ISSN 1608-5043 (Print)
ISSN 1608-5078 (Online)

SCIENTIFIC AND TECHNICAL JOURNAL

GEORESOURCES

www.georesjournal.ru

V. 22. No. 2. 2020

GEORESURSY GEORESOURCES. SCIENTIFIC AND TECHNICAL JOURNAL

SCIENTIFIC AND TECHNICAL JOURNAL
GEORESURSY
www.geors.ru
e-mail: mail@geors.ru
ISSN 1608-5043 (Print)
ISSN 1608-5078 (Online)
V. 22. Is. 2. 2020
Key title: «Georesursy». Parallel title: «Georesources»

Publisher: Georesursy LLC
Editorial and Publisher's address:
1-10, Mayakovsky st., Kazan, 420012, Russian Federation
Phone: +7 843 2390530, e-mail: mail@geors.ru

Georesursy (Georesources) is a peer-reviewed scientific and technical journal published since 1999.

The journal is included/indexed in:
- **Scopus;**
- **Web of Science (ESCI);**
- **Directory of Open Access Journals (DOAJ);**
- **CAS (Chemical Abstracts Service) databases;**
- **GeoRef database;**
- **EBSCOhost™ databases;**
- **Ulrich's Periodicals Directory.**

The full-text e-versions of the articles are available on: **www.geors.ru**

Registered by the Federal Service for Supervision of Communications and Mass Media No. PI FS77-38832

The Journal is issued 4 times a year. Circulation: 250 copies
Issue date: June 30, 2020

Table of Contents

ORIGINAL ARTICLE
DOI: https://doi.org/10.18599/grs.2020.2.2-7

Influence of the pore space structure and wettability on residual gas saturation

R.S. Khisamov[1], V.G. Bazarevskaya[2], N.A. Skibitskaya[3], I.O. Burkhanova[3], V.A. Kuzmin[3], M.N. Bolshakov[3], O.O. Marutyan[3]*

[1]*Tatneft PJSC, Almetyevsk, Russian Fedeartion*
[2]*Institute TatNIPIneft Tatneft PJSC, Bugulma, Russian Fedeartion*
[3]*Oil and Gas Research Institute of the Russian Academy of Sciences, Moscow, Russian Fedeartion*

Abstract. A significant part of hydrocarbon deposits in Russia is in the late stage of development. The distribution of residual oil and gas reserves is determined by the properties of the holding rocks. Estimating of deposits' residual gas saturation is an important scientific task. The allocation of zones with the maximum undeveloped gas reserves will allow to select areas in long-developed fields for the intensification of production in the most efficient way. To search for such "sweet" zones, it is necessary to determine the factors that provide the value of the residual gas saturation.

The article proposes a method for estimating of residual trapped in pores gas saturation based on quantitative characteristics of the pore space structure and rock wettability.The influence of formation pressure value and behaviour on making up of residual gas saturation during field development is not accounted in this work.

The study of a wide collection of core sampled from productive deposits of the Orenburg oil and gas condensate field, the Vuktylskoe oil and gas condensate field, oil and gas field of Orenburg region, and also three areas in the East Caucasian petroleum province confirmed that the value of structure-trapped oil and gas saturation of carbonate and terrigenous rocks is directly proportional to the ratio of pore diameters and channels connecting them. Herewith the angular coefficient of the regression equation for this relationship for carbonate rocks directly depends on the quantitative characteristics of the predominant (relative) wettability.

The obtained relationships make it possible to predict the value of residual gas saturation based on knowledge about the pore space structure and the surface properties of rocks.

Keywords: residual gas saturation, trapped gas saturation, structure-trapped gas saturation, pore space structure, selective wettability, relative wettability, predominant wettability

Recommended citation: Khisamov R.S., Bazarevskaya V.G., Skibitskaya N.A., Burhanova I.O., Kuzmin V.A., Bolshakov M.N., Marutyan O.O. (2020). Influence of the pore space structure and wettability on residual gas saturation. *Georesursy = Georesources*, 22(2), pp. 2-7. DOI: https://doi.org/10.18599/grs.2020.2.2-7

Introduction

Late stages of field development call for improvement of oil and gas recovery. For this purpose, it is necessary to understand the distribution of residual petroleum reserves, which is dependent on reservoir rock properties as well as technology-related factors (Mikhailov, 1992; Surguchev et al., 1984).

Two types of residual hydrocarbon reserves are distinguished. These are of macro-and micro scales. Macro-scale residual oil and gas reserves are located in by-passed zones, lenses and unswept intervals, while micro-scale residual hydrocarbons are accumulated in the flooded areas of the formation (Mikhailov, 1992).

The paper considers a scenario of the buildup of residual gas saturation at the micro scale, particularly behind the flood front under depletion-drive development.

Stronger water-wet properties of a porous gas-saturated medium provide higher residual gas saturation. This results from ever-increasing growth of gas bubbles due to increase in the curvature and concavity of the meniscus of moving water at capillary imbibition front and ever-greater advance of meniscus edges relative to the center during their closure and formation of a new meniscus upon reaching pore contraction point at the subsequent entry into the channel. The larger the pores and the thinner the pore connecting channels (i.e. the greater than unity is the ratio between average diameters of pores and

*Corresponding author: Natalia A. Skibitskaya
E-mail: skibitchka@mail.ru

connecting channels $d_{pore}/d_{channel}$), the larger the trapped gas bubbles and the higher the trapped gas saturation behind capillary imbibition front at observed reservoir pressures (Bolshakov et al., 2014).

Since residual gas trapping in pores is largely determined by pore structure of reservoir rocks, the resultant residual gas saturation and the corresponding pore volume can be defined as structure-trapped. The fraction of the net productive reservoir volume filled with water intruded during capillary imbibition is defined as producing or dynamic reservoir volume. The extent of this continuously bounded dynamic volume depends substantially on average diameter of pore connecting channels $d_{channel}$ and physical and chemical properties of the surface (Bolshakov et al, 2014, Skibitskaya et al., 2010).

Spot-to-spot variation of water cut in reservoir rocks of gas-condensate and oil-gas-condensate fields, developed generally under depletion drive, is dominated by capillary imbibition behavior depending on porosity and permeability, physical and chemical properties and structure-and-capacity properties of the rocks at macro- and micro scales. The stronger the water-wet state of a gas-saturated reservoir, the greater the rate of direct-flow capillary imbibition. Various studies have demonstrated that the rate of direct-flow capillary imbibition in oil-wet gas-saturated carbonate reservoirs can reach as low as zero (Skibitskaya et al., 2018). Reservoirs with heterogeneous water wetting properties will more likely tend to contain unswept regions at micro- and macro-scales.

Materials and Methods

A comprehensive study of rock samples using lithological and petrophysical, geochemical, physical and chemical methods provided a unique database for the

Fig. 1. A location map of the examined fields and areas. GOF-1 – a gas-oil field located in the Orenburg Region, A1, A2, A3 – production areas of the East Predcaucasus petroleum region.

Location	Field	Lithology	Age	Tectonic confinedness	Number of samples examined in SEM
Volga-Ural Petroleum Province	Orenburgskoye	Carbonate rocks	P_1 - C	Sol-Iletsk Dome	51
Timan-Pechora Petroleum Province	Vuktylskoye	Carbonate rocks	P_1 - C	Northern part of Upper Pechora Depression Pre-Urals Foreland Basin	49
Volga-Ural Petroleum Province	Gas-oil field (GOF-1)	Carbonate rocks	P_1	Sol-Iletsk Dome	21
East Predcaucasus Petroleum Region	Area 1	Carbonate, terrigenous rocks	T_1	Northern edge of East-Manychsky Trough	25
	Area 2	Terrigenous rocks	K_1, J_2, T_3	Chograisky Trough of Manuchsky Troughs zone	22
	Area 3	Carbonate, terrigenous rocks	D_3	South-Western part of Pre-Caspian Depression	10
				Total:	178

Table 1. Characteristics of examined sediments

Orenburgskoye oil-gas-condensate field, Vuktylskoye oilgas-condensate field, a gas-oil field in the Orenburg Region (GOF-1), as well as three areas of the East Predcaucasus petroleum region (A1, A2, A3) (Fig. 1, Table 1) (Khisamov et al., 2014). The aggregated dataset covers the Devonian, Carboniferous, Permian, Triassic, Jurassic, and Cretaceous sediments.

The samples represent, for the most part, carbonate rocks, however terrigenous sediments have also been examined. It is important to note that extraction of the samples did not intend to preserve the native wetting state of the rock surface. Pore structure and wettability of pore surfaces are considered to be the main rock properties responsible for oil trapping effect (Mikhailov, 1992; Surguchev et al., 1984; Dullien et al., 1972).

Results of core studies of the fields listed above enable analysis of these effects. The pore structure of rock samples was examined in a scanning electronic microscope (SEM) using cathode luminescence method (Kuzmin, 1984). Obtained microscopic images of the pore space were processed in *Collector* software program. Its computation algorithm relies on understanding of the void space as a system of pores and channels (Bolshakov et al., 2007). The program allows evaluation of different structural parameters of the pore space, including the ratio between average diameter of pores and the average diameter of pore connecting channels $d_{pore}/d_{channel}$.

Residual (trapped) gas saturation factor S_{gr} was determined by means of direct-flow capillary water imbibition of unextracted rock samples in a state of residual water saturation (Skibitskaya et al., 2018). The authors believe that this method for simulation of residual gas saturation in a core sample most closely reflects residual gas saturation buildup processes during field operation.

Fractional wettability was evaluated using conventional optical measurements of contact angle based on estimated angles of the meniscus formed on sample surface in water/ hydrocarbon fluid system which were updated with state of-the-art digital instruments (Skibitskaya et al., 2016). Water contact angles of hexane-saturated samples in hexane medium $\theta_{w\text{-}h}$ and hexane contact angle of water-saturated samples in water medium $\theta_{h\text{-}w}$ were estimated.

Given that the examined rocks are characterized by complex composition and complex structure of the void space, and the fact that pore surface is unevenly covered with high-molecular oil components of different composition from mixed-wet (asphaltenes, heavy resins) to oil-wet (oils), a part of the pore surface may be water-wet while another part is oil-wet.

In this case, the term "predominant wettability" should be used to characterize the surface properties of the rock.

Predominant wettability represents the tendency of one liquid to adhere to the rock surface in presence of another fluid; particularly, oil-versus-water wetting preference. Predominant wettability was quantitatively expressed in terms of relative wettability parameter $\theta_{h\text{-}w}/\theta_{w\text{-}h}$, which is determined as the ratio between rock contact angles with hydrocarbons and with water. Should relative wettability be less than unity, the sample predominantly imbibes hydrocarbons, i.e. the rock is predominantly oil-wet. Otherwise, relative wettability $\theta_{h\text{-}w}/\theta_{w\text{-}h}$ above unity is indicative of water-wet rock.

Results

Experimental studies of core samples from the central part of the Orenburgskoye oil-gas-condensate field has revealed that residual gas saturation of productive carbonate rocks is defined by the ratio between average diameters of pores and pore connecting channels $d_{pore}/d_{channel}$ (Skibitskaya et al., 2010). Direct linear relationship between S_{gr} and $d_{pore}/d_{channel}$ is characterized by large correlation coefficient and is common for

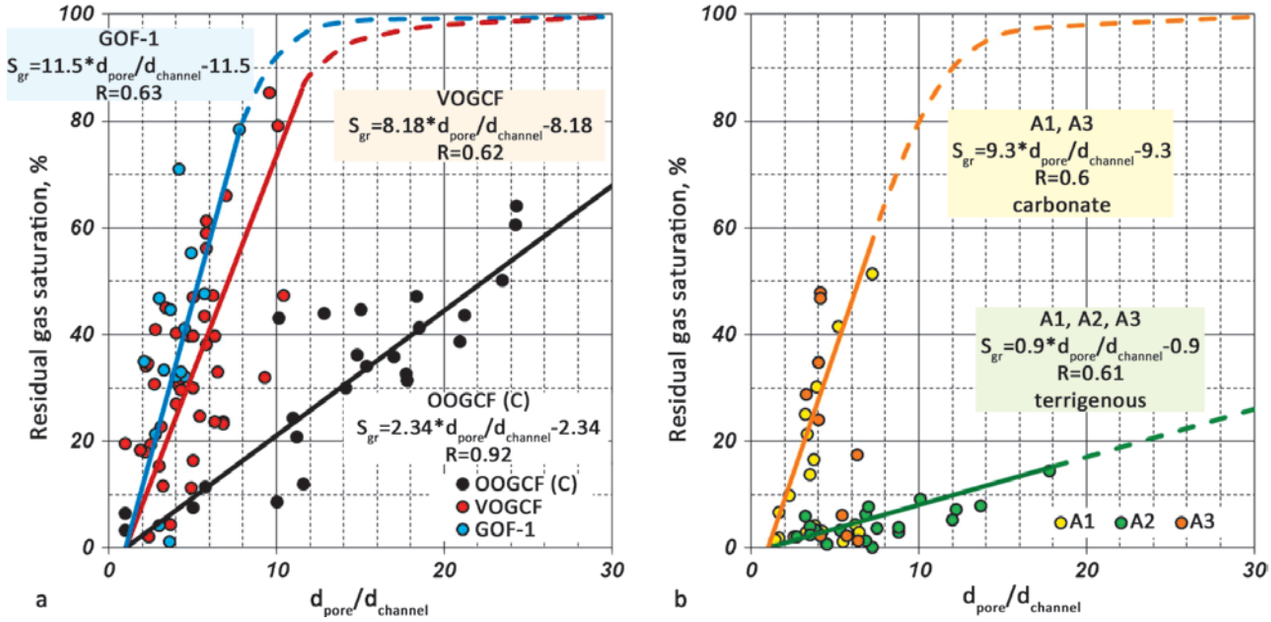

Fig. 2. Relationship between structure-trapped gas saturation factor S_{gr} and the ratio between diameters of pores and pore channel ($d_{pore}/d_{channel}$). a – for productive sediments of the central part of Orenburgkoye oil-gas-condensate field (OOGCF (C)), Vuktylskoye oil-gas condensate field (VOGCF), gas-oil field in the Orenburg Region (GOF-1); b – for productive sediments of Areas 1 (A1), 2 (A2) and 3 (A3) of East Predcaucasus petroleum region.

all stratigraphic units of the field (Fig. 2a). Since gas trapping does not occur if pores and channels have similar diameters, this relationship stems from the point where $d_{pore}/d_{channel}$ equals unity and S_{gr} equals zero. Thus, the regression equation of $S_{gr} = f(d_{pore}/d_{channel})$ takes the form of a linear non-homogeneous equation:

$$S_{gr} = m \cdot (d_{pore}/d_{channel}) - b, \quad (1)$$

where S_{gr} is structure-trapped gas saturation, %; m is slope factor of linear regression equation, %; b is an intercept of linear regression equation, numerically equal to m, %.

Studies of core samples from other fields yielded similar close relationships (Fig. 2a, b). It should be noted that examined core samples from the Orenburgskoye oil-gascondensate field exhibit maximum S_{gr} up to 65% in pores with diameters 24 times greater than channel diameters. The study of core samples from Vuktylskoye oil-gascondensate field and gas-oil field in the Orenburg Region has demonstrated that residual gas saturation reaches 80-90% even at $d_{pore}/d_{channel}$ of approximately 10. At higher pore/channel diameter ratios the function $S_{gr} = f(d_{pore}/d_{channel})$ for these fields will probably be nonlinear (Fig. 2a). However, no actual data has been obtained to confirm it for this set of samples.

Similar dependence plots were obtained for reservoir rocks of production arears 1 (A1), 2 (A2) and 3 (A3) of the East Predcaucasus petroleum region (Fig. 2b). Comparison of linear sections of $S_{gr} = f(d_{pore}/d_{channel})$ functions for different fields have shown that the slope angles of these relationships differ significantly (Fig. 2a, b).

Comprehensive analysis of petrophysical, geochemical and physical-chemical parameters of examined samples has revealed that relative (predominant) wettability $\theta_{h\text{-}w}/\theta_{w\text{-}h}$ is the main factor determining the slope angle of $S_{gr} = f(d_{pore}/d_{channel})$, and, accordingly, the growth rate of the residual structure-trapped gas saturation factor when the pore structure undergoes changes from capillary-like to large-pore structure.

This statement is fair for examined carbonate sediments: rock samples from the central part of the Orenburgskoye oil-gas-condensate field, Vuktylskoye oil-gas-condensate field, gas-oil field in the Orenburg Region, as well as for predominantly carbonate rocks of areas 1, 2, and 3 (Table 2). The $S_{gr} = f(d_{pore}/d_{channel})$ relationships for terrigenous rock samples obtained from areas 1 and 3 have substantially lower percent slope compared to carbonate rocks despite high relative wettability (Table 2).

Since the examined terrigenous rock samples are few in number, further studies of the effects of terrigenous rocks wettability on residual gas saturation are required.

Data analysis has indicated a close relationship between relative wettability and the slope "m" of equation (1) (Fig. 3). Thus, an experimental evidence of the influence of relative (predominant) wettability of rocks on trapped gas saturation of carbonate rocks has been obtained.

Conclusion

Studies have shown that the ratio of average diameter of pores to average diameter of pore connecting channels

Field	Lithology	Average wettability $\theta_{h-w}/\theta_{w-h}$	Slope m, %
Orenburgskoye (central part)	Carbonate rocks	0.83	2.34
Vuktylskoye	Carbonate rocks	0.93	8.18
Gas-oil field	Carbonate rocks	1.15	11.5
Areas 1 and 3 East Predcaucasus region	Carbonate rocks	1.1	9.3
Areas 1, 2 and 3 East Predcaucasus region	Terrigenous rocks	1.06	0.9

Table 2. Comparison of average relative wettabilities $\theta_{h-w}/\theta_{w-h}$ and slopes m of equation for $S_{gr} = f(d_{pore}/d_{channel})$ relationship for various fields

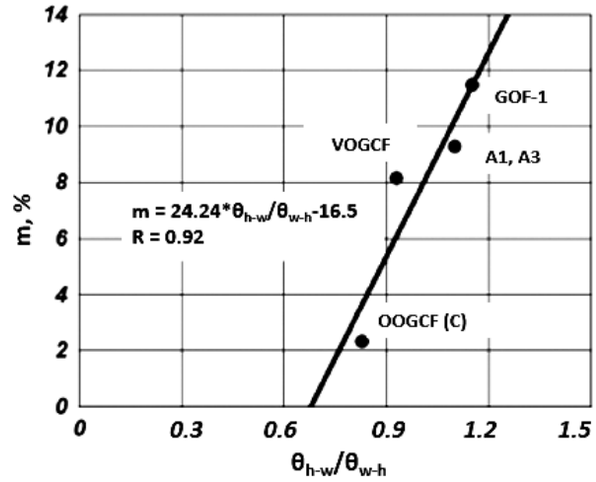

Fig. 3. Relationship between the slope m of the equation $S_{gr} = f(d_{pore}/d_{channel})$ and relative wettability $\theta_{h-w}/\theta_{w-h}$ based on the results of studies of rock samples from the central part of the Orenburgskoye oil-gas-condensate field (OOGCF (C)), Vuktylskoye field oil-gas-condensate field (VOGCF), gas-oil field in the Orenburg Region (GOF-1), areas 1 (A1) and 3 (A3) of East Predcaucasus petroleum region.

controls the volume of trapped gas in both carbonate, and terrigenous rocks. The *S*gr growth rate when carbonate rock pore structure undergoes changes from capillary-like to large-pore structure is dependent on relative (predominant) wettability of the rocks. Attained results enable prediction of residual gas saturation in gas-saturated carbonate sediments of gas-condensate and oil-gas-condensate fields from pore structure and relative (predominant) wettability of rocks. According to conducted studies, predominantly water-wet large-pore carbonate rocks will have the highest trapped gas saturation. Study results confirm the theoretical understanding of the effects of pore structure, physical-chemical rock properties and lithological characteristics on residual gas saturation.

Acknowledgments

The paper has been written as part of the state assignment (subject: "Forecasting the status of the resource base of Russian oil and gas sector based on systematic studies of petroleum potential of natural reservoirs in carbonate, terrigenous and shale formations", No. AAAAA19-119030690047-6).

References

Bolshakov M.N., Skibitskaya N.A., Kuzmin V.A. (2007). Investigation of the Pore Space Structure by a Scanning Electron Microscope Using the Computer Program Collector. *Journal of Surface Investigation. X-Ray, Synchrotron and Neutron Techniques*, 1(4), pp. 493-496. https://doi.org/10.1134/S1027451007040222

Bolshakov M.N., Skibitskaya N.A., Kuzmin V.A., Marutyan O.O. (2014). Determination of residual oil and gas saturation by direct-flow capillary impregnation method. *Neftyanoe khozyaistvo = Oil industry*, 4, pp. 30-32. (In Russ.)

Dullien F.A., Dhavan G.K., Nur Gurak, Babjak L. (1972). A relationship between pore structure and residual oil saturation in tertiary surfactant floods. *SPEJ*, pp. 289-296. https://doi.org/10.2118/3040-PA

Khisamov R.S., Bazarevskaya V.G., Burkhanova I.O., Skibitskaya N.A., Kuzmin V.A., Nikulin B.A. (2014). A systematic approach to the study of the oil and gas source carbonate sequence of a hydrocarbon field in the Orenburg region. *Neftyanoe khozyaistvo = Oil industry*, 7, pp. 12-17. (In Russ.)

Kuzmin V.A. (1984). Methodology and main results of studying rocks – reservoirs of complex structure using a scanning electron microscope. Abstract of diss. Moscow: MINKh i GP im. I.M. Gubkina. (In Russ.)

Mikhailov N.N. (1992). Residual oil saturation of the developed formations. Moscow: Nedra, 270 p. (In Russ.)

Skibitskaya N.A., Bolshakov M.N., Kuzmin V.A., Marutyan O.O. (2018). Regularities of the processes of direct-flow capillary impregnation in productive carbonate deposits of the Orenburg oil and gas condensate field. *Aktualnye problemy nefti i gaza = Actual problems of oil and gas*, 3(22), pp. 13. (In Russ.). http://oilgasjournal.ru/issue_22/skibitskaya-bolshakov.html

Skibitskaya N.A., Kuzmin V.A., Bolshakov M.N., Marutyan O.O. (2010). The influence of the microstructural parameters of carbonate rocks of productive sediments on the residual oil and gas saturation. *Neftyanoe khozyaistvo = Oil industry*, 12, pp. 98-101. (In Russ.)

Skibitskaya N.A., Kuzmin V.A., Marutyan O.O., Bolshakov M.N., Burkhanova I.O., Khaliullina A.F. (2016). Results of studying the selective wettability of carbonate rocks in productive deposits of hydrocarbon deposits. *Georesursy, geoenergetika, geopolitika*, 1(13), p. 3. (In Russ.). http://oilgasjournal.ru/vol_13/skibitskaya-kuzmin.html

Surguchev M.L., Zheltov Yu.V., Simkin E.M. (1984). Physical-chemical microprocesses in oil and gas bearing strata. Moscow: Nedra, 215 p. (In Russ.)

About the Authors

Rais S. Khisamov – Dr. Sci. (Geology and Mineralogy), Professor, Deputy Director General and Chief Geologist

Tatneft PJSC

75, Lenin st., 75, Almetyevsk, 423400, Russian Federation

Venera G. Bazarevskaya – Cand. Sci. (Geology and Mineralogy), Deputy Director for research in the field of geology of hard-to-recover reserves

Institute TatNIPIneft Tatneft PJSC

40, M.Djalil st., Bugulma, 423326, Russian Federation

Natalia A. Skibitskaya – Cand. Sci. (Geology and Mineralogy), Head of the Laboratory of hard-to-recover hydrocarbon reserves, Leading Researcher, Oil and Gas Research Institute of the Russian Academy of Sciences
3, Gubkin st., Moscow, 119333, Russian Federation
E-mail: skibitchka@mail.ru

Irina O. Burkhanova – Cand. Sci. (Geology and Mineralogy), Senior Researcher of the Laboratory of hard-to-recover hydrocarbon reserves, Oil and Gas Research Institute of the Russian Academy of Sciences
3, Gubkin st., Moscow, 119333, Russian Federation

Vladimir A. Kuzmin – Cand. Sci. (Geology and Mineralogy), Leading Researcher of the Laboratory of hard-to-recover hydrocarbon reserves, Oil and Gas Research Institute of the Russian Academy of Sciences
3, Gubkin st., Moscow, 119333, Russian Federation

Mikhail N. Bolshakov – Cand. Sci. (Geology and Mineralogy), Senior Researcher of the Laboratory of hard-to-recover hydrocarbon reserves, Oil and Gas Research Institute of the Russian Academy of Sciences
3, Gubkin st., Moscow, 119333, Russian Federation

Oleg O. Marutyan – Senior Researcher of the Laboratory of hard-to-recover hydrocarbon reserves, Oil and Gas Research Institute of the Russian Academy of Sciences
3, Gubkin st., Moscow, 119333, Russian Federation

Manuscript received 27 March 2020;
Accepted 09 June 2020;
Published 30 June 2020

ORIGINAL ARTICLE
DOI: https://doi.org/10.18599/grs.2020.2.8-14

Evaluation of hydraulic fracturing results based on the analysis of geological field data

*I.N. Ponomareva, D.A. Martyushev**
Perm National Research Polytechnic University, Perm, Russian Federation

Abstract. The relevance of the research is specified by the significant contribution of the oil produced as a result of hydraulic fracturing in the wells in its total production. A correct assessment of the results of actually carried out hydraulic fracturing will allow to develop clear recommendations on the further application of this method of oil production enhancement for the geological and physical conditions of specific fields. It was established that hydraulic fracturing in the well 221 of the Shershnevsky field (the Perm Territory, Russia) led to a change in interaction between wells within the entire element of the development system; it began to work as a single coordinated system. As a result of hydraulic fracturing, there was not just a redistribution of fluid drainage volumes. A synergistic effect arose when fracturing in one well led to an increase in fluid flow rates and coordinated operation of the entire element of the development system. It is likely that hydraulic fracturing in the well 221 led to a significant change in the geological and technological characteristics of the Bobrikovskian deposit of the Shershnevsky field to a greater extent than the volume of the drainage zone of this well. A whole system of channels with reduced filtration resistances appeared instead of a single crack, as is common in the classic representation of hydraulic fracturing.

It should be noted that the approach presented in the article is the first very important step in a comprehensive analysis of the effective reservoir development based on the results of field monitoring. In the future, it is necessary to attract more detailed information about the interaction of wells. Only such a multilevel analysis will allow to substantiate the general conclusion about the hydraulic fracturing on the development of a reservoir and to confirm conclusively the effect of wells on each other, which can be individual in different parts of the reservoir.

Keywords: hydraulic fracturing, terrigenous reservoir, interaction between wells, correlation of flow rates, method of enhanced oil recovery

Recommended citation: Ponomareva I.N., Martyushev D.A. (2020). Evaluation of hydraulic fracturing results based on the analysis of geological field data. *Georesursy = Georesources*, 22(2), pp. 8-14. DOI: https://doi.org/ 10.18599/grs.2020.2.8-14

Introduction

Hydraulic fracturing (fracturing) is currently one of the most effective methods of stimulating oil production worldwide. An adequate assessment of the results of hydraulic fracturing allows, inter alia, evaluating the method prospects in certain geological and technological conditions (Cherepanov et al., 2015).

In the Perm Territory, a wide variety of hydraulic fracturing technologies are used, such as classic proppant fracturing in terrigenous reservoirs, acid proppant fracturing in carbonate reservoirs, acid fracturing with proppant fracturing, nitrogen foam fracturing, etc. (Cherepanov et al., 2015; Voevodkin et al., 2018).The effectiveness of these technologies is usually evaluated by the increase in oil production in wells – objects of exposure (Votinov et al., 2018; Tare A. Ganata et al., 2018). In addition to the increase in flow rate, in some cases technological efficiency indicators are also used such as additional oil production and the duration of the effect, calculating these indicators with respect to the wells where hydraulic fracturing was carried out (Valeev et al., 2018). This approach to assessing the results of hydraulic fracturing is due to the fact that this type of stimulation on the formation is usually attributed to the group of technologies for stimulating flow to wells. In particular, in the works (Kashnikov et al., 2018; Nurgaliev et al., 2017; Yakhina, 2018) it was shown that hydraulic fracturing is carried out in order to increase the reservoir permeability in the bottomhole zone and increase well productivity. However, some researchers (Nurgaliev et al., 2017; Tare A. Ganata et al., 2018; Debotyam Maity et al., 2019; Yuekun Xing et

**Corresponding author: Dmitriy Martyushev*
E-mail: martyushevd@inbox.ru

al., 2019) believe that hydraulic fracturing under certain conditions not only a way to increase the permeability of the bottom-hole zone, and, as a consequence, the productivity of a particular well, but also a deeply penetrating method of exposing the reservoirs in general.

The study of laws of fractures formation is one of the urgent tasks of monitoring hydraulic fracturing. Obtaining reliable information about the spatial position of the fracture(s) and its size will allow not only analyzing hydraulic fracturing in details, but also making justified decision on the appropriateness of replicating this technology to other wells in similar conditions (Jianming He et al., 2017; Voevodkin et al., 2018; Kulakov et al., 2018).

To date, a wide range of research methods and technologies exists and is used widely that allow controlling the process of creating fractures. The method for estimating hydraulic fracture parameters according to microseismic monitoring (MSM) has become widespread (Aleksandrov et al., 2007; Yew Kwang Yong et al., 2018; Lei Li et al., 2019). However, the support of all hydraulic fractures with microseismic monitoring is impractical for both economic and technological reasons (there are areas in which microseismic studies are inappropriate within the Perm Territory) (Alexandrov et al., 2007; Rastegaev et al., 2019).

Field geophysical survey and hydrodynamic well surveys hold a special place among other surveys. Their role is very significant, since these methods provide the predominant amount of information about hydraulic fracturing. It should be noted that the existing technologies for conducting and interpreting hydrodynamic well testing and field geophysical survey are of limited use for solving this problem and have a high potential for improvement and development (Ipatov et al., 2009).

In this regard, a technique seems to be relevant that allows us to solve this problem on the basis of a comprehensive analysis of field data (Tare A. Ganata et al., 2018; Chorny et al., 2019). The accumulated experience of hydraulic fracturing, accompanied by microseismic monitoring, made it possible to develop such a technique as applied to oil assets of the Perm Territory. The reliability of its results is confirmed by the materials of MSM (Rastegaev et al., 2019).

Thus, the availability of a reliable method for estimating hydraulic fracture parameters based on the integrated use of field data allows us to study the results of hydraulic fracturing even if the event was not accompanied by microseismic monitoring. The approach described further in the article is the first step in a comprehensive analysis of the effectiveness of reservoir development based on the results of field monitoring. This article presents the results of solving this problem in relation to the Shershnevsky field.

General information about the object of study

This article provides information on the results of hydraulic fracturing carried out at well 221 of the Shershnevsky oil field (the Perm Territory, Russia) (Fig.1). The well exploits the terrigenous Bobrikovskian deposit. The placement practically in the central part of the structure is its characteristic feature. The deposits of the Bobrikovskian horizon are mainly represented by quartz sandstones, sometimes with interbeds of mudstones and siltstones unevenly clayey, areas of very sandy before transition to sandstone. Sandstones, different-grained with various oil manifestations – from oil effusions in pores to complete oil saturation, can be attributed to channel alluvium, to which industrial oil content is confined. Brief information on the geological and physical characteristics of the operation of well 221 of the Shershnevsky field is presented in Table 1. Information on the other six oil producing wells participating in the assessment of hydraulic fracturing is presented in Table 2.

Standard approaches to determine technological efficiency made it possible to evaluate the results of hydraulic fracturing in this well as very high for the region. The well production rate increased almost three times, the effect persisted for more than 2000 days.

This article has conducted a study of hydraulic fracturing affecting not only on the performance of the well itself – the fracturing object, but also on the nearest surrounding wells, that is, on the element of the development system as a whole. So, in the immediate vicinity of well 221 considered in the article, there are six production wells (No. 64, 214, 215, 222, 228, and 229), which together form a "conditional" first annular row (Fig. 1).

Study of the interaction between wells before and after hydraulic fracturing

If hydraulic fracturing performed in well 221 had a deeply penetrating character, it should be manifested in a change in technological efficiency indicators, i.e. the nearest producing wells should "respond" by changing the values of their production indicators (Nurgaliev et al., 2017; Mukhametshin, 2018; Yudin et al., 2018). To test this hypothesis, field materials were studied and statistically analyzed – oil and liquid production rates, as well as accumulated oil and liquid production values for all wells of the selected development element (Galkin et al., 2017).

At the first stage, performance indicators were compared in the periods before and after hydraulic fracturing. In this case, the indicators before hydraulic fracturing are assigned to class 1 (the sample amounted to n = 69 values), after hydraulic fracturing – to class 2 (n = 81 values). Comparison of average fluid flow rates for grades 1 and 2, that is, before and after hydraulic

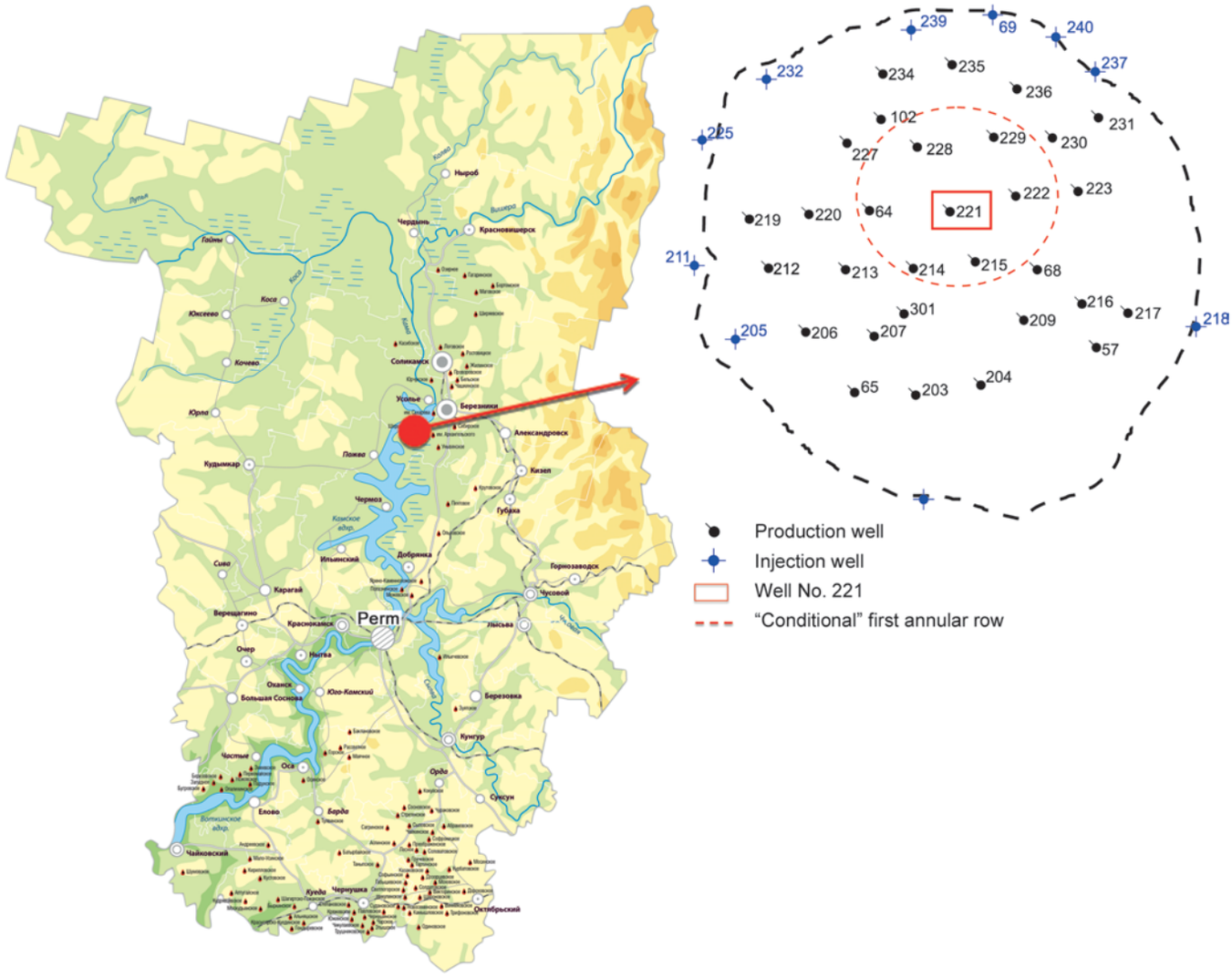

Fig. 1. Map of the location of the Shershnevsky field in the Perm Territory with scheme of the development system element of the Bobrikovskian deposit

fracturing, was performed using mathematical statistics tools (Student's t-test and Pearson's-χ^2 criterion), the comparison results are shown in Table 3.

It can be seen from the table that truly statistical criteria confirm a significant change (increase) in fluid flow rates after hydraulic fracturing for all wells of the selected element of the development system, and not just well 221, the object of the hydraulic fracturing.

As a graphic illustration, a combined graph of the dependence of Q_H on t for all wells was constructed (Fig. 2). It can be seen from the figure that after the hydraulic fracturing, well 221 underwent a restructuring of the system as a whole, which can be well confirmed using regression analysis. In the first case, the connection has the following form: $Q_H = -18.834 + 0.001158$ t, at $r = 0.041$, $p = 0.3628$; in the second: $Q_H = -212.265 + 0.006001$ t, with $r = 0.3611$, $p = 0.0000$. This shows that the change in the system of values of Q_H in time actually occurred.

A similar conclusion was also obtained by comparing oil production rates, cumulative oil and fluid production, typical for the periods of operation before and after hydraulic fracturing. That is, hydraulic fracturing at well 221 led not only to an increase in its production rate, but also to the production rates of all neighboring wells located in close proximity. That is, hydraulic fracturing of well 221 cannot be considered as a geological and technical measure aimed only at intensifying the inflow directly to this well.

It should also be noted that in all cases, the cause of the increase was not the conduct of any other geological and technical measures. That is, the assumption that as a result of hydraulic fracturing, a simple redistribution of drainage volumes between neighboring wells in favor of the well being affected is also not correct, since in this case there would be a decrease in the flow rates of neighboring wells.

For a more detailed analysis of the obtained data, a correlation analysis was used, the results of which are shown in Table 4.

In order to visualize the obtained results, we constructed schemes for changing the correlation

No.	Indicator name, units	Value
1	Absolute elevation of the roof, m	-1846
2	Net oil pay,m	9.9
3	Viscosity of formation oil, mPa*c	3.19
4	Gas saturation of reservoir oil, m^3/t	64.2
5	Bubble-point pressure, MPa	11.94
6	Porosity coefficient, unit fractions	0.17
7	Net-to-gross sand ratio, unit fractions	0.6
8	Average number of permeable intervals, unit fractions	3.21
9	Permeability coefficient (defined by field geophysical survey data), $micron^2$	0.096
10	Water cut before hydraulic fracturing, %	1.0
11	Bottom hole pressure before hydraulic fracturing, MPa	9.55
12	Reservoir pressure before hydraulic fracturing, MPa	12.97

Table 1. Brief information about the well – fracturing object

Well No.	Permeability coefficient, $micron^2$	Net oil pay,m	Reservoir pressure before hydraulic fracturing, MPa	Bottom hole pressure before hydraulic fracturing, MPa	Water cut before hydraulic fracturing, %
215	0.909	8.7	11.59	10.25	1.0
222	0.206	10.8	12.92	10.06	0
229	1.716	11.2	11.21	9.79	0
228	0.111	14.7	12.78	11.76	2.0
64	0.456	5.4	13.10	11.71	3.0
214	0.078	12.6	12.77	9.77	5.0

Table 2. Brief information about the operating parameters of adjoining wells participating in the hydraulic fracturing assessment

Well No.	Statistical performance indicators		Comparison criteria*	
	Class 1 (before HF)	Class 2 (after HF)	Student's t-test	Pearson's-χ^2 criterion
221	19.4±16.1	40.8±6.7	-10.847 0.000	99.603 0.000
64	21.9±17.6	48.1±12.1	-10.724 0.000	85.483 0.000
214	13.8±13.7	22.9±3.7	-5.773 0.000	36.027 0.000
215	29.1±14.4	37.4±5.0	-4.833 0.000	29.127 0.014
222	36.1±15.9	60.3±8.9	-11.681 0.000	135.111 0.014
228	30.5±6.6	43.7±3.9	-14.997 0.000	134.260 0.000
229	47.6±12.9	55.9±5.8	-5.228 0.000	24.509 0.014

*Table 3. Comparison of the average values of fluid flow rates (m^3/day) before and after hydraulic fracturing for wells of a selected element of the development system. *Note: the numerator shows the value of the criterion, the denominator shows the level of its significance.*

coefficients between oil production rates within the development element before (Fig. 3) and after hydraulic fracturing (Fig. 4).

The analysis of the diagram in Fig. 3 shows that for the period preceding the hydraulic fracturing, the maximum positive correlations are characteristic of a pair of wells 221-214, that is, these wells worked concertedly, they simultaneously responded to any events with a unidirectional change in their production rates. The eastern part of the development element is characterized by a rather strong negative correlation. That is, an increase in the flow rate of well 221 led to a decrease in the same indicator in wells 215 and 222.

It is likely that the increase in flow rate of well 221 was due to the redistribution of drainage volumes from the eastern part of the selected development element.

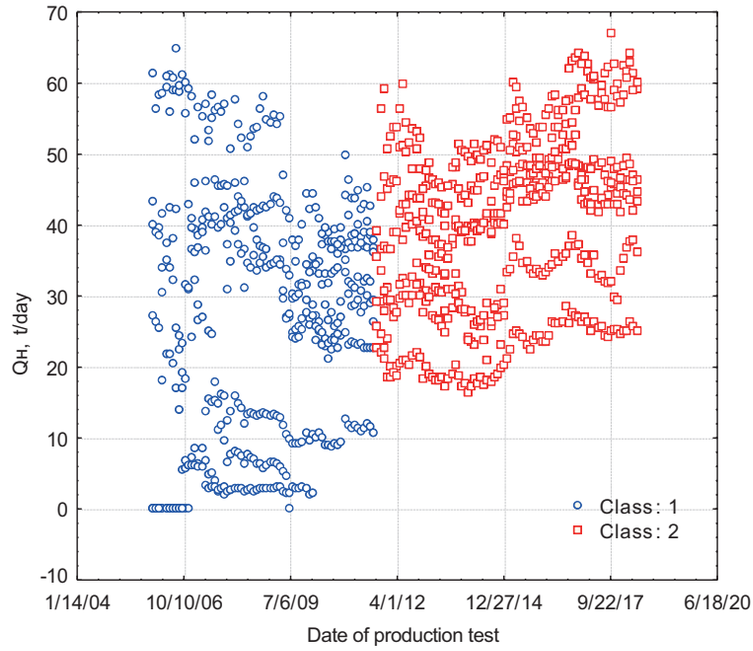

Fig. 2. The change in Q_H in time for producing wells before and after hydraulic fracturing

Well	221	64	214	215	222	228	229
221	1.00 1.00	-0.10 0.68*	0.65* 0.63*	-0.72* 0.69*	-0.81* 0.64*	0.24* 0.69*	-0.17 0.54*
64		1.00 1.00	0.57* 0.93*	-0.29* 0.83*	-0.23 0.67*	-0.05 0.72*	-0.52* 0.73*
214			1.00 1.00	-0.74* 0.82*	-0.74* 0.72*	0.13 0.76*	-0.45* 0.81*
215				1.00 1.00	0.82* 0.75*	-0.02 0.69*	0.32* 0.74*
222					1.00 1.00	-0.08 0.53*	0.38* 0.74*
228						1.00 1.00	-0.13 0.79*
229							1.00 1.00

Table 4. The correlation matrix between the oil production rates of wells of the selected development element (the numerator is before hydraulic fracturing, the denominator is after hydraulic fracturing) Note: -0.65 – significant correlation*

Analysis of changes in the values of the correlation coefficients after hydraulic fracturing clearly demonstrates a significant change in the behavior of the entire selected element of the development system as a result of hydraulic fracturing in well 221. Significant positive correlations are noted within the first annular series between the flow rates of all wells. That is, the whole element began to work as a single unidirectionally coordinated system. The positive nature of the correlation indicates that as a result of hydraulic fracturing, there was not just a redistribution of drainage volumes, but a synergistic effect arose when an event in one well led to an increase in flow rates and coordination of the work of the development system entire element.

Conclusion

The conclusion obtained during the research indicates that the generally accepted model of the hydraulic fracturing result, which consists in visualizing the fracture within the drainage zone of the well – the fracturing object, and in some cases only within the bottom-hole zone of this well, does not reflect the picture that occurred on the Bobrikovskian deposit of Shershnevsky field. It is likely that hydraulic fracturing in well 221 led to a significant change in the filtration parameters of the Bobrikovskian deposit to a greater extent than the volume of the drainage zone of this well. Obviously, on a rather large section of the reservoir, a whole system of channels with reduced filtration resistances arose, rather than a single fracture, as is the

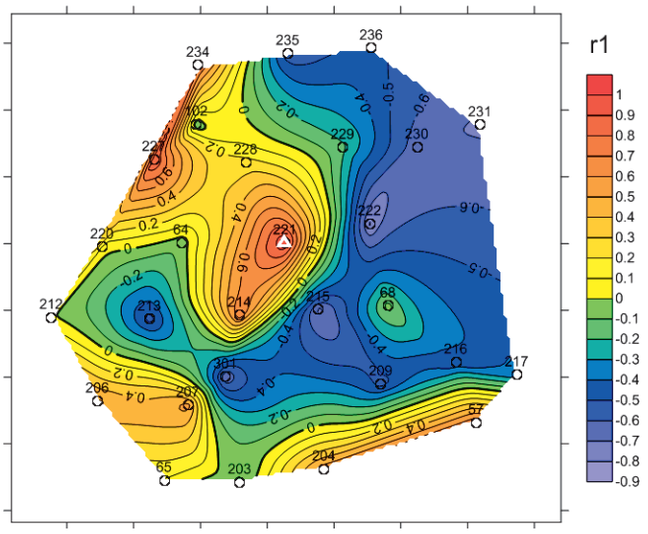

Fig. 3. Scheme for changing the values of the correlation coefficients between oil production rates within the development element before hydraulic fracturing

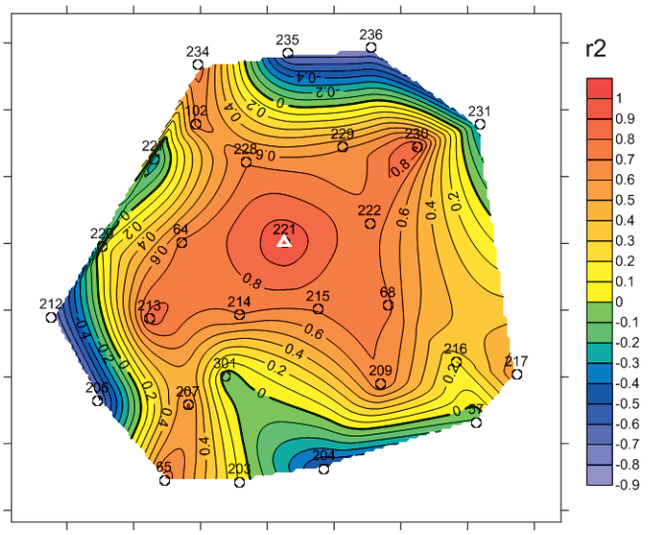

Fig. 4. Scheme of changes in the values of the correlation coefficients between oil production rates within the development element after hydraulic fracturing

case in the classical representation of the use of hydraulic fracturing data. In relation to the hydraulic fracturing field under consideration, it should be considered not as a single, point-based method of stimulating oil production due to an increase in the productivity of the well – the object of impact, but even, to some extent, as a method of increasing oil recovery. It should be noted that the approach described in the article is a very important first step in a comprehensive effectiveness analysis of the deposits development according to the results of the control. The next step in analyzing the effectiveness of hydraulic fracturing is to draw detailed information on the interaction of wells based on long-term monitoring of bottom-hole pressure and costs with the obligatory involvement of information on geological and technological measures carried out in each well. Such a multi-level analysis will allow not only to substantiate the general conclusion about the effect of hydraulic fracturing on the development of a reservoir, but also to confirm conclusively the effect of wells on each other, which can be individual in different parts of the reservoir.

Of course, the singularity of the study does not allow us to draw conclusions about the need to review approaches to assessing the results of hydraulic fracturing. It seems appropriate to conduct similar studies on other wells in this and other regions.

Acknowledgments

The authors are sincerely grateful to V.I. Galkin and A.V. Rastegaev for their support and help in writing the article.

References

Alexandrov S.I., Gogonenkov G.N., Pasynkov A.G. (2007). Passive seismic monitoring to control the geometrical parameters of hydraulic fracturing. *Neftyanoe hozyajstvo = Oil industry*, 3, pp. 51-53. (In Russ.)

Cherepanov S.S., Chumakov G.N., Ponomareva I.N. (2015). The results of acid fracturing with proppant on the Tournaisian-Famennian deposits of the Ozernoye field. *Vestnik PNIPU. Geologiya. Neftegazovoe i gornoe delo = Perm Journal of Petroleum and Mining Engineering*, 14(16), pp. 70-76. (In Russ.) https://doi.org/10.15593/2224-9923/2015.16.8

Chorny A.V., Kozhemyakina I.A., Churanova N.Yu., Soloviev A.V., Khayrullin M.M., Yudin E.V. (2019). Well interference analysis based on field data integration algorithms. *Neftyanoe hozyajstvo = Oil industry*, 1, pp. 36-39. (In Russ.) https://doi.org/10.24887/0028-2448-2019-1-36-39

Debotyam Maity, Jordan Ciezobka (2019) Using microseismic frequency-magnitude distributions from hydraulic fracturing as an incremental tool for fracture completion diagnostics. *Journal of Petroleum Science and Engineering*, 176, pp. 1135-1151. https://doi.org/10.1016/j.petrol.2019.01.111

Galkin V.I., Koltyrin A.N., Kazantsev A.S., Kondratiev S.A., Zhigalov V.A. (2017). Development of a statistical model for predicting the effectiveness of proppant hydraulic fracturing by geological and technological indicators for the Verey carbonate oil and gas complex. *Geologiya, geofizika i razrabotka neftyanyh i gazovyh mestorozhdenij = Geology, geophysics and development of oil and gas fields*, 3, pp. 48-54. (In Russ.)

Ipatov A.I., Nuriev M.F., Jafarov I.S. (2009). The principles of control and management of the development of complex oil fields based on stationary long-term monitoring of reservoirs and wells. *Neftyanoe hozyajstvo = Oil industry*, 9, pp. 40-45. (In Russ.)

Jianming He, Chong Lin, Xiao Li, Yixiang Zhang, Yi Chen (2017). Initiation, propagation, closure and morphology of hydraulic fracturing in sandstone cores. *Fuel*, 208, pp. 65-70. https://doi.org/10.1016/j.fuel.2017.06.080

Kashnikov Yu.A., Ashikhmin S.G., Yakimov S.Yu., Kukhtinsky A.E. (2018). The influence of geomechanical parameters of the massif on the efficiency of hydraulic fracturing. *Geologiya, geofizika i razrabotka neftyanyh i gazovyh mestorozhdenij = Geology, geophysics and development of oil and gas fields*, 1, pp. 46-50. (In Russ.)

Kulakov P.A., Kutlubulatov A.A., Afanasenko V.G. (2018). Predicting the effectiveness of hydraulic fracturing as a component of optimizing its design. *SOCAR Proceedings*, 2, pp. 41-48. (In Russ.) https://doi.org/10.5510/OGP20180200349

Lei Li, Jingqiang Tan, David A. Wood, Zhengguang Zhao, Haichao Chen (2019). A review of the current status of induced seismicity monitoring for hydraulic fracturing in unconventional tight oil and gas reservoirs. *Fuel*, 242, pp. 195-210. https://doi.org/10.1016/j.fuel.2019.01.026

Mukhametshin V.V. (2018). Justification of trends in increasing the level of oil production in the Lower Cretaceous deposits of Western Siberia based on the identification of objects. *Izvestiya Tomskogo politekhnicheskogo universiteta. Inzhiniring georesursov = Bulletin of the Tomsk Polytechnic University. Geo Assets Engineering*, 329 (5), pp. 117-124. (In Russ.)

Nurgaliev R.Z., Gallyamov R.I., Makhmutov A.A., Kornev E.V., Astakhov A.V. (2017). Assessing the effectiveness of hydraulic fracturing taking into account the formed geological bodies. *Geologiya, geofizika i razrabotka neftyanyh i gazovyh mestorozhdenij = Geology, geophysics and development of oil and gas fields*, 3, pp. 57-62. (In Russ.)

Nurgaliev R.Z., Mukhliev I.R., Sagidullin L.R., Schekaturova I.Sh., Rakhmatullin A.A. (2018). Features of the effect of well interference on the efficiency of hydraulic and gas-dynamic fracturing. *Neftepromyslovoe delo = Oil Field Engineering*, 3, pp. 29-34. (In Russ.) https://doi.org/10.30713/0207-2351-2018-3-29-34

Rastegaev A.V., Chernykh I.A., Ponomareva I.N., Martyushev D.A. (2019). Assessment of the results of hydraulic fracturing based on a comprehensive analysis of microseismic monitoring data and geological and field information. *Neftyanoe hozyajstvo = Oil industry*, 8, pp. 122-125. doi: 10.24887/0028-2448-2019-8-122-125

Tarek A. Ganata, Meftah Hrairi. (2018). A new choke correlation to predict flow rate of artificially flowing wells. *Journal of Petroleum Science and Engineering*, 171, pp. 1378-1389. https://doi.org/10.1016/j.petrol.2018.08.004

Valeev A.S., Dulkarnaev M.R., Kotenev Yu.A., Sultanov Sh.Kh., Brilliant L.S. (2018). The reasons for the increase in water cut in wells after hydraulic fracturing in heterogeneous formations. *Izvestiya Tomskogo politekhnicheskogo universiteta. Inzhiniring georesursov = Bulletin of the Tomsk Polytechnic University. Geo Assets Engineering*, 329(6), pp. 140-147. (In Russ.)

Voevodkin V.L., Aleroev A.A., Baldina T.R., Raspopov A.V., Kazantsev A.S., Kondratiev S.A. (2018). The development of hydraulic fracturing technologies in the fields of the Perm region. *Neftyanoe hozyajstvo = Oil industry*, 21, pp. 108-113. (In Russ.) https://doi.org/10.24887/0028-2448-2018-11-108-113

Votinov A.S., Drozdov S.A., Malysheva V.L., Mordvinov V.A. (2018). Restore and increase the productivity of production wells of the Kashirsky and Podolsk facilities at one of the oil fields in the Perm Territory. *Vestnik PNIPU. Geologiya. Neftegazovoe i gornoe delo = Perm Journal of Petroleum and Mining Engineering*, 18(2), pp. 140-148. (In Russ.) https://doi.org/10.15593/2224-9923/2018.4.4

Yakhina Yu.I. (2018). Evaluation of the effectiveness of hydraulic fracturing with two cracks in the vicinity of a single well. *Georesursy = Georesources*, 20(2), pp. 108-114. (In Russ.) https://doi.org/10.18599/grs.2018.2.108-114

Yew Kwang Yong, Belladonna Maulianda, Sia Chee Wee, Dzeti Mohshim, David Eaton (2018). Determination of stimulated reservoir volume and anisotropic permeability using analytical modeling of microseismic and hydraulic fracturing parameters. *Journal of Natural Gas Science and Engineering*, 58, pp. 234-240. https://doi.org/10.1016/j.jngse.2018.08.016

Yudin E.V., Gubanova A.E., Krasnov V.A. (2018). A method for assessing interference of wells using data from the technological modes of their operation. *Neftyanoe hozyajstvo = Oil industry*, 8, pp. 64-69. (In Russ.) https://doi.org/10.24887/0028-2448-2018-8-64-69

Yuekun Xing, Guangqing Zhang, Tianyu Luo, Yongwang Jiang, Shiwen Ning (2019) Hydraulic fracturing in high-temperature granite characterized by acoustic emission. *Journal of Petroleum Science and Engineering*, 178, pp. 475-484. https://doi.org/10.1016/j.petrol.2019.03.050

About the Authors

Inna N. Ponomareva – Cand. Sci. (Engineering), Associate Professor, Department of Oil and Gas Technologies, Perm National Research Polytechnic University

29, Komsomolskiy av., Perm, 614990, Russian Federation

Dmitry A. Martyushev – Cand. Sci. (Engineering), Associate Professor, Department of Oil and Gas Technologies, Perm National Research Polytechnic University

29, Komsomolskiy av., Perm, 614990, Russian Federation

E-mail: martyushevd@inbox.ru

Manuscript received 12 November 2019;
Accepted 21 April 2020;
Published 30 June 2020

ORIGINAL ARTICLE
DOI: https://doi.org/10.18599/grs.2020.2.15-28

Paleoкarst, hydrothermal karst and karst reservoirs of the Franian reefs of the Rybkinsky group

A.P. Vilesov[*], *K.N. Chertina*
Tyumen Petroleum Research Center, Tyumen, Russian Federation

Abstract. More than 20 isolated reefs of the Rybkinsky group were discovered in 2015-2018 in the eastern part of the Rubezhinsky Trough, west of the Sol-Iletsky Arch (Orenburg region; southern part of Volga-Ural Oil and Gas Province), thanks to the use of seismic surveys 3D and exploration drilling. The interval of the stratigraphic distribution of the reefs encompasses Domanikian, Rechitskian and Voronezhian Horizons (=Regional Stages) of the Franian Stage of Upper Devonian. The reefs are cased and overlapped by carbonate-terrigene-clay deposits of the Kolganian Formation that form the seal. High-amplitude oil fields (up to 150 m high) are related to the bodies of reefs. Reefs developed under conditions of significant changes in sea level caused by both eustatic fluctuations and regional tectonics.

Actual data on features of surface and deep karst in different reefs of the Rybkinsky group are given. Three karst epochs are allocated: 1) late Domanikian; 2) late Rechitskian; 3) late Voronezhian. Evidences of the post-franian hydrothermal karst in the reefs are presented. Reservoirs formed as a result of karst are characterized by high complexity of pore space.

Reef reservoirs have a scale permeability effect that is necessary to consider in hydrocarbon reserve calculations.

Keywords: reefs, karst, hydrothermal karst, Franian, reef facies, karst reservoirs, Volga-Ural oil and gas province

Recommended citation: Vilesov A.P., Chertina K.N. (2020). Paleoкarst, hydrothermal karst and karstic reservoirs of the Franian reefs of the Rybkinsky group. *Georesursy = Georesources*, 22(2), pp. 15-28. DOI: https://doi.org/10.18599/grs.2020.2.15-28

Introduction

According to the definition of G.A. Maximovich (1963), «karst is process of chemical and partly mechanical influence of underground and surface off-channel waters on soluble and permeable rocks». Due to karst, voids of various shape and size are formed in the carbonate massif. The ancient karst (or paleokarst) played an important role in the formation of reservoir in carbonate oil and gas complexes of different ages. Franian isolated reefs of the Rybkinsky group, which are located in the south part of the Volga-Ural oil and gas province, within the territory of the Orenburg region, are one example of the mentioned value of the paleokarst. This paper provides new information on the manifestations of karst in these peculiar carbonate reservoirs. The article is a logical continuation of the review publication about the Rybkinsky reefs (Vilesov et al., 2019a).

[*]*Corresponding author: Aleksandr P. Vilesov*
E-mail: apvilesov@mail.ru

It should be noted that for the devonian sedimentary basins of Australia and Canada, where franian and famenian reefs are widespread, numerous factual data on ancient karst have been published (for example: Chow & Wendte, 2011; Playford, 2002; George & Powell, 1997; etc.). At the same time, this important part of the geology of devonian reefs remains a white spot for the Volga-Ural oil and gas province to date.

The first isolated franian reef of the Rybkinsky group with a high-amplitude oil pool (West-Rybkinsky reef) was discovered accidentally in 1990 during prospecting and exploration drilling on the terrigenous sandstone reservoirs of the Middle Devonian. Targeted searches led to the discovery nearby of another organic buildup with a oil pool – the North-Zhokhovsky reef (Nikitin et al., 2011). Reserves of opened oil pools were put on balance as part of the Rybkinskoye Oil Field. According to biostratigraphic studies, it was found that the formation of Rybkinsky reefs occurred in the Rechitsky and Voronezh time of the late Franian. Reefs overlap the upper franian – lower famenian carbonate-terrigenous-clay Colganian Formation. In 2012-2013 on the territory of the Volostnovsky licensed area, that includes the reefs of the Rybkinskoye Oil Field, «Orenburgneft» oil

company performed high-resolution three-dimensional (3D) seismic exploration. As a result, about 30 franian isolated basin reefs (similar to ones of the Rybkinsky Oil Field) were discovered and prepared for drilling (Nikitin et al., 2017, 2018). The height of the reefs varies from 180 to 220 m, diameter – from 0.6 to 1.5 km.

Drilling of reefs was carried out in 2015-2018. New oil pools are open both in reef reservoirs and in the famenian and tournesian carbonate deposits, covering the reefs.

Material

Within the Volostnovsky license area more than 20 productive isolated franian reefs (including ones of the Rybkinskoye Oil Field) have been opened by drilling already (Fig. 1). Core predominantly good quality with diameter 100 and 110 mm was taken from the reef path of section during well drilling. Franian reef at the Volostnovsky license area are characterized by the core unevenly, since the coring was performed mainly from the oil saturated upper part of the section or at separated intervals. Significant coring is made to individual reefs. In particular, continuous coring for more than 100 m was performed on Novozhokhovsky Reef (Shakirov et al., 2019). In total, studies of the core of reef facies were carried out on 19 carbonate buildup.

As a result of the sedimentological analysis of the core, the reconstruction of the history of the Rybkinsky group reefs was carried out, the facies reef zones were characterized, the groups of organisms building the reef and their distribution within reefs were established, the diagenesis off reef rocks was reconstructed (Vilesov et al., 2019a). In the reef section different scale cycles are highlighted and horizons of the subaeral exposure are established. The history of the development of Rybkinsky reefs was compared with the eustatic curve developed by a team of specialists from Moscow University for the Russian Plate (Alekseev et al., 1996). In the reef history were identified three stages, coinciding with three stages of regional sea level fluctuations – Domanikian, Rechitskian and Voronezhian. It has been established that the epochs of paleokarst are associated with the completion of each stage and periods of low sea level.

Tectonics of the Sol-Iletsky Arch had a significant impact on sea level changes during the late Devonian (Nikitin et al., 2013; Vilesov et al., 2019b).

Stratigraphic and tectonic position of the Rybkinsky reef group

The stratigraphic interval of Rybkinsky reefs corresponds to the Domanikian, Rechitskian and Voronezhian horizons (=Regional Stage) of the Franian Stage of the Upper Devonian (Vilesov et al., 2019a). In 2015, a section of the Rybkinsky reefs was allocated to the Rybkinskian formation (Fortunatova et al., 2015). In 2017 the Rybkinskian formation was introduced into the unified subregional stratigraphic scheme of the Upper Devonian of the Volga-Ural subregion (Unified subregional stratigraphic scheme…, 2018). The Rybkinskian formation is underlain by the thin limestone units of the Sargaevian formation. It is covered by carbonate-terrigenous-clay deposits of the Colganian formation and replaced by that to the lateral. The clay rocks of the Lower Famenian, which form a seal over franian deposits edging the Sol-Iletsky arch, are also part of the Colganian formation.

In tectonic terms, the area of the Rybkinsky reef group is located in the joint zone of the Rubezhinsky Trough, Sol-Iletsky Arch and Pavlovskaya Saddle (Nikitin et al., 2011). The reefs of the Rybkinskoye Oil Field together with the Zhokhovsky reef are located on the Devonian tectonic flexure, oriented according to the sedimentation bench of the late franian carbonate platform in the northwestern part of the Volostnovsky license area (Fig. 1). Most of the reefs located between flexure and sedimentation bench form subparallel lines. It is possible that these reefs are also controlled by low-amplitude tectonic breaks.

Paleogeographic position of the Rybkinsky reef group

The area of distribution of Rybkinsky reefs in paleogeographic terms is confined to the northeastern shelf edge of the paleocontinent Laurussia (Fig. 2). As can be seen on the palinspathic map of C.Scotese (2014), this part of the continental shelf in franian time was in the equatorial zone of the northern hemisphere. Other palinspathic reconstructions give a similar paleogeographic position (for example: Orenburg tectonic…, 2013; Golonka, 2002; and others).

The equatorial climatic zone is characterized by high temperatures, heavy rainfall, and high humidity. All these factors are favorable for the intensive development of karst in carbonate deposits brought to the conditions of the subaeral exposure (Moor, 2001; Wilson, 2012).

Isolated basin reefs of the Leduk Formation of Western Canada (Atchley et al., 2006; Switzer et al., 1994; and other) are similar age analogues of Rybkinsky reefs. They were also formed in the equatorial zone, only on the western shelf margin of Laurussia.

Facial structure of Rybkinsky reefs

During sedimentological analysis of core of Rybkinsky reefs facial complexes of the reef core and reef slope, as well as zones of karst and hydrothermal karst manifestations, were identified (Vilesov et al., 2019a). Signs of ancient karst (paleokarst) and hydrothermal karst cross the rocks of the facial complexes of the reef core and reef slope.

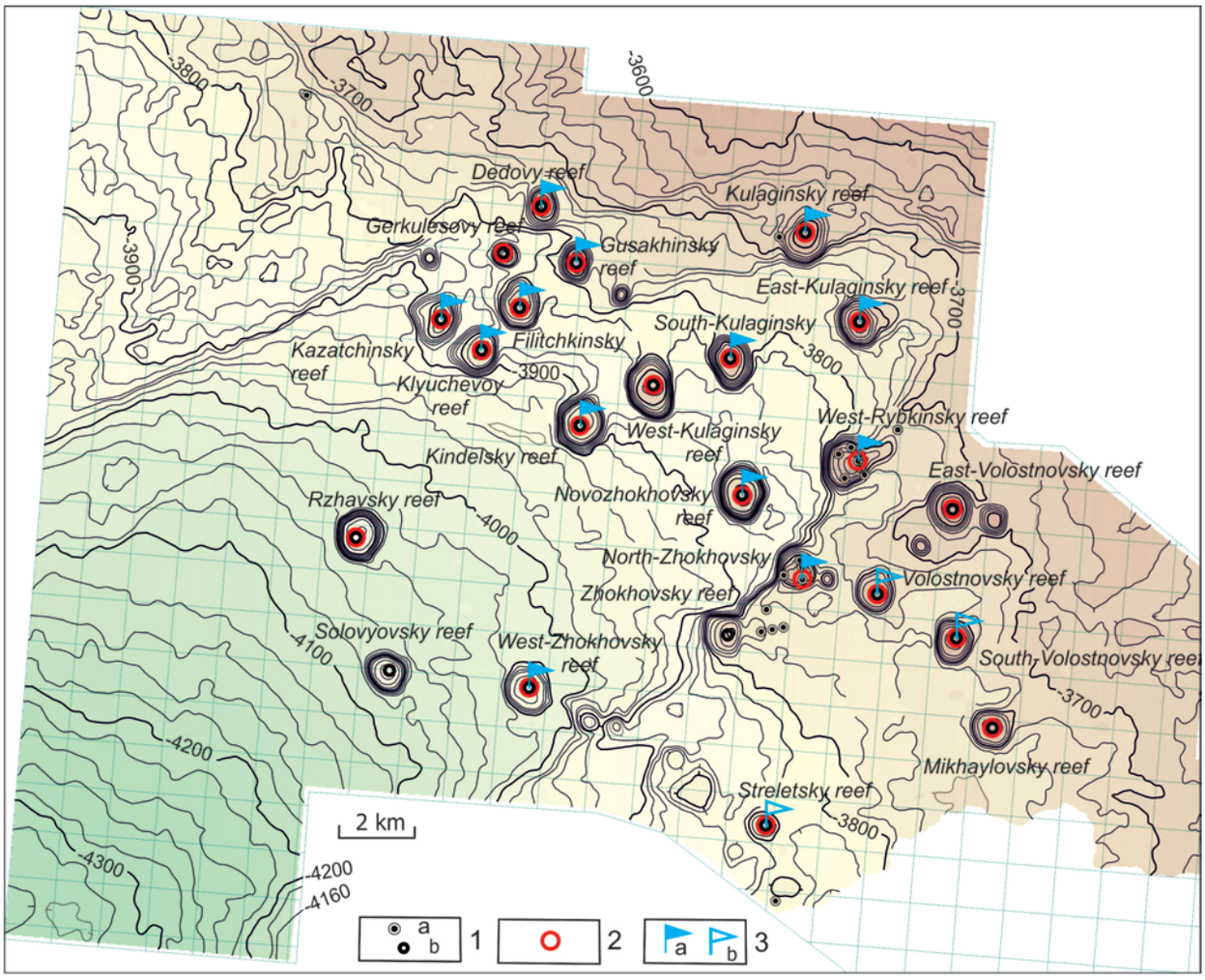

Fig. 1. Rybkinsky group of franian reefs: structural map on the surface of the Voronezhian regional stage (Nikitin et al., 2017). 1a – old wells, 1b – wells drilled in 2015-2018; 2 – reefs with signs of surface karst and deep karst in the core; 3 – reefs with signs of hydrothermal karst in the core (a – intense, b – weak)

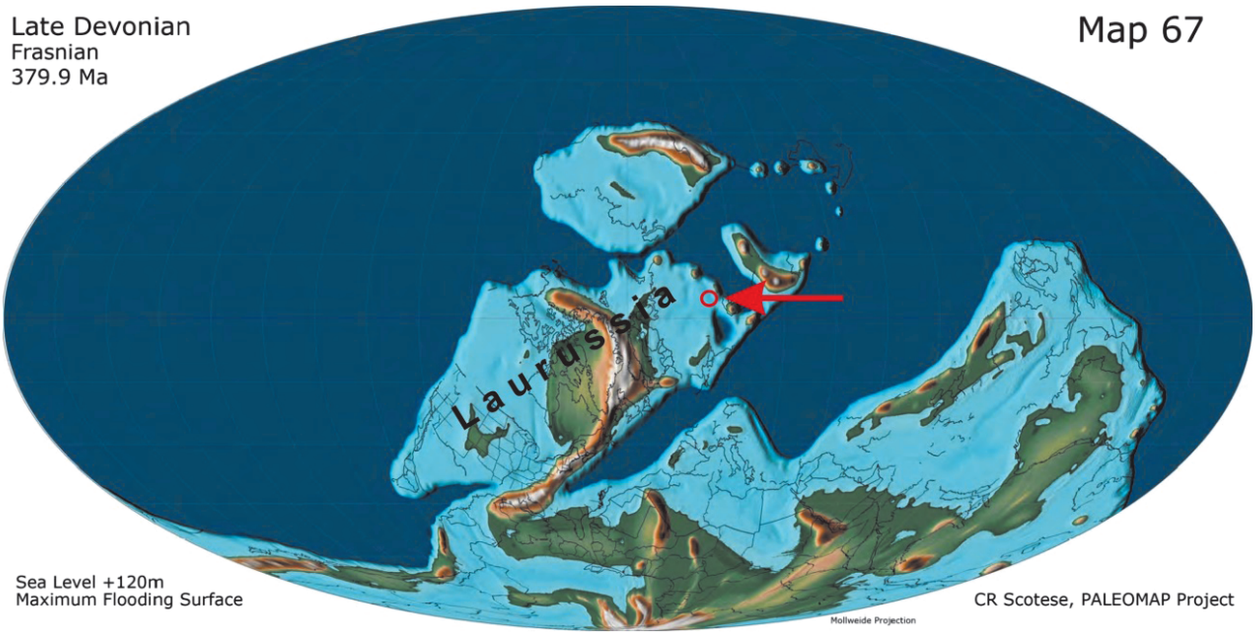

Fig. 2. Paleogeographic map of the franian time of the Devonian period on a palinspatic basis (Scotese, 2014). The area of the Rybkinsky reef group is shown by a red circle and arrow

According to lithological features, the following facies are distinguished ***in the facial complex of the reef core***: 1) the ridge zone of the reef; 2) the back-reef zone; 3) reef shallow subtidal zone; 4) up-reef tidal flat; 5) reef lagoon. Massive, tabular and combined skeletons of stromatoporoids, forming a strong framework resistant to wave influence, are characteristic for rocks of the ridge zone of the reef. Large stromatoporoids with a combined mushroom-like skeleton and abundant microbial fouling are most typical for limestones of the back-reef zone. Numerous thick-branched stromatoporoids are found in the limestone of reef shallow subtidal zone; various skeletal grains are distributed among their skeletons. The rocks of the up-reef tidal flat are represented by different-grained limestones with a texture from grainstone to rudstone. The facies of the reef lagoon are characterized by mad limestones with dispersed bioclastic material.

Due to karst, the different-age parts of the reef core are connected into a integrated hydrodynamic system. Limestones in the reef core zone are chemically pure. The appearance of impurities (for example, clay minerals, quartz) is due to their injection through the karst voids system.

The facial complex of the reef slope is divided into two facies: the upper part of the reef slope and the lower part of the reef slope.

The facies of the upper part of the reef slope are divided into the following subfacies: 1) biogerms of the upper part of the slope; 2) granular deposits of the reef apron of the upper part of the slope; 3) carbonate debrites of the upper part of the slope; 4) ladge syndepositional fracture of reef margin – neptunian dyke.

Biogermal rocks of the upper part of the reef slope are characterized by lamellar and leaf-shaped forms of frame-forming organisms – stromatoporoids, corals, and hydroids.

Granular deposits of reef apron are represented by different-grained limestones with the texture of rudstone, grainstone, packstone, floatstone. Carbonate grains are diverse: lithoclasts, bioclasts, cortoids, peloids. Skeleton fragments of echinoderms and thick-branching stromatoporoids dominate among other bioclast grains. Granular deposits of the reef apron reach a maximum length and thickness in the rear (leeward) part of the reefs and can form a significant part of the reef complex (Vilesov et al., 2019a).

Carbonate debrites of the upper part of the slope are represented by breccias and conglomerates with a different-grained carbonate matrix. The size of the debris varies from small rubble to blocks in the first tens of centimeters. The most typical texture of debris are stromatoporoid and coral boundstone. The texture of the matrix containing the debris varies from wackestone to different-grained rudstone.

In the matrix of debrites crinoid fragments predominate among other bioclasts. In some cases, the distribution of debris in the bed sequence is gradational: large debris at the bottom, small debris at the top, and contact with the underlying bed is erosive.

Neptunian dyke subfacies of the reef slope has been diagnosed in several reef buildings. The visible length of dykes in the core reaches 1.5 m. The walls of the dykes are relatively even, inclined, formed by the bedrocks of the reef slope. The sediments filling the dykes differ sharply in structure from the containing bedrock subjected to break. Different-grained limestones from packstones to rudstones and limestone breccias are distinguished in dyke filling. In some cases, one can observe distinct vertical zonality in the filling of dykes, which is expressed in the form of a noticeable enlargement of grains from top to bottom or a change of texture from granular to breccia. Significant signs of karst can be traced along neptunian dykes.

The rocks of the upper reef slope, like the rocks of the facial complex of the reef core, are characterized by chemical purity.

The facies of the lower part of the reef slope are represented by detrital clay limestones to varying degrees dolomitic, with an uneven admixture of insoluble sediment (clay mineral, quartz and feldspar grains from silt to thin sand dimension, pyrite). Clay limestones can pass into marls with interlayers of calcareous claystones. The predominant texture of limestones is a different-grained floatstone. The clay-carbonate matrix of floatstones is unevenly dolomitic; various bioclasts and carbonate lithoclasts are included in it.

Karst of Rybkinsky reefs

According to the main dissolution agent, *meteoric water karst* and *thermal water karst* (hydrothermal karst) were identified in reef rocks. In the first case, the dissolution of carbonate rocks occurred due to filtration into reef arrays of atmospheric precipitation. In the second case, hot deep waters enriched with a specific complex of dissolved chemical elements affected reef rocks.

In relation to the terrestrial paleo-surface, meteoric water karst can be divided into surface and deep karst. Surface karst (or epikarst) is manifested at exposure surfaces of reefs and is represented by such characteristic morphological karst forms as ponors and karren. Deep karst (or subsurface karst) crosses a significant interval of the reef section. It was formed in the zone of vertical percolating of fresh waters, as well as along the surface of the fresh water mirror and below it, up to the zone of mixing with sea pore waters. Caves are the most significant morphological forms of the deep karst.

Surface karst

Attributes of surface karst (Fig. 3) was observed at or beneath subaerial exposure unconformities. In Rybkinsky reef sections three such levels have been identified: 1) top of the Domanikian regional stage; 2); top of the Rechitskian regional stage; 3) top of the Voronezhian regional stage (Table 1).

Features of surface karst are most fully represented on well core in the upper part of the Voronezhian regional stage. Limestones from this stratigraphic interval were coring on twelve reefs. In all cases, sharp lithological contact can be observed in the core: gray and dark-gray clay silt-sandstones of subtidal with small brachiopods and trace fossil Zoophycos lay on eroded light-gray limestones of the reef complex (Fig. 3a, b, e). In the western part of the area, silt-sandstones are replaced by dark-gray clay-silt limestones with a texture of bioclastic floatstone. Skeletons of thin-branched rugosa and stromatoporoids, shell of brachiopods, echinoderm detritus are unevenly distributed in the microcrystalline calcite matrix of floatstones.

Morphological varieties of surface karst are represented by karren and ponors. *Karren* are furrows on the surface of reef limestones (Fig. 3b), *ponors* are small funnels or tubular recesses on it (Fig. 3a, e). Ponors are filled with terrigenous-clay material (Fig. 3a). A breccia-like detachment of the bedrock can be observed along their walls. The visible width of ponors can reach 5-6 cm, depth – 0.5-1.5 m.

The facts about surface karst features of different stratigraphic levels and different reefs recorded on the well core are given in Table 1.

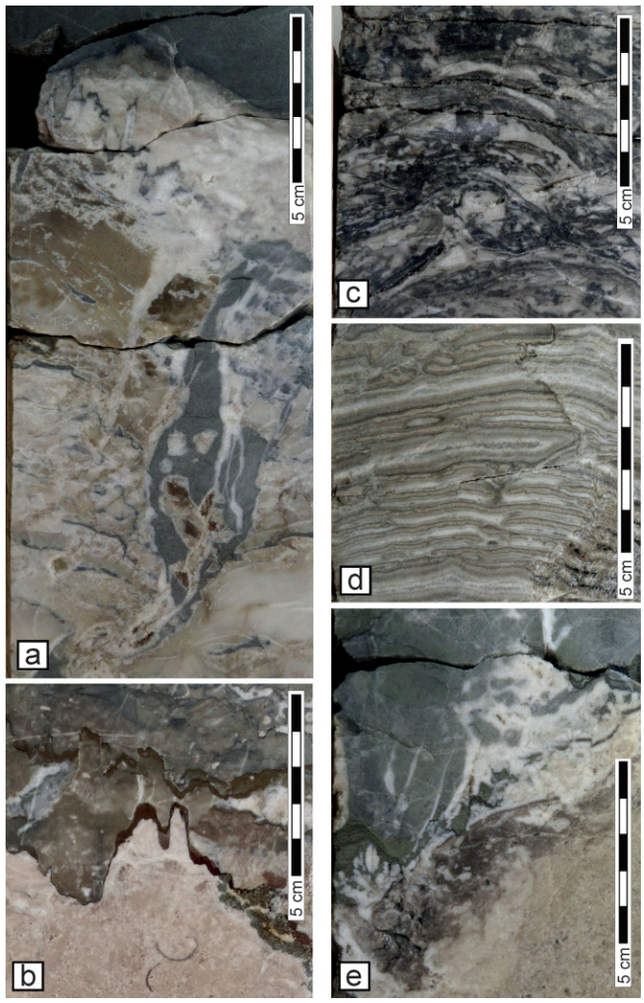

Fig. 3. Features of epikarst in the reefs of the Volostnovsky license area: a – narrow funnel-shaped ponor at the top of voronezhian reef limestones (Novozhokhovsky reef); b – karren on the surface of reef limestones of the Voronezhian regional stage (Gusakhinsky reef); c – limestones of the palaeosol (top of the Rechitskian regional stage, Streletsky reef); d – microbial tuff limestones of the karst-water unloading zone (Streletsky reef); e – large funnel-shaped ponor at the top of voronezhian reef limestones (East-Kulaginsky reef).

Deep karst

Deep karst was diagnosed in the well core for 22 reefs. According to the available material, various forms of subsurface karst for the Rechitskian and Voronezhian intervals are identified (Table 2; Fig. 4). In particular, caves were identified in the well core, which are characteristic morphological varieties of deep karst. Systems of small karst cavities and karst fracture are associated with caves. Deep karst forms and features are located significantly lower than installed surfaces of subaeral exposure.

The width of *karst caves* significantly exceeds the diameter of the core, their height varies from 0.1 to 4.0-7.5 m. The largest paleokarst caves were found in the core of the East-Volostnovsky, Kindelsky and East-Kulaginsky reefs (Table 2). These caves are filled with sandy, silt-clay and clay dolomite, in which angular blocks of reef bedrocks are found. Natural localization of coarse angular fragments of the collapse breccia to the lower part of caves is observed. Clay and terrigenous material at the stages of sea level falling and sea level lowstand (LST) in significant volumes was carried by rivers from Sol-Iletsk island to Rubezhinsky Trough. At the stages of sea level rise, these precipitation was redistributed by wave processes and through systems of vertical karst voids fell into cavities formed by deep karst. The increased content of terrigenous and clay material in the filling of karst voids is most characteristic of the Voronezhian part of the reefs.

Intervals of caves in wells are diagnosed by the gamma-ray log (GR) based on increased natural radiation.

Karst cavities reach a width of 5-10 cm. They are quite common in reef section, have different shapes and, as a rule, are accompanied by fractures. Systems of cavities associated with fractures can be often observed. Cavities can be filled with clay dolomite,

Reef	Top of the Voronezhian regional stage	Top of the Rechitskian regional stage	Top of the Domanikian regional stage
Rybkinsky	terrigenous sediments lie with erosion on frame limestone	-	-
Novozhokhovsky	karren and ponors, filled with clay silt-sand material	karren fracture, wedging down and filled with clay dolomite	-
Volostnovsky	-	-	limestone breccia
Kulaginsky	small karren corroded with stylolites	dolomite breccia	-
South-Volostnovsky	gentle karren	-	-
Mikhaylovsky	coarce clast limestone breccia	-	-
South-Kulaginsky	small karren, brecciated limestone	coarce clast carbonate breccia	coarce clast carbonate breccia
East-Kulaginsky	funnel-shaped ponor, passing down into a large karst cavity filled with dolomite breccia and sand-silt dolomite	-	-
Kazatchinsky	terrigenous sediments lie with erosion on frame limestone	-	-
Klyutchevoy	small karren, almost vertical fractures with carbonate-clay filling	small karren	-
Rzhavsky	terrigenous sediments lie with erosion on frame limestone	-	-
West-Zhokhovsky	-	coarce clast carbonate breccia	-
Gusakhinsky	deep karren (до 5 sm)	-	-
Gerkulesovy	small karren	-	-
Streletsky	-	carbonate palaeosol with rhizoliths, microbial tuffs of karst water unloading zone	-

Table 1. Features of surface karst and subaeral exposure surfaces of franian reefs of the Rybkinsky group diagnosed on the well core

clay-silt sandstone, carbonate rubble in clay-dolomite and silt-sand-dolomite matrix. The walls of the cavities are uneven, corroded; at contacts with the bedrock, large-toothed and large-amplitude stylolitization is often developed. Slit-like karst cavities with a width from 2-5 mm to 3-6 cm are quite common in well sections.

Karst fractures have a variable width and shape. They are filled with carbonate rubble, clay dolomite, clay silt-stone. Systems of elongated vugs, karst cavities are often developed along karst fractures.

A specific group of karst fractures, coupled with a system of almost vertical neptunian dykes, has been identified in the slope zone of reefs. Such fractures developed along the contacts of the reef bedrock and the various granular filling of dykes.

Within reefs, karst zones form areas of increased permeability, since almost always voids, even with dense filling, are accompanied by systems of open fractures and microfractures. Later hydrothermal karst textures intersects often the systems of paleokarst fractures and cavities (Fig. 4a), complicating significantly the pore space of reservoir and increasing its capacity. In cases of intense properties of hydrothermal dolomitization, signs of the preceding deep karst cannot be diagnosed practically.

The formation of the secondary dolomite zone according to the model of mixing meteoric and sea pore waters is an important result of the development of deep karst. This conclusion was made based on the results of the study of the West-Rybkinsky and North-Zhokhovsky reefs (Vilesov et al., 2013). The interval of secondary different-crystal dolomites with increased porosity and permeability is located 60-70 m below the top of the Voronezhian part of the reefs. The thickness of the dolomite units varies from 10-12 to 15-18 m. The pore space in the dolomites of the mixing zone is represented by numerous intercrystalline pores, molds (by dissolved fossils) and wugs (leaching caverns).

Hydrothermal karst of Rybkinsky reefs

Hydrothermal karst (or hydrothermokarst) refers to the process of leaching rocks with heated solutions with the formation and subsequent filling of cavities (Maksimovich, 1969; Dublyansky, 1985; etc.). In carbonate rocks, hydrothermal karst can be accompanied by intense dolomite metasomatosis. One of the models

Reef	Voronezhian regional stage	Rechitskian regional stage	Domanikian regional stage
West-Rybkinsky	karst fractures	-	-
North-Zhokhovsky	karst fractures with systems of small cavities filled with clay dolomite	-	-
Rybkinsky	inclined karst fractures with systems of cavities partially filled with terrigenous-clay material	-	-
Novozhokhovsky	inclined fractures of various widths; a system of fractures and various cavities, filled with silt-clay and carbonate-clay material, carbonate rubble	small karst cavities filled with carbonate rubble in clay-carbonate matrix	-
East-Volostnovsky	karst cave 17 m from the surface; height more than 5 m; cave filling – dolomite rubble and dolomite breccia, silt-clay-dolomite material	-	-
Volostnovsky	inclined fractures of various widths filled with silt-clay and carbonate-clay material	almost vertical and inclined fractures of various widths, filled with silt-clay, clay-dolomite material and carbonate rubble	inclined tortuous fractures of various widths filled with silt-clay-dolomite material
Kulaginsky	diverse in width inclined fractures with dolomite and dolomite-clay filling; cavities with clay filling; subhorizontal cave up to 30-50 cm high with layered dolomite filling and angular carbonate fragments	almost horizontal and inclined cavities up to 30 cm high with carbonate breccia in clay and dolomite-clay matrix	-
South-Volostnovsky	diverse almost vertical and inclined fractures, small cavities with sand-silt-clay, dolomite-clay and calcite filling; rare almost horizontal cavities with carbonate breccia	-	-
Mikhaylovsky	inclined fractures with dolomite-clay and sand-silt-clay filling; inclined cavities filling with carbonate block and rubble in dolomite-clay matrix	caves up to 2 m high, filled with dolomite breccia; extended inclined karst slot-like cavities along neptunian dykes with carbonate rubble filling	-
West- Kulaginsky	inclined karst fractures with clay-dolomite filling	-	-
South-Kulaginsky	almost vertical tortuous fractures with crystalline calcite and dolomite filling; almost horizontal and inclined cavities with dolomite breccias; single cavities filled with anhydrite	-	-
East-Kulaginsky	karst caves from 2.0 to 3.5 m (or more) high, filled with different block dolomite breccia	cave up to 0.5 m high, filled with dolomite breccia with dolomite-clay matrix	-
Kindelsky	a system of karst caves from 1 to 8 m high, filled with dolomite breccias, dolomite conglomerates, lithoclastic floatstone and dolomadstone	-	-
Kazatchinsky	inclined karst fractures with systems of small cavities filled with dolomite-clay material	-	-
Klyuchevoy	inclined and almost vertical fractures with variable width filled with different crystalline dolomite	-	-
Rzhavsky	vertical karst fractures with systems of small cavities	-	-
Filichkinsky	rare isometric cavities with clay-dolomite filling	-	-

Table 2. Features of deep karst diagnosed on the well core of franian Rybkinsky reefs

West-Zhokhovsky	complex system of almost vertical fractures and fracture cavities	a system of numerous almost vertical fractures, cavities and caves (from 0.5 to 1.5 m high). Filling - clay and clay-dolomite material. In large cavities and caves - broken fragments of reef bedrock	-
Gusakhinsky	small karst cavities and fractures filled with carbonate crushed stone, dolomite and anhydrite	-	-
Dedovy	large karst cavities filled with carbonate breccia and clay dolomite	a system of cavities filled with clay dolomite	-
Gerkulesovy	small karst cavities filled with clay dolomite	-	-
Streletsky	karst cavities up to 12 cm high with clay-dolomite filling	-	-

Table 2. Continuation. Features of deep karst diagnosed on the well core of franian Rybkinsky reefs

for the formation of secondary diagenetic dolomites is called hydrothermal (Warren, 2000).

Secondary dolomites of Rybkinsky reefs formed as a result of hydrothermal karst are unevenly found in section and area (Table 3; Fig. 1, 5). Signs of hydrothermal metasomatosis in individual reefs are recorded in intervals with a continuous vertical length of more than 30 m (for example, in the upper part of the South-Kulaginsky and West-Rybkinsky reefs). In other reefs, signs of hydrothermal exposure occur at frequent intervals of variable thickness (from 1-2 to 6-12 m) throughout the reef section. In the third group of reefs, hydrothermal karst is found in rare and small areas, or not diagnosed at all in the core. It should be noted that the signs of hydrothermal karst are installed in the core only from Voronezhian and Rechitskian intervals of reef sections (Table 3).

Rocks formed as a result of hydrothermal karst are represented by multicrystalline dolomites with characteristic features: saddle-shaped crystals, zebroid and spotted color, the development of crystalline veins, complex fracture systems with coarse crystal inlays, uneven development of the ore iron sulfide (in the form of crystalline veins and pyrite inclusions). The primary texture of reef rocks subjected to hydrothermal metasomatosis is often not preserved practically.

The hydrothermal nature of secondary dolomites is confidently diagnosed according to the results of laboratory geochemical studies by the method of X-ray fluorescence analysis: in coarse crystalline secondary dolomites of Rybkinsky reefs the content of manganese and iron is increased (Fig. 6a, b), that is typical for dolomites of the hydrothermal model (Warren, 2000). Strontium content in dolomites is reduced compared to slightly modified limestones (Fig. 6c).

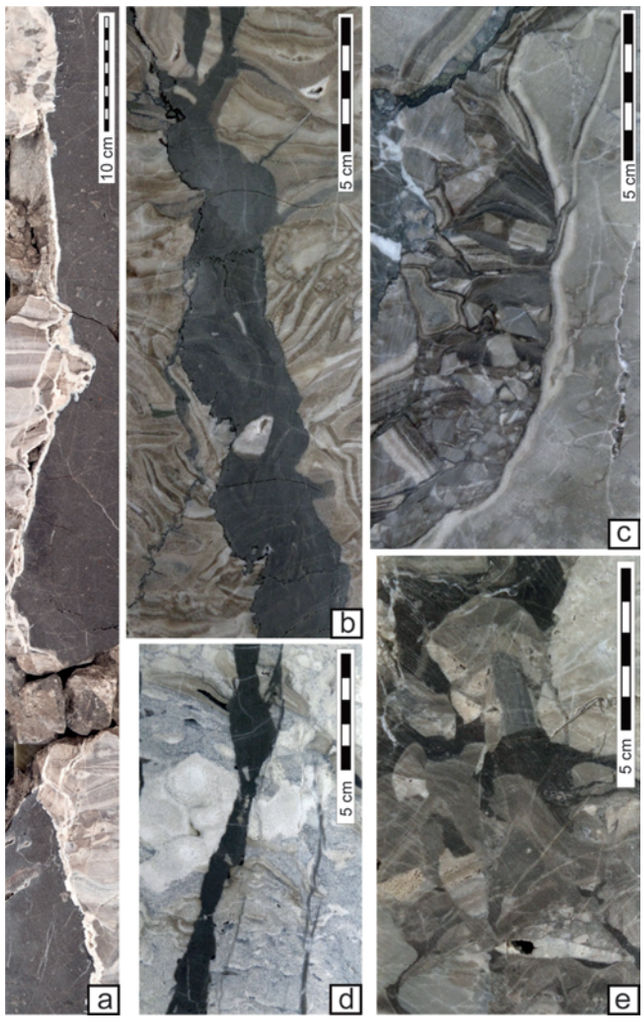

Fig. 4. Deep karst in the reefs of the Rybkinsky group: a - a cave filled with dark-gray clay microcrystalline dolomite; along the walls of frame limestones are the veins of hydrothermal dolomite (Kindelsky Reef, Voronezhian regional stage); b – inclined slit-like karst cavity in frame stromatoporoid limestone filled with clay dolomite (Volostnovsky reef, Rechitskian regional stage); c – karst cavity filled with carbonate rubble (Kulaginsky reef, Voronezhian regional stage); d - slit-like karst fracture in bioherm limestone of reef slope with clay-dolomite filling (West-Zhokhovsky reef); e – limestone collapse breccia of the bottom part of the karst cave (Kindelsky reef, Voronezhian regional stage)

Reef	Voronezhian regional stage	Rechitskian regional stage
West-Rybkinsky	coarce crystalline dolomites with saddle-like crystals	-
North-Zhokhovsky	spotted dolomitization zones with large dolomite crystals; extended inclined fractures inlaid with saddle crystalline dolomite and pyrite	-
Rybkinsky	numerous inclined fractures with inlays of coarse crystal saddle dolomite	-
Novozhokhovsky	beds of multicrystalline dolomites with thickness from 1-2 to 5-6 m distributed unevenly along the section; saddle-like crystals; uneven incrustation by pyrite	frequent units of different crystalline dolomites with a thickness of 0.5 to 3.0 m and with saddle-like crystals; uneven pyritization, including as crystalline veins
Volostnovsky	rare saddle crystals of dolomite along the walls of vugs	-
Kulaginsky	crystalline veins of saddle dolomite with pyrite	various crystalline veins of saddle dolomite with pyrite; units of secondary multicrystalline dolomites up to 1.5 m thick
South-Volostnovsky	rare saddle crystals of dolomite along the walls of vugs	-
South-Kulaginsky	intensive dolomitization along the section; units of multicrystalline dolomites with a thickness of 6 to 11 m; saddle dolomite forms various crystalline veins and inlays fractures; uneven pyritization, including as crystalline veins	saddle dolomite is developed in the form of crystalline veins and incrustations along fractures; pyrite meets with him
East-Kulaginsky	intensive dolomitization in the upper part of the reef, units of multicrystalline dolomites up to 4 m thick; saddle dolomite is represented in the form various crystalline veins, it inlays extended fractures; uneven pyritization across dolomites	-
Kindelsky	intensive dolomitization; units of multicrystalline dolomites from 2 to 4 m thick; saddle dolomite is represented in the form crystalline veins, it inlays fractures; pyritization is unevenly distributed among dolomites	-
Kazatchinsky	white coarse crystal saddle dolomite forms crystalline veins along karst fractures	-
Klyuchevoy	intensive dolomitization throughout the sections in the form of crystalline veins of saddle dolomite, inlays on fractures and vugs; uneven pyritization, including in the form of pyrite veins	-
Filitchkinsky	intensive dolomitization throughout the sections; units of multicrystalline dolomites from 2 to 7 m thick; saddle dolomite is represented in the form crystalline veins; it, together with pyrite, is distributed among extended fractures	-
West-Zhokhovsky	units of multicrystalline dolomites up to 6 m thick; saddle dolomite is represented in the form crystalline veins; together with pyrite, it is distributed to various directed fractures	units of multicrystalline dolomites reach a thickness of up to 1 m; saddle dolomite forms crystalline veins and inlays multi-directional fractures
Gusakhinsky	units of multicrystalline dolomites from 0.3 to 1.2 m thick; saddle dolomite forms crystalline veins and inlays fractures and vugs; there are usually veins of ore pyrite along the section	-
Dedovy	intensive dolomitization along the section with units dolomites with zebra-structures; saddle dolomite forms extended tortuous crystalline veins, inlays fractures	uneven dolomitization along the section; white saddle dolomite forms tortuous crystalline veins
Streletsky	rare fractures with inlays of coarse crystal saddle dolomite and pyrite	-

Table 3. Features of hydrothermal karst diagnosed on the well core of Rybkinsky reefs

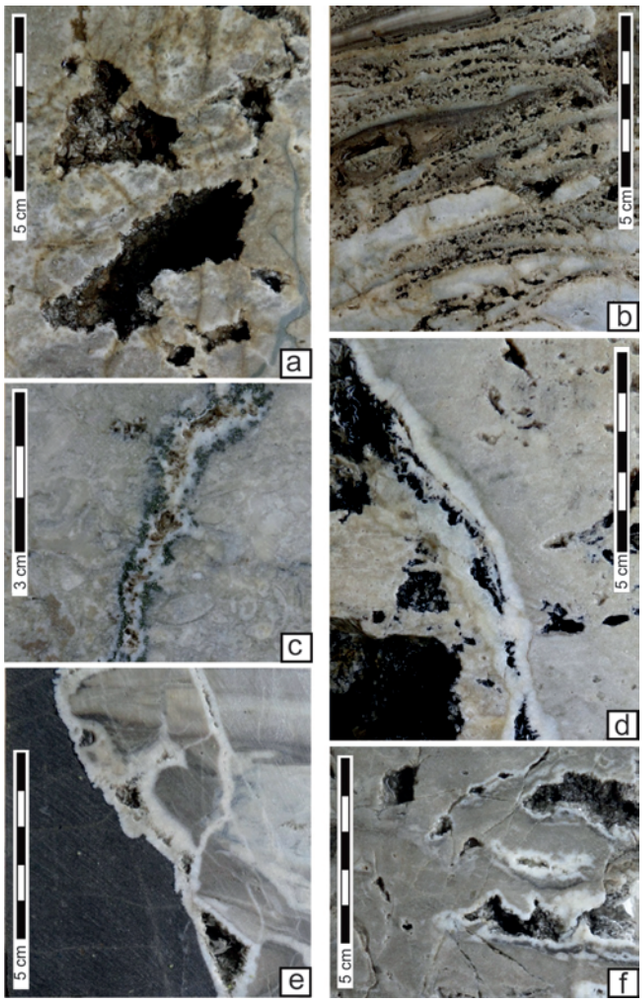

Fig. 5. Hydrothermal karst on Novozhokhovsky (a, b, c), South-Kulaginsky (d), Kindelsky (e) and West-Zhokhovsky (f) reefs: a – zebra-structures of secondary large-crystal dolomite with a system of vugs, cavities and microfractures; b – secondary multicrystalline hydrothermal dolomite with relics of stromatoporoid skeletons; c – crystalline dolomite vein with a chain of vugs and a pyrite fringe; d – secondary dolomite with large cavities and vugs, with coarse-crystal saddle dolomite; e – crystalline vein of large-crystal hydrothermal dolomite along the walls of the karst cave; f – zebra-structures of hydrothermal dolomite with a system of cavities, vugs and fractures.

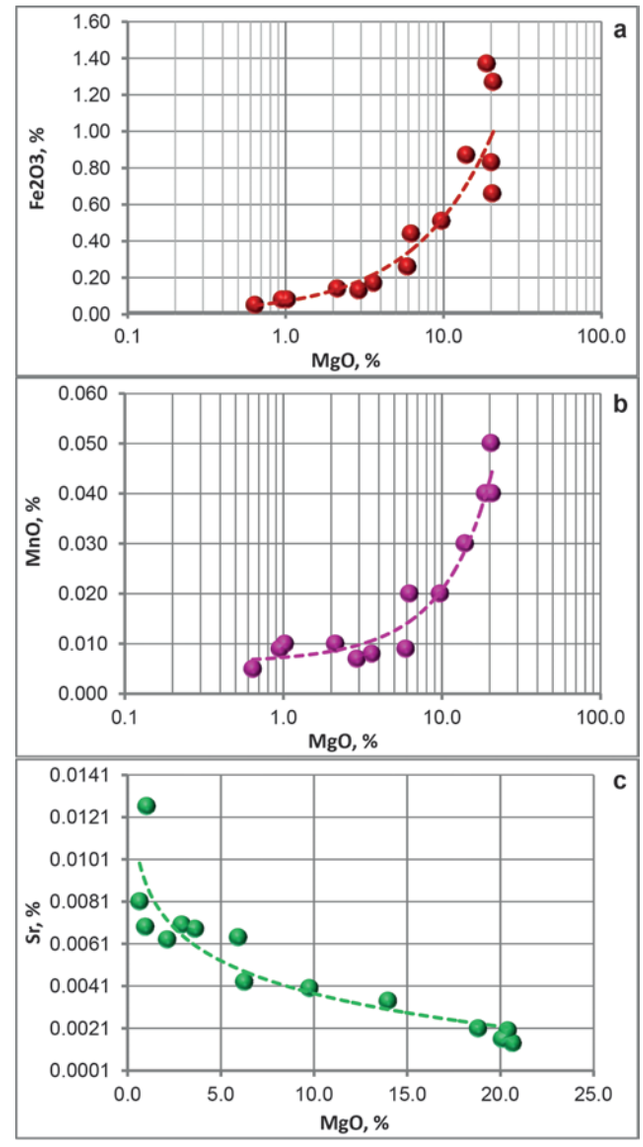

Fig. 6. Connection of individual chemical elements content with the intensity of hydrothermal dolomitization (using the example of rocks of the West-Zhokhovsky reef): a – Iron; b – Manganese; c – Strontium

Hydrothermal karst developed most strongly along the primary permeable rocks of the paleokarst zones. Therefore, combining two different forms of diagenetic changes is quite usual. The features of hydrothermal karst are especially characteristic of reefs located within linear zones. For example, hydrothermokarst is recorded at the core of all wells in the linear zone of Klyuchevoy reef – Filitchkinsky reef – Gusakhinsky reefs (Fig. 1). He was diagnosed in the linear zone of the Kindelsky reef – West-Kulaginsky reef – South-Kulaginsky reef. Hydrothermal karst is not fixed within separate reefs located outside pronounced linear zones (for example, in the Mikhailovsky and Gerkulesovy reefs). At the same time, it was very intensively formed in the section of the Novo-Zhokhovsky reef, which is located in the linear zone of another direction: Gusakhinsky reef – West-Kulaginsky reef – Novozhokhovsky reef – North-Zhokhovsky reef (Fig. 1).

Limestones of the franian reefs within the Volostnovsky license area underwent hydrothermal diagenesis in post-franian times, much later than the sedimentation stage. The replacement of limestones with secondary dolomites was caused by the rise and filtration into reef massifs of hot deep waters enriched with magnesium and iron ions.

Rocks subjected to hydrothermal diagenesis are characterized by the development of a system of the most diverse voids (intercrystalline pores, vugs, fractures, cavities) and, accordingly, the most complex structure of the pore space. Hydrothermal voids, unlike paleokarst ones, that usually filled with products of destruction

of bedrocks and introduced material (clay dolomite, clay silt-sandstones, etc.), remained largely empty. Their walls are unevenly inlaid with coarse crystalline dolomite, pyrite and more later in crystallization time sulfates. However, fully filled hydrothermal cavities are much less common than paleokarst ones.

Reef rocks that have experienced hydrothermal metasomatosis are almost always complex highly productive fracture-vug and fracture-vug-pore reservoirs. The thickness of the units of secondary highly porous dolomites in the reef section can reach 15-30 m, and in some cases 50-60 m.

Karstic epochs in the development of Rybkinsky reefs

In the history of the formation of Rybkinsky reefs, three epochs of surface and deep karst (hypergenesis) can be distinguished. They are associated with periods of significant falls in sea level, caused both by eustatic fluctuations and the influence of inversion tectonic processes in the Sol-Iletsky Arch area.

The first epoch of paleokarst (Later Domanikian). At the end of Domanikian time, as a result of a significant decrease in sea level (Alekseev et al., 1996), Rybkinsky reefs underwent weathering and karst. Carbonate breccia horizons are observed at this level in the core. Mosaic carbonate platforms framing the Sol-Iletsky island from the north were also subjected to Late Domanikian karst and weathering (Vilesov et al., 2019b).

The second paleokarst epoch (Late Rechitskian) is associated with a significant regional falling of sea level at the end of the Rechitskian time. It was mainly caused by tectonic processes in the Sol-Iletsky Arch zone (against the background of a global eustatic rise). In the reefs of the Rybkinsky group, a second level of paleokarst is formed with a various karst fractures, cavities and caves. The karst water unloading zone with characteristic tuff-like microbialites was identified in the well core of the Streletsky Reef (Fig. 3d).

The third paleokarst epoch (Late Voronezhian) is associated with a significant global falling of sea level at the end of Voronezhian time (Alekseev et al., 1996; Johnson et al., 1985). Numerous and various signs of the late Voronezhian karst are revealed in reef sections: karst relief of the reef surface with karren and ponors, systems of karst cavities and caves with collapse breccia, karst fractures, vug zones. Intensive supply of terrigenous-clay material and its introduction by karst voids into reef buildings is characteristic of the third stage. An important feature of the third karst epoch is the formation of secondary dolomitization zones in reef reservoirs according to the mixing model (Vilesov et al., 2013).

Late Voronezhian and Late Rechitskian karst epochs are comparable to each other in the scale of karst manifestations. An important difference between them is the more significant presence of clay-terrigenous impurities in the filling of karst voids of Late Voronezhian karst.

Formation of the Rybkinsky reefs did not resume after the Late Voronezhian karst epoch. Layered subtidal carbonate-terrigenous-clay sediments deposited on reefs at the stage of Evlanovian transgression. Siliciclastic sediment, which was discharge from Sol-Iletsky island, played the role of an important limiting factor for the development of highly organized groups of frame builders. It is possible also that the Late Franian crisis in marine ecosystems was an equally important reason for the cessation of reef formation (Copper, 2002).

The development of hydrothermal karst in the reefs of the Rybkinsky group falls on the post-franian time. It is possible that it is associated with the intense block movements of the Sol-Iletsky Arch at the turn of the Franian and Famenian centuries. Taking into account the fact that there are no signs of hydrothermal karst at the well core higher in the section (in famenian and tournesian limestones), this time limit of hydrothermal activation is most likely.

Karst reservoirs of Rybkinsky reefs

Thus, complex karst reservoirs of Rybkinky reefs were formed as a result of three stages of hypergenesis, as well as the later period of hydrothermal karst. Various secondary voids, such as vugs, fracture, cavities and caves, were formed during periods of development of surface and deep karst (hypergenesis stages) as a result of atmospheric water filtration through carbonate reef massifs. Large paleokarst voids (caves and cavities) were filled with products of destruction of reef bedrocks, as well as clay-terrigenous sediments discharged from Sol-Iletsk land. Hydrothermal karst processes developed in reef massifs following karst permeable zones. Unlike large karst voids, hydrothermokarst cavities were only partially filled with newly formed minerals

Karst reservoirs of Rybkinsky reefs are characterized by a complex structure of pore space. Voids are presented by all variety – pores, vugs, fractures, cavities, caves. The high complexity of the pore space of karst reef reservoirs can be observed especially clearly from images obtained by X-ray computed tomography on an entire core column (Fig. 7).

Systems of oriented fractures (Fig. 7a, h), cavities connected by fractures (Fig. 7b, c, e), areas with multiple vugs (Fig. 7d, g), the directed systems of the touch-vug channels (Fig. 7f), a system of vugs connected by a porous matrix (Fig. 7i) can be diagnosed on tomographic sections. In fact, due to the presence of large voids and fractures, the well core from the intervals of karst reservoirs cannot be studied by standard methods in the petrophysical laboratory. Standard size samples (small core plug 30 mm/1 inch in diameter) may be made in

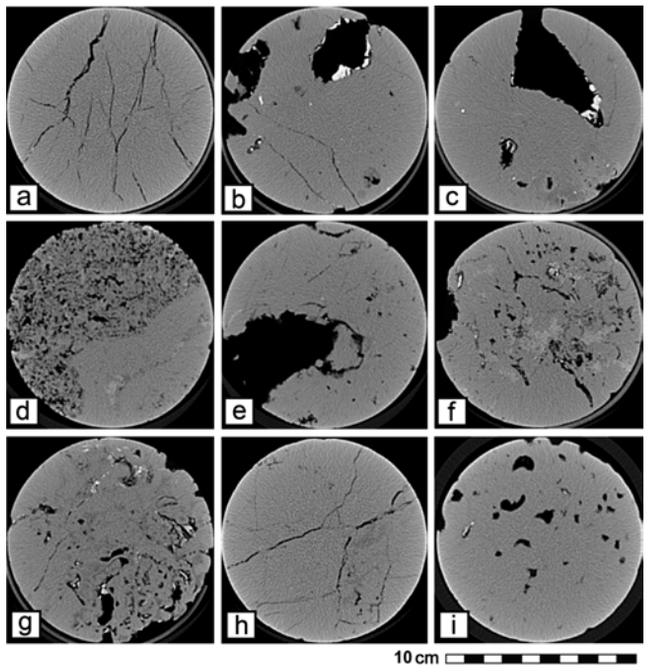

Fig. 7. Visualized images of the pore space of the karst reservoirs of Rybkinsky reefs obtained on the core column using X-ray computed tomography: a-c – Kindelsky reef, d-e – Novozhokhovsky reef, f-g – South-Kulaginsky reef, h – South-Volostnovsky reef, i – West-Kulaginsky Reef. Dark – pore space, light – dense part of rock. Explains to the images in the text. Tomograph operator – Kuznetsov E.G. (Core Research Center TNNC)

areas of porous or moderately cavernous rocks, but they do not characterize rocks with extended conductive fractures or a system of large vugs and cavities. The transition to the study of porosity and permeability of karst reservoirs according to the method of full-diameter core samples (with diameter 100 mm) to some extent allows us to solve this problem, since larger pores are involved in the research.

When studying the filtration properties of complex reservoirs of Rybkinsky reefs on small core plugs (that is, standart samples) and full-diameter samples, the "scale effect" is clearly manifested. It is a noticeable difference between standard and full-size samples in permeability. In Russia this direction of laboratory core analysis of carbonate reservoirs began to actively develop during the transition to the study of borehole core with a diameter of 100 or more millimeters, coring using the latest core-saving technologies (Mikhailov, Gurbatova, 2011; Gurbatova et al., 2011; Gurbatova, Mikhailov, 2011). Analysis of full-size core makes it possible to characterize not only pore channels of rock (available for study on standard samples of 1-inch diameter), but also filtering pores of larger size (fractures, cavern channel systems). As a result, at similar porosity values, the permeability of full-diameter samples can be one to two orders of magnitude higher than that of standard samples (Fig. 8). Taking into account the "*scale effect*" when working with complex reef reservoirs allows you to correctly estimate reserves (Nemirovitch et al., 2016; Shakirov et al., 2019).

However, the most accurate filtration characteristics of karst reservoirs can be obtained only when analyzing hydrodynamic studies of wells. Oil inflows from 190 to 380 m^3/day obtained by testing the karst intervals of Rybkinsky reefs (Vilesov et al., 2019a) indicate a significant role in the fluids filtration of cavern channels and fractures with high permeability. The results of laboratory core analysis using only small core plugs do not explain such production property of oil reservoirs.

Conclusions

Various attributes of surface and deep paleokarst as well as hydrothermal karst were diagnosed in the franian isolated reefs of the Rybkinsky group as a result of laboratory sedimentological studies of the borehole core.

The three epochs of the paleokarst, the Late Domanikian, Late Rechitskian and Late Voronezhian, are distinguished in the history of the formation of

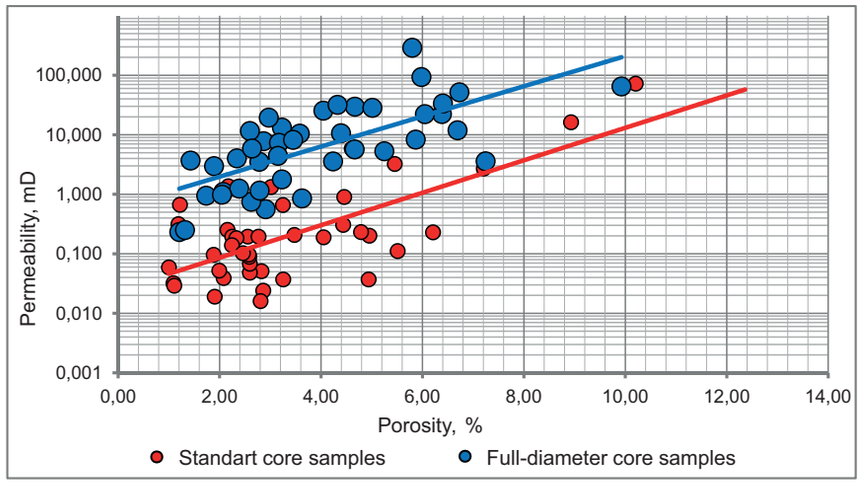

Fig. 8. Porosity-permeability cross plot for core samples of standart and full-diameter sizes (according to the results of laboratory core analysis of karst reservoirs of the South-Kulaginsky reef)

Rybkinsky reefs. Signs of surface and subsurface karst are established for each of them.

Carbonate breccias are assigned to the signs of surface karst in the upper part of the Domanikian regional stage. Karst at this level was caused by a regional decrease of sea level.

The late Rechitskian karst epoch was caused by significant inversion tectonic processes in the Sol-Iletsky Arch and its neighboring blocks against the background of global sea level rise. Surface karst is expressed by limestone breccias and carren, deep karst – by caves, fractures and cavities. Caves and cavities are filled mainly with carbonate and clay-carbonate sediment.

The Late Voronezhian paleokarst was caused by a significant eustatic falling of sea level and positive movements of the tectonic blocks of the Sol-Iletsky Arch. Ponors, carren and carbonate breccias are the results of surface karst. Deep karst formed such structures as caves, fractures, cavities. Filling karst voids at this stratigraphic level is the most diverse in terms of material composition that is represented by carbonate breccias, terrigenous-clay and clay-carbonate material.

The stages of the Late Rechitskian and Late Voronezhian karst are comparable in scale. Significant development of deep karst attributes is characteristic of each of these time lines.

Rybkinsky reefs were exposed to hydrothermal karst possibly at the turn of Late Franian – early Famenian ages. Hydrothermal karst developed mainly along permeable zones formed earlier by deep karst. An important result of hydrothermal karst is secondary high-porous hydrothermal dolomites.

Signs of the hydrothermal karst are distributed unevenly in area. They are developed most intensively along some linear zones, apparently associated with low-amplitude tectonic faults.

Reservoirs in the body of Rybkinsky reefs were formed as a result of a complex diagenetic history in which paleokarst (hypergenesis) and hydrothermal karst played leading roles.

The complex structure of the pore space is characteristic for the karst reservoirs of Rybkinsky reefs. Voids are presented here by all morphological types – pores, vugs, fractures, cavities, caves.

Acknowledgements

The authors are grateful to the management and geological service of «Orenburgneft» JSC for the systematic coring from isolated franian reefs and the possibility of core laboratory studies.

We would also like to thank the reviewer – professor Valentina A. Zhemchugova – for the careful analysis of the manuscript and valuable comments on the initial version of the work, which contributed to a noticeable improvement in the quality of publication.

References

Alekseev A.S., Kononova L.I., Nikishin A.M. (1996). The Devonian and Carboniferous of the Moscow Syneclise (Russian Platform): stratigraphy and sea-level changes. *Tectonophysics,* 268(1-4), pp. 149-168. https://doi.org/10.1016/S0040-1951(96)00229-6

Atchley S.C., West L.W., Sluggett J.R. (2006). Reserves growth in a mature oil field: The Devonian Leduc Formation at Innisfail field, south-central Alberta, Canada. *AAPG Bulletin*, 90(8), pp. 1153-1169. https://doi.org/10.1306/03030605193

Chow N., Wendte J. (2011). Palaeosols and palaeokarst beneath subaerial unconformities in an Upper Devonian isolated reef complex (Judy Creek), Swan Hills Formation, west-central Alberta, Canada. *Sedimentology*, 58(4), pp. 960-993. https://doi.org/10.1111/j.1365-3091.2010.01191.x

Copper P. (2002). Reef development at the Frasnian/Famennian mass extinction boundary. *Palaeogeography, Palaeoclimatology, Palaeoecology*, 181, pp. 27-65. https://doi.org/10.1016/S0031-0182(01)00472-2

Dublyanskiy Ju.V. (1985). Hydrothermal karst as process of the ore conditioning. Novosibirsk: Institut geologii i geofisiziki AN SSSR. Preprint. 18 p. (In Russ.)

Fortunatova N.K., Zaytseva E.L., Bushueva M.A., Shvets-Teneta-Guriy A.G., Baranova A.V., Kononova L.I., Rakhimova E.V., Mikheeva A.I., Oleneva N.V., Mushin I.A. (2015). Verkhniy devon Volgo-Uralskogo subregiona: materialy po aktualizatsii stratigraficheskikh skhem (Upper Devonian of the Volga-Ural subregion: materials on updating stratigraphy schemes). Moscow: VNIGNI, 174 p. (In Russ.)

George A.D., Powell C.McA. (1997). Paleokarst in an upper devonian reef complex of the Canning basin, Western Australia. *Journal of sedimentary research*, 67(5), pp. 935-944. https://doi.org/10.1306/D4268680-2B26-11D7-8648000102C1865D

Golonka J. (2002). Plate-tectonic maps of the Phanerozoic. Phanerozoic reef patterns (eds. Kiessling W., Flugel E., Golonka J.). *SEPM (Society for Sedimentary Geology), Special Publication*, 72, pp. 21-75. https://doi.org/10.2110/pec.02.72.0021

Gurbatova I.P., Kuzmin V.A., Mikhailov N.N. (2011). Influence of pore space structure on the scale effect in studying permeability storage capacity of complicatedly built carbonate reservoirs. *Geologiya Nefti i Gaza = Russian Oil and Gas Geology*, 2, pp. 74-81. (In Russ.).

Gurbatova I.P., Mikhailov N.N. (2011). Scale and anisotropic effects in experimental determination of physical properties of complex reservoirs. *Karotazhnik*, 7(205), pp 138-145. (In Russ.)

Hunt, D.W., Fitchen, W.M., Kosa, E. (2002). Syndepositional deformation of the Permian capitan reef carbonate platform, Guadalupe Mountains, New Mexico, USA. *Sediment. Geol*., 154, pp. 89-126.https://doi.org/10.1016/S0037-0738(02)00104-5

Johnson, J.G., Klapper, G., Sandberg, C.A. (1985). Devonian eustatic fluctuations in Euramerica. *Geol. Soc. Am. Bull*., 96, pp. 567-587. https://doi.org/10.1130/0016-7606(1985)96<567:DEFIE>2.0.CO;2

Maximovich G.A. (1963). The basics of karst science. Vol. 1: *Questions of karst morphology, speleology and hydrogeology of karst*. Perm, 443 p. (In Russ.)

Mikhailov N.N., Gurbatova I.P. (2011). Scale Effect at Laboratory Determination of Permeability and Porosity Properties of Complex Structured Carbonate Reservoirs. *Tekhnologii nefti i gaza = Oil and Gas Technologies*, 4, pp. 32-36. (In Russ.)

Moor C. (2001). Carbonate Reservoirs: Porosity Evolution and Diagenesis in a Sequence Stratigraphic Framework. *Developments in Sedimentology*, 55, pp. 1-444.

Nemirovitch T.G., Serkin M.F., Vilesov A.P. (2016). Secondary voidage of carbonate formations and its role in anisotropy of rock permeability. *Nauch.-tekh. vestnik OAO NK «Rosneft»*, 44, pp. 38-43. (In Russ.)

Nikitin Yu.I., Rikhter O.V., Makhmudova R.K., Vilesov A.P. (2013). Late Devonian Geodynamic and Paleogeographic Conditions for Oil Traps Formation in the Volga-Ural Province, Russia. *75th EAGE Conference & Exhibition incorporating SPE EUROPEC 2013*. London, UK. https://doi.org/10.3997/2214-4609.20131043

Nikitin Yu. I., Ostapenko S.V., Scheglov V.B. (2011). New branch of activities pertaining to geological prospecting in Orenburg region. *Geologiya, geofizika i razrabotka neftyanyh i gazovyh mestorozhdeniy = Geology, geophysics and development of oil and gas fields*, 11, pp. 13-18. (In Russ.)

Nikitin Yu.I., Astafyev E.V., Akhtyamova I.R., Shakirova G.V., Shirokovskich O.A. (2017). Exploration and research of oil and gas bearing zones controlled by reef using the regional criteria. *Neftyanoe khozyaystvo = Oil Industry*, 9, pp. 64-69. (In Russ.) https://doi.org/10.24887/0028-2448-2017-9-64-69

Nikitin Yu.I., Vilesov A.P., Koryagin N.N. (2018). Oil-bearing upper-fransian reefs – a new direction of geological exploration in orenburg region.

Geologiya, geofizika i razrabotka neftyanyh i gazovyh mestorozhdeniy = Geology, geophysics and development of oil and gas fields, 5, pp. 4-11. (In Russ.) https://doi.org/10.30713/2413-5011-2018-5-4-11

Nikitin Yu.I., Vilesov A.P., Chikina N.N. (2015). Late franian single reefs of the southern Orenburg region. *Proc. AllRuss. litologic. meet.: Geology of reefs*. Syktyvkar: IG Komi NTs UrO RAN, pp. 112-113. (In Russ.).

Nolting A., Zahm C.K., Kerans C. Nikolinakou M.A. (2018). Effect of carbonate platform morphology on syndepositional deformation: Insights from numerical modeling. *Journal of Structural Geology*, 115, pp. 91-102. https://doi.org/10.1016/j.jsg.2018.07.003

Orenburg tectonic junction: geological structure and petroleum potential. (2013). Ed. Volozh Yu.A and Parasyna V.S. Moscow, 264 p. (In Russ.)

Playford P.E. (2002). Palaeokarst, pseudokarst, and sequence stratigraphy in Devonian reef complexes of the Canning Basin, Western Australia. *Proceedings of the Western Australian Basins Symposium*, pp. 763-793.

Puchkov V.N. (2000). Paleogeodynamics of the Southern and Middle Urals. Ufa: Dauria, 146 p. (In Russ.)

Tikhomirov, S.V. (1985). Stages of Sedimentation of the Russian Platform Devonian and general questions of the structure and development of the stratisphera. Moscow: Nedra, 268 p. (In Russ.)

Unified subregional stratigraphic scheme of the Upper Devonian of the Volga-Ural subregion. (2018). Explanatory note. Fortunatova N.K., Zaytseva E.L., Bushueva M.A. et al. Moscow: VNIGNI, 64 p. (In Russ.)

Scotese C.R. (2014). Atlas of Devonian Paleogeographic Maps, PALEOMAP Atlas for ArcGIS, volume 4, The Late Paleozoic, Maps 65-72, Mollweide Projection, PALEOMAP Project, Evanston, IL.

Shakirov V.A., Vilesov A.P., Chertina K.N., Istomina N.M., Koryagin N.N. (2019). Oil reserves distribution in complicatedly-built fractured collectors of the franian reefs of Volostnovsky area in Orenburg region. *Geologiya, geofizika i razrabotka neftyanyh i gazovyh mestorozhdeniy = Geology, geophysics and development of oil and gas fields,* 5, pp. 12-21. (In Russ.) https://doi.org/10.30713/2413-5011-2019-5(329)-13-21

Switzer S.B., Holland W.G., Christie D.S., Graf G.C., Hedinger A.S., McAuley R.J., Wierzbicki R.A., Packard J.J. (1994). Devonian Woodbend-Winterburn Strata of the Western Canada Sedimentary Basin. *The Geological Atlas of the Western Canada Sedimentary Basin* (compilers: Mossop G. and Shetsen I.). Calgary, pp. 165-202.

Vilesov A.P., Nemirovich T.G., Lashmanova A.A. (2013). Franian single reefs of the Orenburg region and its hudrocarbon potential. *Proc. VII AllRuss. litologic. meet.: Sedimentary basins, sedimentation and post-sedimentation processes in geological history*. Novosibirsk: INGG SO RAN, 2013, vol. 1, pp. 158-163. (In Russ.)

Vilesov A.P., Nikitin Yu.I., Akhtyamova I.R., Shirokovskikh O.A. (2019) The frasnian reefs of the Rybkinsky group: facial structure, formation stages, oil potential. *Geologiya, geofizika i razrabotka neftyanyh i gazovyh mestorozhdeniy = Geology, geophysics and development of oil and gas fields*, 7, pp. 4-22. (In Russ.). https://doi.org/10.30713/2413-5011-2019-7(331)-4-22

Vilesov A.P., Nikitin Ju.I., Rikhter O.V., Makhmudova R.Kh. (2019). Sedimentological model of the Colganian Formation (Upper Devon) on the northern frame of the Sol-Iletsky Vault. *Coll. papers: Ekzolit – 2019. Facial Analysis in Lithology: Theory and Practice*. Moscow: MSU, pp. 31-34. (In Russ.)

Warren J. (2000). Dolomite: occurrence, evolution and economically important associations. *Earth-Science Reviews*, 52, pp. 1-81. https://doi.org/10.1016/S0012-8252(00)00022-2

Wilson M.E.J. (2012). Equatorial carbonates: an earth systems approach. *Sedimentology*, 59(1), pp. 1-31. https://doi.org/10.1111/j.1365-3091.2011.01293.x

About the Authors

Aleksandr P. Vilesov – Cand. Sci. (Geology and Mineralogy), Associate Professor, Expert in Lithology and Sedimentology

Tyumen Petroleum Research Center

42, M.Gorky st., Tyumen, 625048, Russian Federation

E-mail: apvilesov@mail.ru

Kseniya N. Chertina – Head of the Petrographic Research Laboratory

Tyumen Petroleum Research Center

42, M.Gorky st., Tyumen, 625048, Russian Federation

Manuscript received 19 September 2019;
Accepted 20 April 2020; Published 30 June 2020

ORIGINAL ARTICLE
DOI: https://doi.org/10.18599/grs.2020.2.29-36

Facies variability of pennsylvanian oil-saturated carbonate rocks (constraints from Bashkirian reservoirs of the south-east Tatarstan)

A.N. Kolchugin[1], G. Della Porta[2], V.P. Morozov[1], E.A. Korolev[1], N.V. Temnaya[1], B.I. Gareev[1]*
[1]*Kazan Federal University, Kazan, Russian Federation*
[2]*Università Degli Studi di Milano, Milano, Italy*

Abstract. One of the strategic ways of the old oil-producing regions is to further prospecting for potentially promising areas for hydrocarbon. One of these exploration areas is the Volga-Ural region. These reservoirs consist of Carboniferous carbonate rocks, which contain high viscous hydrocarbons and are characterized by complex facies architecture and reservoir properties influenced by diagenesis. The high degree of facies variability in the studied area does not allow reliable distribution of potential reservoir rocks not only between different areas but even within the same oil field. Based on textural and compositional features of carbonate facies, 5 main facies associations were identified and characterized with respect to the depositional settings in the Bashkirian basin. The facies associations correspond to: distal middle ramp facies, open marine proximal middle ramp facies, high-energy innershoal facies, inner ramp facies of restricted lagoons, facies of affected by subaerial exposures. From west to east in the study the following trends in facies characterare identified: 1) a decrease open marine middle ramp facies and in the total thickness of the Bashkirian sections; 2) an increase in evidences of sub aerial exposures; 3) a decrease in the proportion of potential reservoir rocks. A general shallowing of the depositional setting was identified in an eastward direction, where potentially promising reservoir facies of shallow high-energy environments were replaced by facies of restricted lagoon and facies affected by subaerial exposures and meteoric diagenesis (palaeosols, dissolution). The applied approach based on detailed carbonate facies analysis allows predicting the distribution of potentially promising cross-sections within the region.

Keywords: Bashkirian stage, carbonate ramp, facies, reservoirs, correlation

Recommended citation: Kolchugin A.N., Della Porta G., Morozov V.P., Korolev E.A., Temnaya N.V., Gareev B.I. (2020). Facies variability of pennsylvanian oil-saturated carbonate rocks (constraints from Bashkirian reservoirs of the south-east Tatarstan). *Georesursy = Georesources*, 22(2), pp. 29-36. DOI: https://doi.org/10.18599/grs.2020.2.29-36

Introduction

Currently, the prospects for oil production are becoming increasingly important in the Volga-Ural region, which includes the southeastern part of Tatarstan. The main reasons are deposit inundation of clastic reservoirs and involvement in the development of deposits with unconventional resources (bitumen deposits and black shale formations of the Domanic type).

At the same time, according to the authors, small attention is paid to carbonate reservoirs, as objects that have significant prospects of oil production and can ensure the region's energy stability soon.

These reservoirs include regionally oil-bearing carbonate rocks of the Bashkirian stage. The difficulty of their exploration lies in the high facies variability of reservoir rocks in the studied area and the difficulty of correlating of facies from section to section.

Attempts to correlate using different methods for comparing sections were carried out by various authors (Mukhametshin, 1982; Kochneva, Koskov, 2013; Galkin, Efimov, 2015; Kolchugin, Morozov et al., 2013, etc.). The authors used correlation techniques based on a statistical analysis of deposits, comparing data from geophysical well surveys, where the core analysis of the studied sections was not assigned the most significant role. The authors of this article believe that the lithological and facial principle of comparing sections based on core analysis and should be the basis for the correlation of deposits in the area. Such an approach will allow qualitatively dissecting the studied sections and established the all variety of

[*]*Corresponding author: Anton N. Kolchugin*
E-mail: anton.kolchugin@gmail.com

lithotypes which composing the sections and the laws of their change both vertically (along the section) and horizontally (over the area).

The object was core material selected from Middle Carboniferous units from the Bashkirian strata. The sections were studied from the most fully represented core wells since drilling of the Bashkirian section is often incompletely and is limited only to the productive zone. The studied core characterized deposits located on a line from west to east from deposits on the eastern side of the Melekesskaya depression to deposits located within the South Tatar anticline (Fig. 1).

The boundaries of the Bashkirian strata were detected according to GIS data. Also, the upper boundary is reliably detected by core analysis: by changing of Bashkirianlimestones to carbonate-clayish strata of the Verey horizon (Moscovian), as well as by changing fossils (Khalymbadzha, 1962; Khvorova, 1958).

The thicknesses of the Bashkirian sections of the studied area on average 40 meters, however, there is a general tendency to decrease (with minor variations) the thicknesses of the sections in the direction from west to east: from the eastern side of the Melekesskaya depression to the South Tatar anticline. Thus, the thickness of the studied Bashkirian sections varied from 60 to 18 meters. On the western slope of the South Tatar anticline, the volume of the studied sections is formed by the successions of the Kamsky horizon and the Cheremshansky horizon. Horizons unconformity cover the Serpukhovian strata. In the top of sections, the Bashkirian strata are unconformity overlap by Moscowian strata (Geology of Tatarstan, 2003).

It is believed that the sections of the Melekesskaya depression are more complete. In the Upper Bashkir section is detected the Melekessky horizon, up to 12 m thick, covers the Cheremshansky horizon (Geology of Tatarstan, 2003). However, the occurrence of the Melekessky horizon is noted in sections of the axial part of the Melekesskaya depression and it is possible on the eastern side of depression thickness may be less or they may completely disappear. In practice, horizons are not distinguished, which is caused by small volumes of paleontological studies and difficulties in comparing fragments of the section according to well log data. Traces of regional unconformity of rocks found in the sections. There are brecciated limestones and the loss of a certain group of fossils, according to V.S. Gubareva (Gubareva et al., 1982). In industry special studies of fossils are practically not provided.

The authors propose a methodology for identifying patterns of variability and correlation of deposits, based on the allocation and tracking of facies in the area. One of the ways based on a qualitative description of core material and analysis of petrographic sections. The practical side of the study is the possibility of using the proposed methodology to track potentially promising reservoir rocks by area and, conversely, to identify low promising areas.

Research methods and study methods

Macroscopic study of core samples

The studied sections were characterized by continuously selected core material with an actual core yield of 90-100%. This allowed the authors qualitative

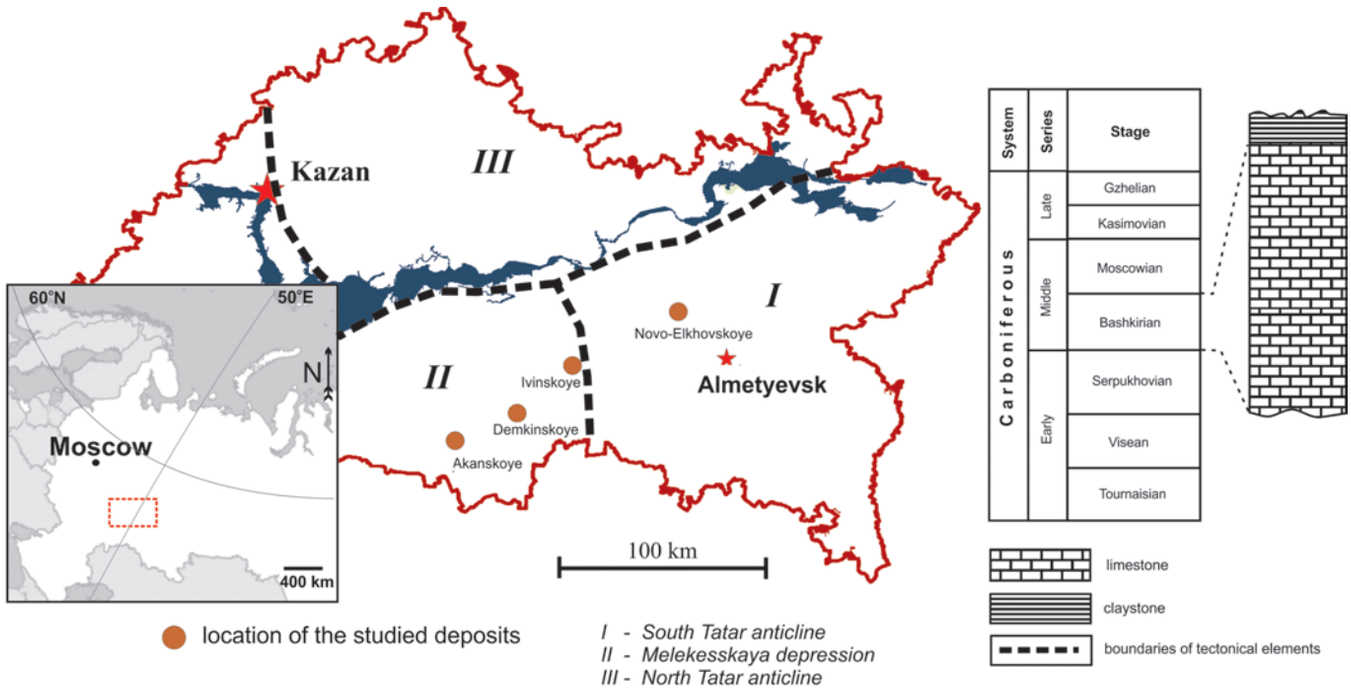

Fig. 1. The location scheme of the studied deposits, the main tectonic elements of the region, and a brief lithological and stratigraphic characteristic of the Carboniferous system

describe the sections and selected in detail rock samples for research. Work with the core material began from preliminary sawing along the axis. It is necessary for a qualitative description and identification of structural and textural characteristics of the rock, fluid saturation, and other features. The description was from bottom to top along the section. Such an approach allows us to reliably establish the patterns of change of rock types under the conditions of the Bashkirian sea: variation in the depth of the basin, intraformational erosion, subaerial exposures, etc. Special focus was paid to the relationship of lithotypes, lithological and paleontological composition, structural and textural features of the rocks. Samples were selected with step from 30 to 70 cm, depending on the facial variability and fluid saturation of rocks

Optical microscopic studies

Petrographical analysis of thin sections was made using an Axio Imager A2 polarizing microscope. Analysis of the thin sections included determination of the mineral composition, identification of the microtexture and structure of the rocks, fossil fragments, determination of facies. The structural classification of Dunham (Dunham, 1962) was chosen as a classification of carbonates, used by the international community and most of the oil companies in Russia, in recent years.

The methodology of lithological and facial reconstructions

The lithofacies model was used to determine the type of facies of allocated lithotypes. This model of distribution of facies determines the presence of lithotypes in various physical and geographical settings. They are controlled by the morphology of coastline, changes in the depth of the water basin, the topography of the seafloor, distance from land, etc. Distribution of facies has a certain pattern, in conditions of increasing depths of basin. The authors created a distribution scheme for the facies of the Bashkirian sea for the studied area (Fig. 2), based on the analysis of several models of marine carbonate precipitation (Immenhauser et al., 2004; Della Porta et al., 2004). Latin letters are used: *A, B, C, D, E*, for the convenience of detected facies. Detailed interpretation of the facies will be done in the "Results" part.

Results

Bashkirian successions were formed in the conditions of gentle slope carbonate ramp, based on analysis of the composition of the rocks (Proust et al., 1998). Precipitation of carbonates was in normal marine environments of low latitudes (Kolchugin, Immenhauser et al., 2016). The studied region can be defined as a transition zone between the inner and middle ramp with typical carbonate sedimentation (Kolchugin, Della Porta et al., 2017). The authors proposed to distinguish 5 main types of facies, which differ in the lithological and paleontological composition.

Facies A is limestone, represented by skeletal packstones, rarely wackestone with an abundance of fragments of brachiopods and spines, crinoids, benthic foraminifera, and peloids (Fig. 3A), fragments of corals.

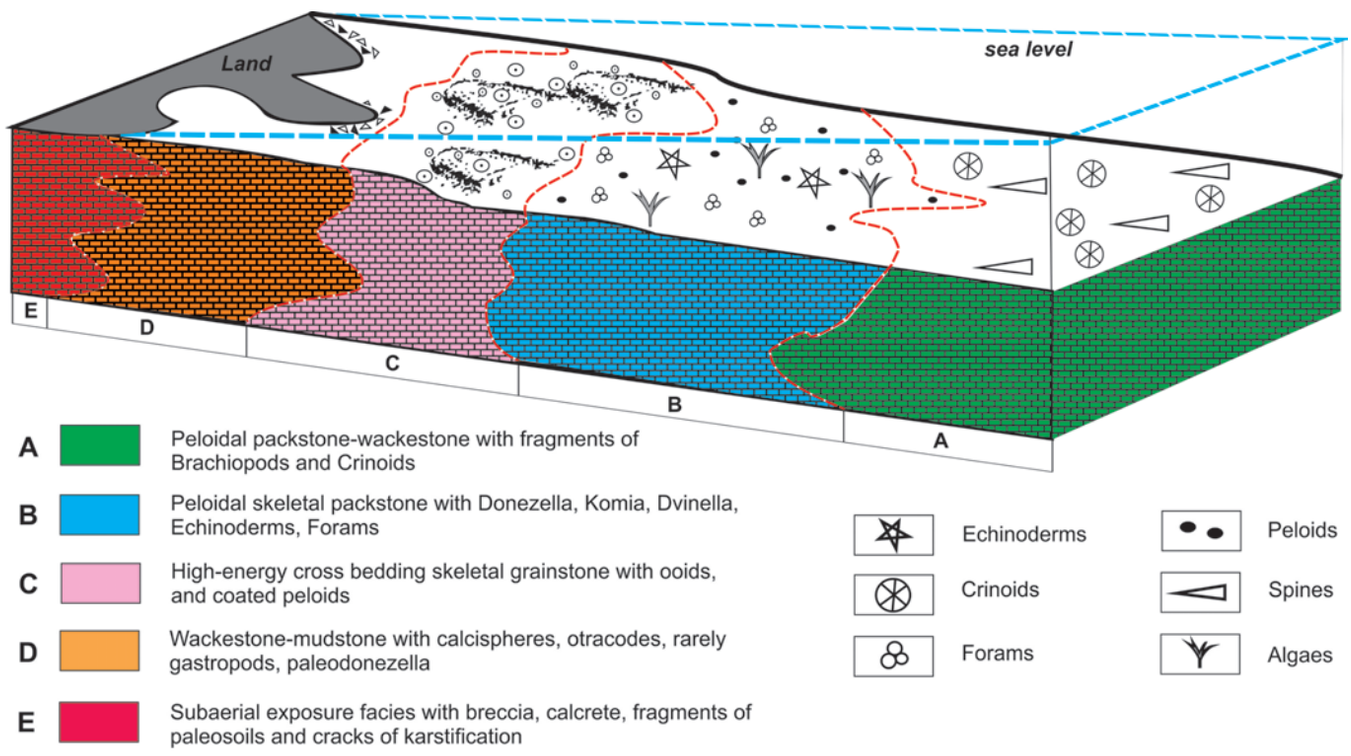

Fig. 2. The main groups of Bashkirian facies

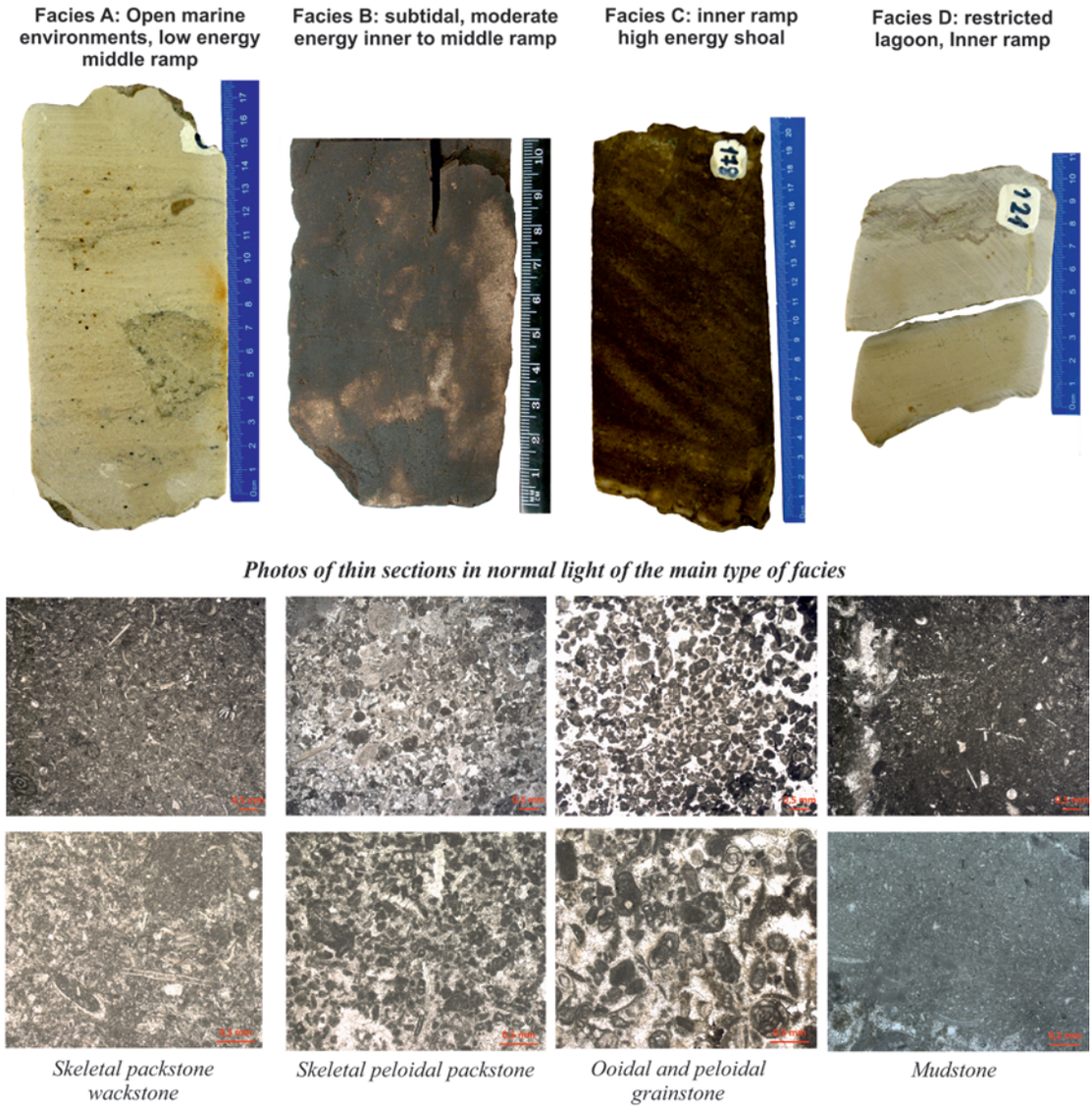

Fig. 3. Photos of samples and thin sections in the normal light of the main identified facies, as an example of limestones of the Ivinsky deposit. The distribution and composition of the facies are shown in the legend to Fig. 2.

Facies B is represented by skeletal peloid packstones, sometimes by grainstones with an abundance of benthic foraminifera (Glovivaluvulina, Climacammina, Dvinellalovilvulina, Climacammina, Bradyina), fragments of echinoderms and bryozoans (Fig. 3B).

Facies C is represented by well-sorted grainstones, with crossed lamination with an abundance of ooids, bioclasts, and fragments of various grains and intraclasts. The facies is characterized by the intergrain type of porosity, isopahous rims of marine fibrous cement (Fig. 3C).

Facies D is represented by mudstones (Fig. 3D) and wackestones with rare grains of peloids, calcispheres, beresellidealgaes gastropods, and ostracods.

Facies E is composed of various types of limestones: brecci as (Fig. 4A), mudstones and wackestones, sometimes bundstones (Fig. 4B), and packstones. All facies have traces of secondary iron mineralization and recrystallization. Rocks are often characterized by the presence of sediment or cracks of karstification (Fig. 4C) with fragments of subaerial leaching and fragments of paleosols and calcrete. Breccias are often characterized by the black pebbles (Fig. 4A).

The authors selected the most typical sections which are characterizing the eastern side of the Melekesskaya depression and the Western slope of the South Tatar anticline and analysis of the variability of rocks in the studied area. One of the most western sections is the section of the Bashkirian strata of the Akansky deposit, located on the eastern side of the Melekesskaya depression. The Novo-Elkhovsky deposit was selected as the most eastern section in the studied area. A significant number of sections were studied, between "opposite" sections on the line from west to east. However, sections of Ivinsky and Demkinsky deposits were chosen as the model between the selected, since they were best characterized by core samples (Fig. 5). It was possible to give a detailed description of the

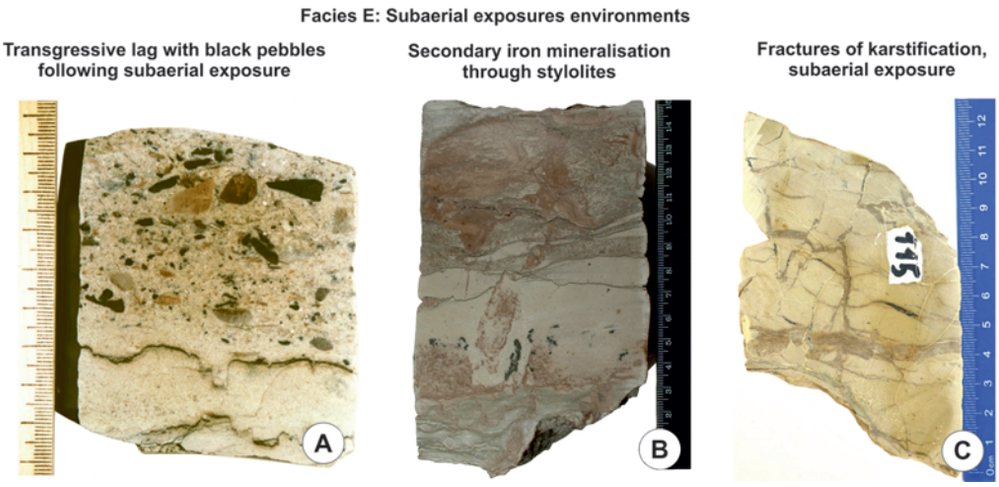

Fig. 4. Photo of samples of facies E. Example of samples with traces of subaerial exposures of Novo-Elkhovskoye (A) and Ivinsky deposits (B, C). A – carbonate breccia, B – Mudstone-boundstone with iron mineralization, C – Mudstone with cracks of karstification and iron mineralization, filled by clay minerals.

types of rocks and establish the boundaries of change lithotypes.

An important feature of all studied sections is the presence of traces of subaerial exposures. In sections, they are marked as facies E and highlighted in red. The proportion of facies E varies from section to section and generally increases from west to east. Another feature is a decrease in the total thickness of the Bashkirian sections. The thickness of the deposits is 45-60 m on the eastern side of the Melekesskaya depression and does not exceed 20-25 m on the western slope of the South Tatar anticline.

Discussion

The variability of the Bashkirian successions from west to east mostly caused by more intraformational erosion of strata within the western slope of the South Tatar anticline. This is indicated by an increasing share of brecciated limestones in sections, traces of subaerial exposures, and meteoric diagenesis. This type of diagenesishas often explained the lack of effective porosity in grainstones, which seem to be the most promising rocks as potential reservoirs. The pore space of such grainstones is almost filled by early diagenetic calcite. The periodic outbreak of rocks above sea level takes a negative role inthe preservation of primary high porosity. Meteoric waters change the physicochemical parameters of precipitation conditions and produce recrystallization of rocks and calcite cementation, filling of pore space by secondary calcite (Badiozmani, Mackenzie, 1977; Moore, 1989).

The presence of reddish colors of rocks indicates the periodic outbreak of rocks above sea level. It is caused by the appearance of iron oxides and hydroxides as markers of subaerial exposures (Fig. 4). Breccias contain black pebbles and found in sections of the western slope of the South Tatar anticline. The black color of pebbles is caused by humic organic matter (fragments of ancient paleosols). This indicates a relatively long time of continental subcontinental environments where could form soils.

The Bashkirian basin is an epicontinental basin with extremely insignificant depth differences. Periodic glacioeustatic oscillations of the marine basin drained some areas. It led to the erosion of previously accumulated carbonates. Bashkirian time was a time of active fluctuations in sea level and produced by global glaciation (Bishop, Montañez et al., 2009; Mii, Grossman et al., 2001).

Probably, glacioeustatic oscillations were a key factor in sea-level change. Traces of erosion are captured only in the form of thin brecciated limestones, in the western sections. In the eastern sections are limestones with traces of secondary iron mineralization, limestones with polygonal cracks of the early stages of karstification, and meteoric type of diagenesis, in addition to brecciated limestones (Fig. 4). It indicates relatively deeper marine environments in the west of the studied region (the modern eastern side of the Melekesskaya depression) and more shallow in the east (modern western slope of the South Tatar anticline). Moreover, the authors do not exclude that even more characteristic tracers could simply be eroded of the existence of rocks in subaerial exposures and changing of sea level.

Correlation of sections between deposits difficult task, because of the high degree of facial variability in the studied area. However, such correlation is quite realistic based on the frequency of certain facies and the patterns of their change along the section, as well as the tracking of intervals of subaerial exposures (Fig. 5). It seems that the intervals of subaerial exposures can be considered as some benchmarks for the correlation of

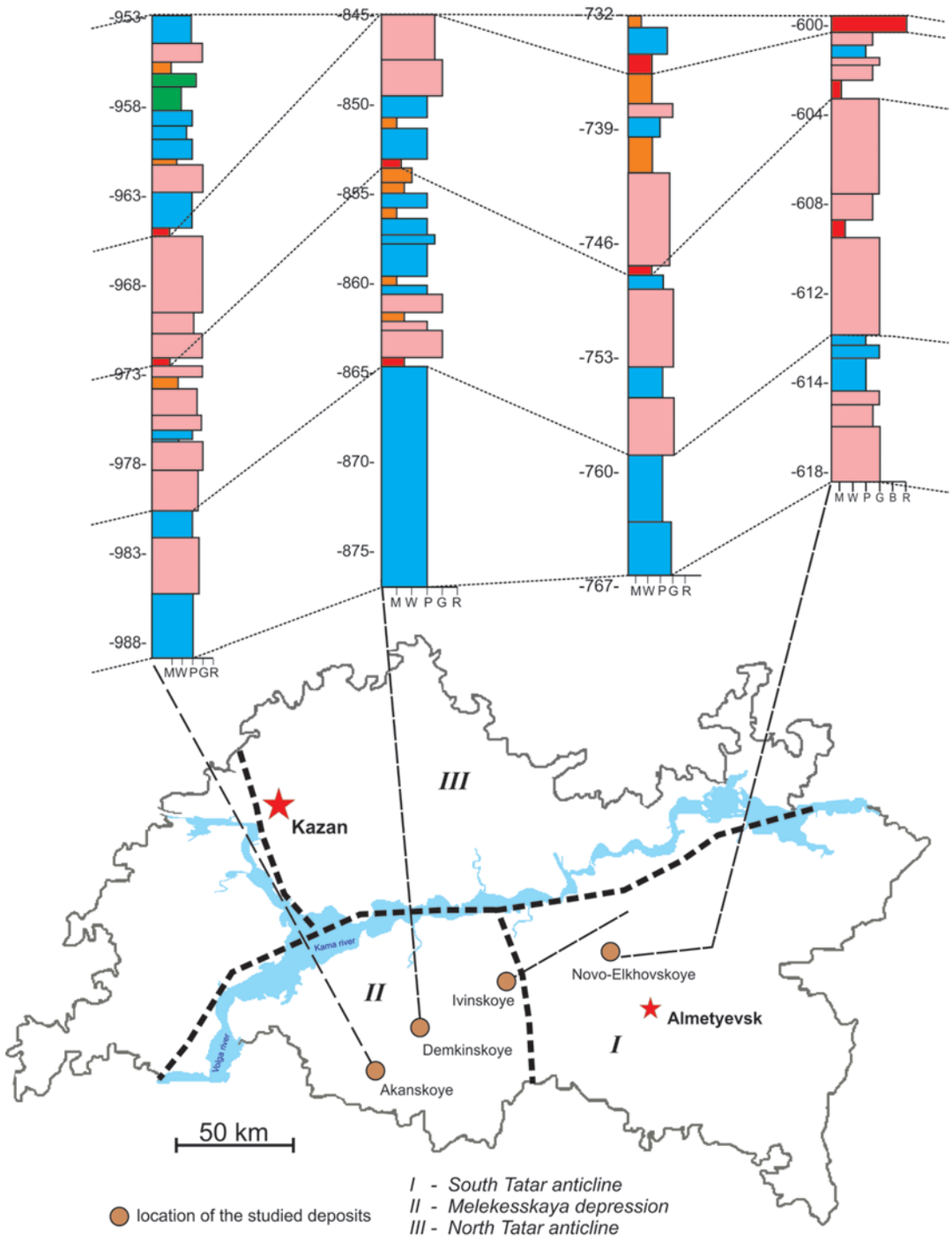

Fig. 5. The position of the studied sections on the profile from west to east. The sections show the distribution of selected facies. The color of the facies is shown in Fig. 2.

sections. Studying the Bashkirian sections shows that all the sections have at least two intervals of subaerial exposures in the middle and upper parts of the sections. Probably, they were the most obvious stages of subaerial environments. It can find a larger number of such intervals in the eastern sections, located on the western slope of the South Tatar anticline. It caused by more shallow marine environments of carbonate precipitation. Moreover, such "regional breaks" of sedimentation are well distinguished in sections and can be used to compare strata.

It is noted variability in productivity and oil saturation, in addition to facies changes within the selected profile from west to east. First of all, this is connected with the potential reservoir rocks represented by packstones and grainstones, which are thinning to the east. If the packstones almost disappear in the eastern sections, grainstones lose porosity in conditions of subaerial diagenesis. The industrial production of such sections is lost, and often rocks do not have any signs of oil saturation.

Conclusions

An analysis of the composition of the studied sections and the position of the sections studied area allowed to draw several conclusions.

1. It is observed a decrease in the share of normal marine environments from the west (the eastern side of the Melekesskaya depression) to the east (the western slope of the South Tatar anticline), at the same time, an increase in the share of restricted lagoon facies and subaerial exposures. In the same direction is observed a general decrease in the thickness of the Bashkirian sections.

2. It is reduced the industrial productivity of sections and the overall oil saturation of the rocks from west to east in the studied area. This is due to two main factors: 1) it is lithological and facies composition of the section, due to a decrease in the share of potential reservoir rocks (packstones and grainstones); 2) it is the type of diagenesis of carbonate sediments, where potentially promising reservoir properties of rocks were lost under the subaerial conditions and the influence of meteoric diagenesis.

3. The high facies variability of the Bashkirian strata caused by global glacioeustatic sea-level fluctuations, and the amplitude of which sea-level change could be up to several tens of meters. In this case, a significant part of sections could be thining (up to 10-15 m) due to erosion.

Acknowledgments

The authors thank the management of Tatneft, Kara-Altyn, Tatex, and Tatnefteprom companies for the opportunity to study core material.

Research supported by the Russian Science Foundation, project No.19-77-00019.

The authors acknowledge the constructive and valuable comments, critical analysis of reviewers.

References

Badiozmani K., Mackenzie F.T., Thortenson D.C. (1977). Experimental carbonate cementation: salinity, temperature and vadose-phreatic effects. *J.Sed.Petrol,* 47(2), pp. 529-542. https://doi.org/10.1306/212F71CB-2B24-11D7-8648000102C1865D

Bishop J.W., Montañez I.P., Gulbranson E.L., Brenckle P.L. (2009). The onset of mid-Carboniferous glacio-eustasy: Sedimentologic and diagenetic constraints, Arrow Canyon, Nevada. *Palaeogeography, Palaeoclimatology, Palaeoecology*, 276(1-4), pp. 217-243. https://doi.org/10.1016/j.palaeo.2009.02.019

Della Porta G., Kenter J.A.M. & Bahamonde J.R. (2004). Depositional facies and stratal geometry of an Upper Carboniferous prograding and aggrading high-relief carbonate platform (Cantabrian Mountains, N Spain). *Sedimentology*, 51(2), pp. 267-295. https://doi.org/10.1046/j.1365-3091.2003.00621.x

Dunham R.J. (1962). Classification of carbonate rocks according to depositional texture. Classification of carbonate rocks: *Simp. Amer. Assoc. Petrol. Geol. Mem*. Ed. W.E.Ham, 1, pp. 108-121.

Galkin V.I., Efimov A.A. (2015). Development of forecasting models for assessing the oil mobility coefficient taking into account facies environments (for example, the Bsh Kokuysky deposit). *Neftepromyslovoe delo = Oil Field Engineering*, 8, pp. 11-15. (In Russ.)

Geology of Tatarstan: stratigraphy and tectonics (2003). Ed. B.V. Burov. Moscow: GEOS, 402 p. (In Russ.)

Gubareva B.C., Dalmatskaya I.I., Kotelnikova E.D. (1982). Bashkirian deposits in the east of the Russian plate. Scale of the Carboniferous system in the modern data. Moscow: Nauka, pp. 94-102. (In Russ.)

Hvorova I.V. (1958). Atlas of carbonate rocks of the middle and upper carbon of the Russian platform. Moscow: Academy of Sciences of the USSR Publ., 170 p. (In Russ.)

Immenhauser A., Hillgärtner H., Sattler U., Bertotti G., Schoepfer P. Homewood P., Vahrenkamp V., Steuber T., Masse J. P., Droste H., Taal-Van Koppen. J., Van der Kooij B., Van Bentum E., Verwer K., Hoogerduijn-Strating E., Swinkels W., Peters J., Immenhauser-Potthast I., Al-Maskery S. (2004). Barremian-Lower Aptian Qishn Formation, Haushi-Huqf area, Oman: A new outcrop analogue for the Kharaib/Shu'aiba reservoirs. *GeoArabia*, 9(1), pp. 153-194.

Khalymbadzha V.G. (1962). Middle Carboniferous Deposits of the Northern, Central, and Western Regions of Tataria. Kazan: KSU Publ., 239 p. (In Russ.)

Kochneva O.E., Koskov V.N. (2013). Lithological and facial correlation of Bashkirian carbonate deposits according to field geophysical studies. *Neftepromyslovoe delo = Oil Field Engineering*, 9, pp. 32-38. (In Russ.)

Kolchugin A., Della Porta G., Morozov V. (2017). Lower Pennsylvanian reservoir facies from the foreland basin carbonate ramp of the Volga-Ural region, east of Russian platform, Russian Federation. *33 International Meeting of Sedimentology. Abstract book*. Toulouse, p. 467.

Kolchugin A.N., Immenhauser A., Walter B.F., Morozov V.P. (2016). Diagenesis of the palaeo-oil-water transition zone in a Lower Pennsylvanian carbonate reservoir: Constraints from cathodoluminescence microscopy, microthermometry, and isotope geochemistry. *Marine and Petroleum Geology*, 72, pp. 45-61. https://doi.org/10.1016/j.marpetgeo.2016.01.014

Kolchugin, A.N., Morozov, V.P., Korolev, E.A., Eskin, A.A., Gazeeva, F.M. (2013). Typical sections of Bashkirian carbonate rocks and structure of oil deposits in the southeast part of the Republic of Tatarstan. *Neftyanoe khozyaystvo = Oil Industry*, 11, pp. 84-86. (In Russ.)

Mii H.-S., Grossman E.L., Yancey T.E., Chuvashov B., Egorov A. (2001). Isotopic records of brachiopod shells from the Russian Platform – Evidence for the onset of mid-Carboniferous glaciations. *Chemical Geology*, 175(1-2), pp. 133-147. https://doi.org/10.1016/S0009-2541(00)00366-1

Moore C.H. (1989). Carbonate Diagenesis and Porosity. Ser. *Developments in Sedimentology*, Vol. 46. Elsevier Publishing Co., 338 p.

Mukhametshin R.Z. (1982). The use of statistical methods for optimal partitioning and correlation of carbonate strata. *Oil and gas geology and geophysics Ser.* Moscow: VNIIOENG, No. 6, pp. 25-27. (In Russ.)

About the Authors

Anton N. Kolchugin – Cand. Sci. (Geology and Mineralogy), Deputy Director for Science, Institute of Geology and Petroleum Technologies, Kazan Federal University

18, Kremlevskaya st., Kazan, 420008, Russian Federation

Tel: +7(843)2337954

E-mail: Anton.Kolchugin@gmail.com

Giovanna Della Porta – PhD, Associate Professor, Università Degli Studi di Milano

7, Via Festa del Perdono, Milan, 20122, Italy

Vladimir P. Morozov – Dr. Sci. (Geology and Mineralogy), Professor, Head of the Department of Mineralogy and Lithology, Institute of Geology and Petroleum Technologies, Kazan Federal University

18, Kremlevskaya st., Kazan, 420008, Russian Federation

Eduard A. Korolev – Cand. Sci. (Geology and Mineralogy), Head of the Department of General Geology and Hydrogeology, Institute of Geology and Petroleum Technologies, Kazan Federal University

18, Kremlevskaya st., Kazan, 420008, Russian Federation

Natalya V. Temnaya – Graduate Student, Institute of Geology and Petroleum Technologies, Kazan Federal University

18, Kremlevskaya st., Kazan, 420008, Russian Federation

Bulat I. Gareev – Research Engineer, Institute of Geology and Petroleum Technologies, Kazan Federal University

18, Kremlevskaya st., Kazan, 420008, Russian Federation

Manuscript received 28 November 2019;
Accepted 22 April 2020; Published 30 June 2020

ORIGINAL ARTICLE

DOI: https://doi.org/10.18599/grs.2020.2.37-44

Biodegraded bitumens dispersed in Vendian (Neoproterozoic) rocks of the Khatyspyt Formation, Northeastern Siberia

D.S. Melnik[1,2], T.M. Parfenova[1,2], V.I. Rogov[1]*

[1]*Trofimuk Institute of Petroleum Geology and Geophysics of the Siberian Branch of the Russian Academy of Sciences, Novosibirsk, Russian Federation*

[2]*Novosibirsk State University, Novosibirsk, Russian Federation*

Abstract. The organic matter of the Vendian (Neoproterozoic) Khatyspyt Formation was investigated. The new data obtained from the GC and GC-MS analyses include: high UCM humps and heightened peaks of steranes and terpanes against the backdrop of C_{27}+ alkanes on chromatograms of saturated hydrocarbons fractions of five samples; predominance of C_{21}-C_{26} in n-alkanes distribution; the presence of 12- and 13-monomethylalkanes on chromatograms and demethylated terpanes on filtered chromatograms (m/z 191 and 177). Besides, dispersed bitumens with biodegraded hydrocarbons have been for the first time identified in carbonate and carbonate-siliceous rocks of the Khatyspyt Formation. Also 8,14-sekohopanes resistant to biodegradation and gammacerane were established.

The revealed features of the composition and distribution of hydrocarbons showed that their source was the autochthonous (syngenetic) organic matter of the Khatyspyt Formation, one of the potential hydrocarbon source rock of Northeastern Siberia. The composition and content of bitumen are found to be controlled by the inputs of primary organisms (eukaryotes and prokaryotes) which lived in Vendian seas, by changing redox conditions of sediment deposition and transformation, as well as by relatively little effect of temperature and high degree of biological oxidation in hypergenesis.

The patterns of bitumen distribution throughout the section show, that besides the overlying deposits, their accumulations can be discovered in the Khatyspyt Formation.

Keywords: organic geochemistry, potential source rock, dispersed bitumens, saturated hydrocarbons (biomarkers), biodegradation, Khatyspyt Formation, Vendian (Neoproterozoic), Siberian Platform

Recommended citation: Melnik D.S., Parfenova T.M., Rogov V.I. (2020). Biodegraded bitumens dispersed in Vendian (Neoproterozoic) rocks of the Khatyspyt Formation, Northeastern Siberia. *Georesursy = Georesources*, 22(2), pp. 37-44. DOI: https://doi.org/10.18599/grs.2020.2.37-44

Introduction

Extensive geological and exploration works within Olenek Uplift which were conducted in the 30s of the 20th century revealed bitumen occurrences in rock cavity and pore space in Turkut Formation, Kessysa Formation and Upper Paleozoic deposits (Gusev, 1950). It has been known since 1950s that Khatyspyt Formation of Vendian (Neopreterozoic) age is developed on the Olenek Uplift slopes (Zhuravlev, Sorokov, 1954). Presently, the age of the Khatyspyt Formation (its lower limit) can be estimated at ~553-558 Ma based on paleontological data (Grazhdankin, 2004; Rogov et al., 2012; Rogov et al., 2013; Soldatenko et al., 2019). However, geochemical data also indicate that the age of the Formation may be younger, ~545 Ma (Kaufman, 2019). Thus, the Khatyspyt Formation is of Vendian age and is overlain by the Turkut Formation of Nemakit-Daldyn age. The latter contains skeletal fossils *Cambrotubulus decurvatus* (Karlova, 1987). In turn, the Turkut Formation is overlain by stratiform breccias being the product of tuff breccias decay, whose age is 543.9 Ma (Bowring et al., 1993; Rogov et al., 2015). The Khatyspyt Formation provides a unique object of study – the Ediacaran biota along with its habitat and burial setting (Rogov et al., 2012; Nagovitsin et al., 2015; Cui et al., 2016).

Some of the research conducted in the 1960s showed that the Khatyspyt Formation rocks are enriched with organic matter (OM) (Natapov, 1962). For more than 50 years, they have been viewed as source rock in the northeast of the Siberian Platform (Bazhenova et al., 1981; Kashirtsev, 1988; 2004; Kontorovich et al., 1995, 2000; Parfenova et al., 2010). Even today, the question about the role of the Khatyspyt Formation as possible oil and gas source in the Russian Arctic sector remains actual (Stupakova et al., 2017; Kashirtsev et al., 2018,

*Corresponding author: Dmitrii S. Melnik,
E-mail: melnikds@ipgg.sbras.ru

2019). Some researchers point out, that the Khatyspyt limestones and dolostones depleted and poorly enriched with OM include carbonate siliceous rocks and black shales, whose generative potential has been realized and they therefore are interpreted as the main source for Olenek and East Anabar bitumen fields (Kashirtsev, 1988; Parfenova et al., 2010; Kashirtsev et al., 2018, 2019; Melnik et al., 2019).

The present work sets out to study the patterns of bitumen occurrences in rocks within the Khatyspyt section, along with geochemical signatures of hydrocarbons-biomarkers.

Materials and methods

The Khatyspyt rocks were sampled in the Neoproterozoic section outcropping along Khorbusuonka River and its tributaries (Fig. 1), and previously studied by geologists (Rogov et al., 2012; Nagovitsin et al., 2015; Cui et al., 2016). The collection including 43 samples was analyzed at the Laboratory of Petroleum Geochemistry of the Trofimuk Institute of Petroleum Geology and Geophysics of the Siberian Branch of the Russian Academy of Sciences (IPGG SB RAS) with an aim of studying the organic geochemistry as part of the project supported by the Russian Science Foundation (grant 17-17-01241). Rocks were powdered in >0.25 mm fraction. Obtaining an insoluble residue (IR) involved dissolution of small weights of ground sample material in 10% HCl. Total organic carbon (TOC) content was determined using express analyser AN-7529 by burning insoluble residues in oxygen flow. Bitumen was extracted with chloroform using a centrifuge and was subsequently purified from elemental sulfur and fractionated by column chromatography. Bulk bitumen content (b_{chl}), bitumen coefficient ($\beta = 100\%*b_{chl}/(1.33*TOC)$) and fraction composition of bitumens were calculated. Saturated fractions of bitumens were analyzed using gas liquid chromatograph Agilent 5890 series II with quartz capillary column 30 m*0.25 mm with HP-5 phase and carrier gas helium. Terpane and sterane hydrocarbons (HCs) were investigated using a gas chromatography-mass spectrometry instrument Agilent (6890 series gas chromatograph and mass-selective detector 5973N). The identification of individual compounds was carried out using data from the NIST 02 mass spectra library and published spectra. The new results of geochemical studies were presented at scientific conferences (Melnik et al., 2019a, b).

Five samples (Fig. 2) showed elevated the bitumen coefficient values, and molecular signs of biodegradation of saturated HCs in bitumen extracts. It is known, that the biological oxidation of HCs by microorganisms is possible only for natural bitumens concentrated in open pore space (also caverns, fissures) at the contact with water (Peters et al., 2005). This primarily was the

Fig. 1. Sample collection area

reason why we concluded that the microscopic bitumen occurrences had been studied. The presence of bitumen is established in limestones (samples K604-1.4 and K602-42.9), siliceous limestones (samples K601C-(-2.5) and K602-53.3), calcareous silicite (sample K602-38.2) (Fig. 2). Additional study of thin sections using petrographic microscopic Carl Zeiss AxioScope A1 showed the presence of microcracks and caverns filled with redistributed organic matter (Fig. 3). Further in this paper, we will discuss only established characteristics of rocks containing dispersed biodegraded bitumens and of their organic compounds.

Results and discussion

Occurrences of free bitumens are reported not only in lowermost and uppermost horizons of the Khatyspyt Formation, but also in the middle part of the section (Fig. 2). The insoluble residue constitutes 4-57% (19% on average) in rocks, TOC content is 0.07-0.87% (Table 1). Bitumen content varies from 0.009 to 0.125%. Calcareous silicite is the most enriched with OM. It is known, that average TOC is 0.3-2.0% within the Khatyspyt section, rising occasionally up to 4-6% and 12-14% in limestones and black shales, respectively (Natapov, 1962; Kashirtsev, 2004; Parfenova et al., 2010; Cui et al., 2016; Melnik et al., 2019). The values of the bitumen coefficient vary from 8.5 to 11.3%, while β values for syngenetic bitumens of the Khatyspyt Formation are generally lower (Kashirtsev, 1988; Parfenova et al., 2010; Melnik et al., 2019).

Bitumens differ by the bitumen group composition (Table 1). Usually, resins dominate. Saturated HCs constitute 22%, aromatic compounds 13% and their sum 35%, accordingly; the sum of asphaltenes and

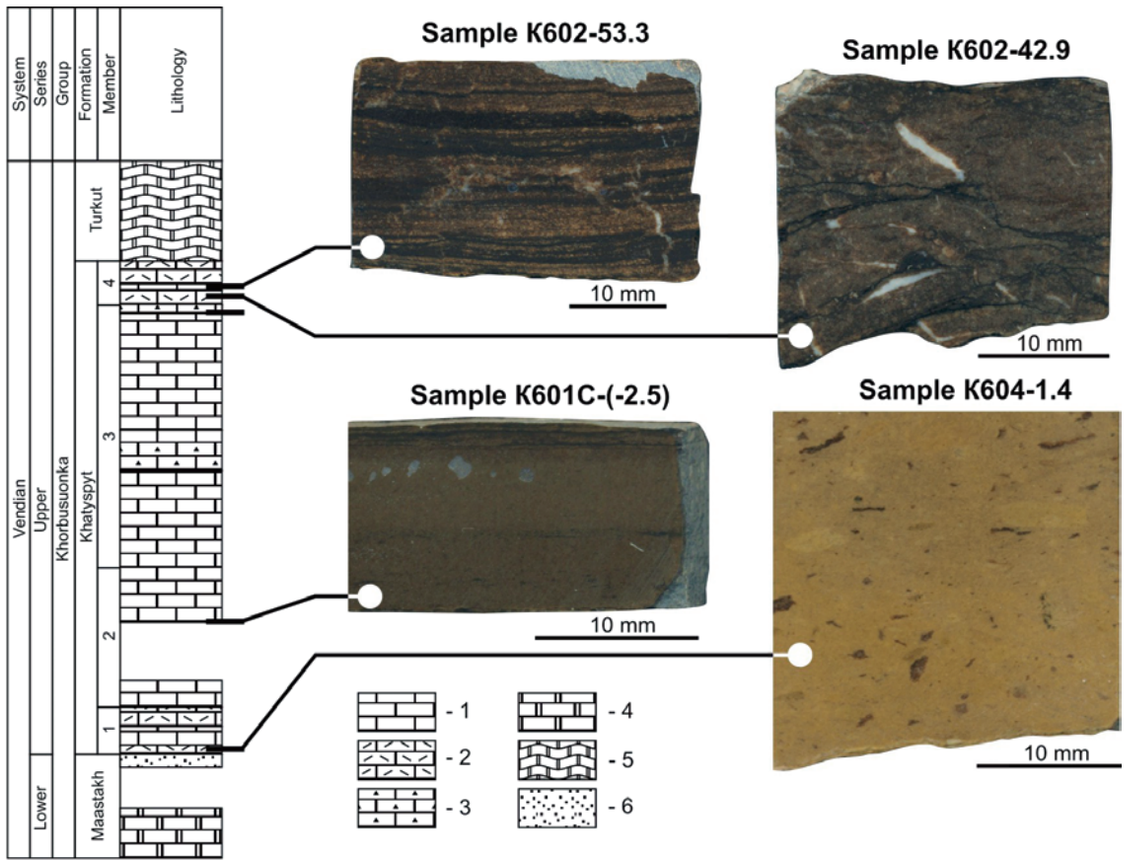

Fig. 2. Stratigraphy and lithology of the Khatyspyt Formation (according to Nagovitsin et al., 2015, modified). 1 – limestone, 2 – intraclastic limestone, 3 – siliceous limestone/calcareous silicite, 4 – dolostone, 5 – microbialitic dolostone, 6 – sandstone.

Sample		K604-1.4	K601C-(-2.5)	K602-38.2	K602-42.9	K602-53.3
IR, %		8	10	57	4	14
TOC, %		0.07	0.18	0.87	0.23	0.33
b_{chl}, %		0.009	0.02	0.125	0.034	0.045
β, %		9.1	8.5	10.8	11.3	10.3
The content in bitumen, %	Saturated HCs	20.3	48.2	15.1	15.2	11.9
	Aromatic HCs	1.4	5.0	16.7	23.9	16.5
	The sum of HCs	21.6	53.2	31.8	39.0	28.4
	Resins	78.4	46.8	59.3	54.5	61.1
	Asphaltenes	undefined	undefined	8.9	6.5	10.5

Table 1. Geochemical characteristic of rocks and dispersed bitumens of the Khatyspyt Formation

resins accounts for more than 60%. Syngenetic bitumens are commonly characterized by a higher content of saturated hydrocarbons against lower concentrations of aromatic hydrocarbons, while resins and asphaltenes remain at approximately the same level (Kashirtsev, 1988; Parfenova et al., 2010; Melnik et al., 2019a, b). The revealed elevated contents of resins and asphaltenes allows us to attribute most of the studied bitumens to asphalts, and one sample (K601C-(2.5)) to "malts" (according to Bazhenova et al., 1981).

Below we consider characteristics of the saturated hydrocarbons from free bitumens.

The normal alkanes distribution is typically characterized by a maximum at n-C_{23-25}. The n-C_{27}/n-C_{17} ratio varies between 0.5-1.6. Such a pattern was noted earlier for some of the Khatyspyt bitumen samples. Usually, n-C_{17-20} predominate among their alkanes (Kontorovich et al., 1995; Kashirtsev, 2004; Parfenova et al., 2010; Melnik et al., 2019). The GL chromatograms exhibit high humps of unresolved complex mixture (UCM) and high steranes and terpanes peaks against the background of alkanes (Fig. 4). The Pr/Ph isoprenoids ratio varies from 0.3 to 1.0 (Table 2). The Pr/n-C_{17} and Ph/n-C_{18} ratios are generally higher, amounting to 0.34-0.37 and 0.39-0.51 respectively. The ratio of the sum of n-alkanes to the sum of isoprenoids, averaging 12.7, is lower, as compared to syngenetic bitumens (Parfenova et al., 2010; Duda et al., 2016; Melnik et al., 2019).

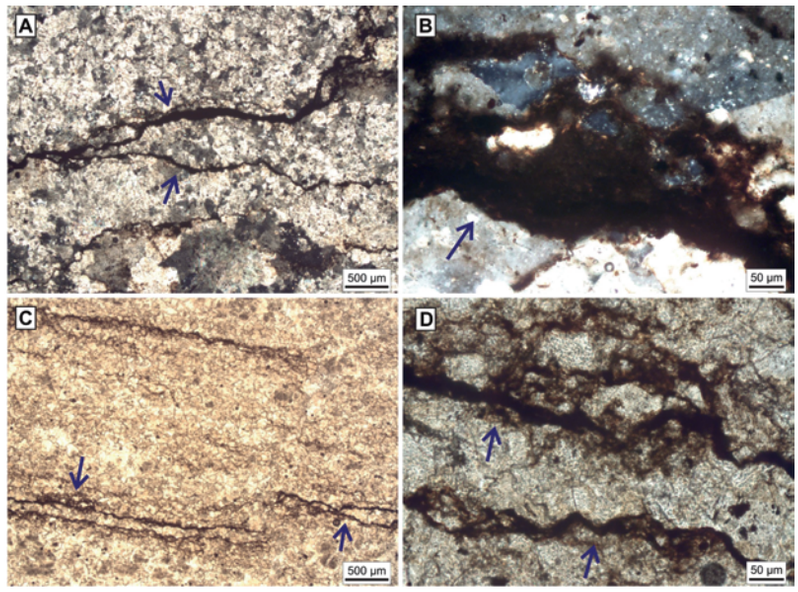

Fig. 3. Typical bitumen occurrence in microfissures in the Khatyspyt rocks. Thin sections, transmitted light microscopy: A, B – sample K602-42.9 (limestone); C, D – sample K602-53.3 (siliceous limestone).

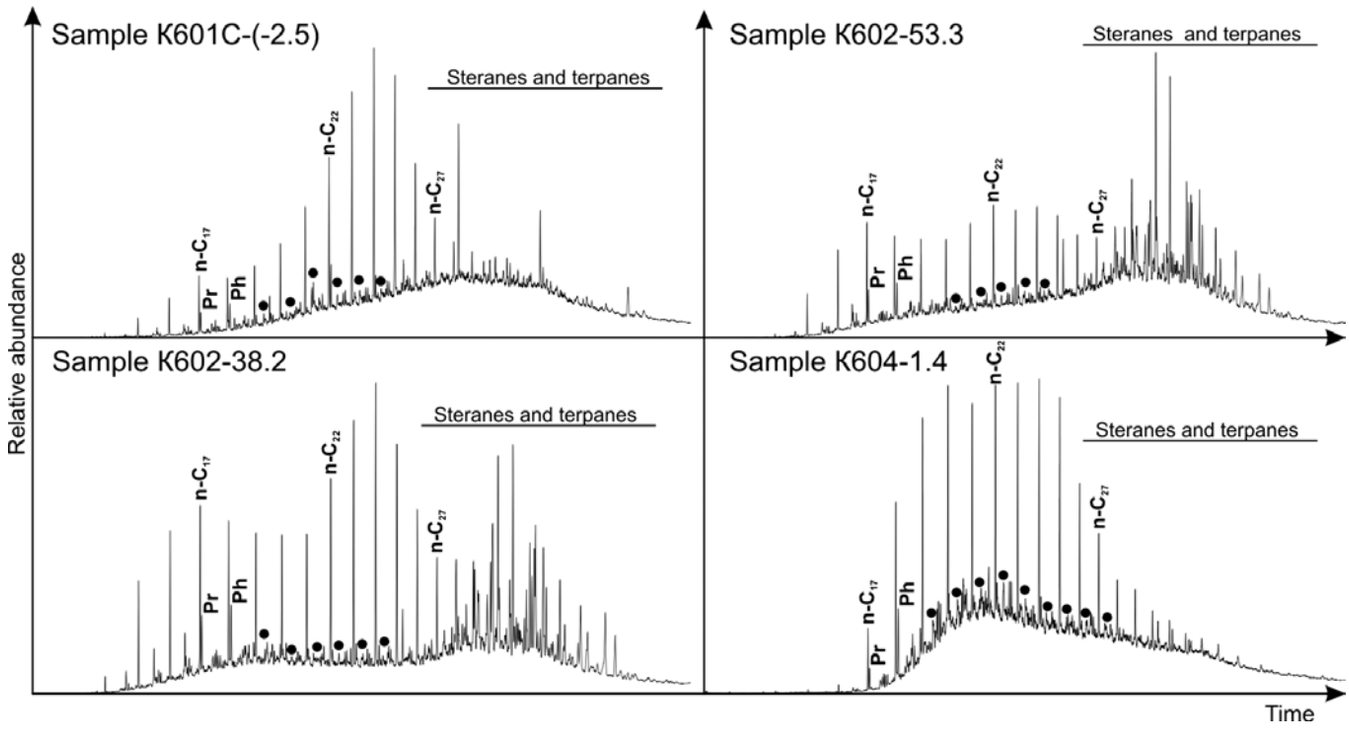

Fig. 4. Chromatograms of the saturated fractions of bitumens from the Khatyspyt Formation rocks. n-C_i – normal alkanes, Pr – pristane, Ph – phytane, black dots – 12- and 13-monomethylalkanes and their low molecular homologues.

The carbon preference index (CPI, Table 2) values for studied bitumens average 1.1, likewise for syngenetic bitumens of the Khatyspyt Formation (Parfenova et al., 2010; Duda et al., 2016; Melnik et al., 2019).

The analyzed chromatograms of saturated fractions of bitumens displayed low concentrations of 12- and 13-monomethylalkanes (Fig. 4). They were first noted in several syngenetic bitumen samples (Melnik et al., 2019). Previously, the possibility for diagnosing these hydrocarbons of the Precambrian OM from the available single samples (Petrov, 1984; Peters et al., 2005) had been dismissed (Kontorovich et al., 1995; Kashirtsev, 2004; Parfenova et al., 2010 etc.).

Analysis of steranes on m/z *217*, *218*, *231* mass-chromatograms permitted to establish two types of steranes distribution both for free bitumens, and syngenetic bitumens. The representative contents include: cholestane between 21 and 35% (per sum of C_{27}-C_{30} steranes), methylcholestanes(16-27%), ethylcholestanes (35-59%), propylcholestanes (1-4%). The C_{29}/C_{27} ratio varies from 1.0-1.3 to 2.4-2.9. The presence of 4-methylstigmastane (according to m/z *217*

	Sample	K604-1.4	K601C-(-2.5)	K602-38.2	K602-42.9	K602-53.3
Alkanes	Pr/Ph	0.31	0.78	0.91	0.83	0.96
	Pr/n-C_{17}	0.36	0.37	0.35	0.35	0.34
	Ph/n-C_{18}	0.41	0.51	0.43	0.39	0.44
	n-C_{27}/n-C_{17}	1.6	1.2	0.6	0.7	0.5
	∑n-C/∑izo-C	9.5	13.8	12.9	16.3	10.8
	CPI*	1.2	1.5	1.0	1.0	1.1
Steranes	C_{29}/C_{27}	1.0	1.3	2.4	2.9	2.6
	20S/(20S+20R)	0.4	0.4	0.4	0.5	0.5
	βα/(αα+ββ)	0.6	0.5	0.2	0.2	0.2
Terpanes	Ts/Tm	0.8	0.9	0.5	0.4	0.4
	Hopanes C_{29}/C_{30}	0.9	0.9	0.8	0.9	0.9
	Hopanes C_{35}/C_{34}	0.8	0.9	1.3	0.9	0.9
	Moretane C_{32}S/R	0.9	0.5	1.4	1.2	1.1
	Ga, %	0.02	0.5	7.2	7.3	6.4

Table 2. Characteristics of hydrocarbons of saturated fractions from bitumens of the Khatyspyt Formation. Note: Asterix (*) denotes Carbon preference index. CPI=0.5((C_{25}+C_{27}+C_{29}+C_{31}+C_{33})/(C_{26}+C_{28}+C_{30}+C_{32}+C_{34})+((C_{25}+C_{27}+C_{29}+C_{31}+C_{33})/(C_{26}+C_{28}+C_{30}+C_{32})) (according to Peters et al., 2005).*

and *231*), acting as dinoflagellate biomarker (Peters et al., 2005), was established. Previously, this HC was identified in bitumen and HyPy-pyrolisate of the Khatyspyt rock sample (Duda et al., 2016). One of the objectives of the Russian Science Foundation project was searches for biomarkers of ancient sponges, however neither 24-isopropylcholestan (Peters et al., 2005) nor 26-methylstigmastan (Zumberge et al., 2018) have thus far been identified. The cholestane isomers ratio C_{29} 20S/(20S+R) remains at the level of 0.4-0.5. The ratio of diasteranes to regular steranes ((βα/(αα+ββ)) varies from 0.15 to 0.55 (Table 2).

Analysis of hopanes and homohopanes, moretanes and gammacerane studied among terpanes, cheilantanes, tetracyclanes, on m/z *191* mass-chromatograms (Fig. 5) revealed the dominance of hopanes and homohopanes (up to 81%). The Ts/Tm and C_{29}/C_{30} hopane ratios are 0.6 and 0.9, on average. The established two types of homohopanes distribution are: $C_{35}>C_{34}$, $C_{32}\geq C_{31}$ and $C_{31}>C_{32}>C_{33}>C_{34}>C_{35}$, the homohopane index C_{35}/C_{34} (Vaz Dos Santos et al., 1998; Kashirtsev, 2004) values vary from 0.8 to 1.3. The cheilantanes are presented in the range from 12-13 to 22-28% in the sum of terpanes, with homologs C_{21} and C_{23} prevailing among them; the tricyclane index ($2*\sum C_{19-20}/\sum C_{23-26}$) values vary within 0.3-1.1 (the average is 0.7). The content of moretanes usually is not more than 5% by the sum of terpanes, with the C_{32}S/R isomers of moretane averaging 1.0. Gammacerane was detected both in high (7.3%) and low (0.02%) concentrations with respect to the sum of terpanes.

The distributions and ratios of HCs established for alkanes, steranes and terpanes of syngenetic bitumens of the Khatyspyt Formation have demonstrated close affinity (Kashirtsev, 2004; Parfenova et al., 2010; Duda et al., 2016; Kashirtsev et al., 2018; Melnik et al., 2019 a, b). This indicates that their source was OM of the Khatyspyt deposits.

A wide range of Pr/Ph ratio and homohopane index values and gammacerane content of HCs in bitumens suggests primarily that their source was sediments formed under changing redox conditions in the Vendian marine basin in the north-east of the Siberian Platform. The distributions of alkanes, isoprenoids, terpanes and steranes of bitumens indicate that archaea, algae and bacteria served as initial inputs of the biomaterial for the organic matter (Petrov et al., 1984; Peters et al., 2005).

Results of this study of bitumens the saturated fractions include pioneering identification of not only demethlated hopanes and homohopanes, but also tetracyclanes and tricyclanes on *m/z 177* mass-chromatograms (Fig. 5). It is commonly noticed, that the latter elute before regular terpanes, since their molecular weight is 14 units lower. Their presence is indicative of a high degree of HCs biodegradation (Petrov, 1984; Kashirtsev, 1988; Peters et al., 2005). The 8,14-sekohopane resistant to biological oxidation of HCs was diagnosed based on molecular mass 414 and fragment-ions 123 and 193 (Peters et al., 2005).

It is known that normal alkanes are the first to undergo bacterial oxidation, then isoprenoids, then hopanes and homohopanes and finally tetracyclanes and tricyclanes (Petrov, 1984; Kashirtsev, 1988; Peters et al., 2005). The fact that both demethylated terpanes and alkanes were found in saturated fractions of the studied samples probably attests to the mixing of bitumens from different stages of generation and filling

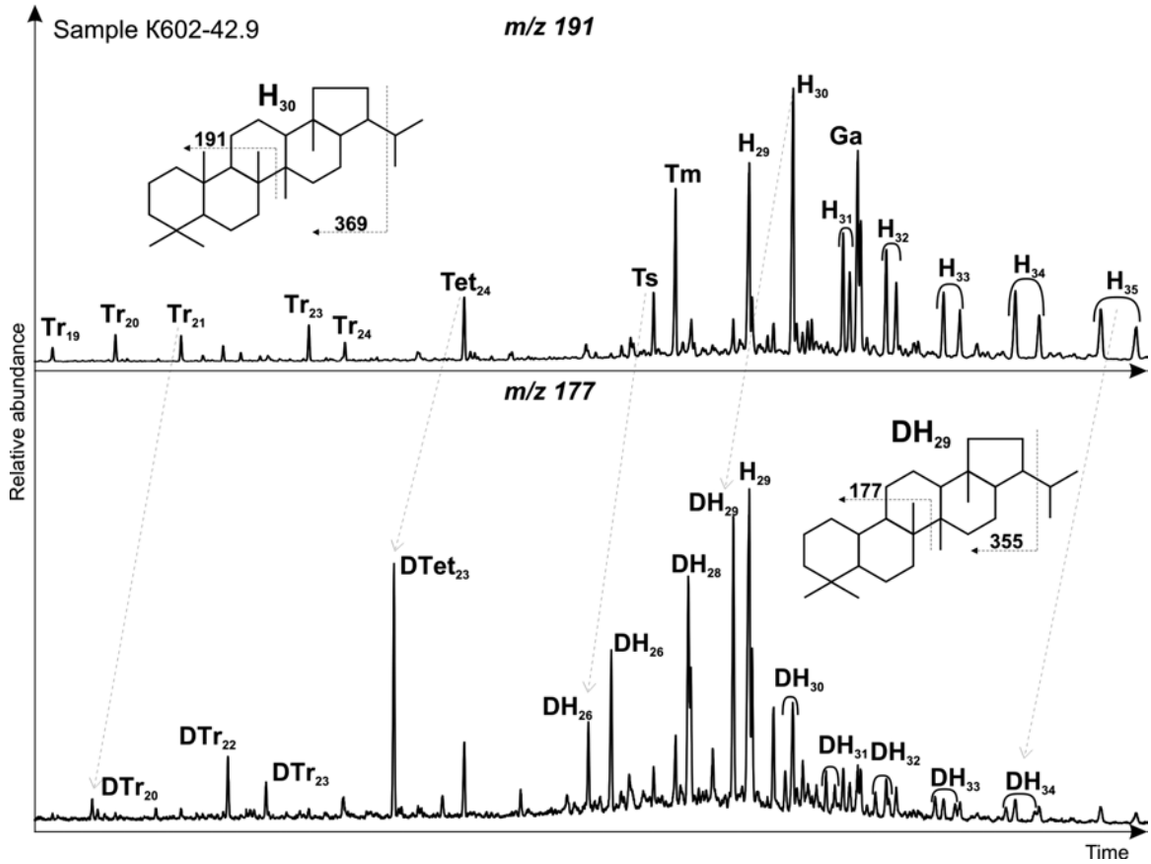

Fig. 5. Mass-chromatograms (m/z 191 and 177) of the saturated fraction of the bitumen from the Khatyspyt Formation rock. Ts – trisnorneohopane, Tm – trisnorhopane, Tr_i – cheilantanes (tricyclic terpanes), Tet_{24} – tetracyclic terpane C_{24}, H_i – hopanes and homohopanes; demethylated terpanes: DTr_i – tricyclic, $DTet_{23}$ – tetracyclic, DH_i – hopanes and homohopanes; Ga – gammacerane.

of the pore space. Bitumens that formed during the first stage were exposed to strong bacterial oxidation, with demethylated terpanes remaining in their saturated fractions. Hydrocarbon generation and migration that followed led to the secondary enrichment of bitumens with alkanes and isoprenoids. The chromatograms (gas-liquid chromatography, Fig. 4) show the ratio of alkanes and terpanes in bitumens to differ significantly, which indicates different intensities of the repeated processes of filling the pores with bitumens and their biodegradation.

Previous studies of the atomic and molecular composition of bitumens from the Turkut Formation of Vendian and Kessysa group of Vendian and Cambrian age within the Olenek Uplift allowed to establish signatures of their HCs composition (high gammacerane content, steranes distribution with ethylcholestanes dominance, absence of 12- and 13-monomethylalkanes). This proves the OM of the Khatyspyt Formation to be their source (Kontorovich et al., 1995, 2000; Kashirtsev, 2004; Parfenova et al., 2010, etc.). Recently updated characteristics of bitumens (oils) generated by Vendian rocks enriched with OM with the geochemistry of aromatic biomarkers (Kashirtsev et al., 2018) have shown that Vendian and Lower Cambrian natural bitumens within the East Anabar and Central Olenek fields owe their origin to the realization of generative potential of the Khatyspyt Formation rocks. Our materials, which supplement the previous results, demonstrate the expanded molecular parameters complex characterizing bitumen genetically associated with autochtonous OM of the Khatyspyt Formation (Melnik et al., 2019a, b). The bottom lines of our findings include: new distribution of steranes with similar concentrations of cholestanes and ethylcholestanes; presence of 12- and 13-monomethylalkanes in low concentrations; low gammacerane content, etc; oil and bitumen accumulations genetically related to the organic matter of the Khatyspyt Formation can be found in sedimentary basins in the Arctic section of Eastern Siberia.

Conclusions

Results of the conducted geochemical study of the organic matter from the Khatyspyt Formation of Vendian age have prompted the following conclusions.

1. The identified occurrences of dispersed bitumen in the Khatyspyt Formation rocks are interpreted as a direct sign of petroleum potential. Most features of the bitumen HCs composition are largely inherited from the OM of the Khatyspyt Formation oil source rock. The maturity

of bitumen and parent OM during mesocatagenesis (early oil window) was estimated from average values of Ts/Tm ratio (0.6), CPI (1.1), and cholestane C_{29}20S/(20S+R) ratio (0.5).

2. The revealed geochemical signatures of the saturated biomarkers indicate that bitumens of the Khatyspyt Formation are biodegraded in hypergenesis. The group composition of bitumens and HCs composition of their saturated fractions resulted from the bitumens mixing which occurred during several stages of their generation, primary migration and biological oxidation.

3. The placement of dispersed bitumens in different parts of the Khatyspyt Formation section within the Olenek Uplift area demonstrates that under favorable geological conditions, oil or bitumen accumulations can be detected in the Khatyspyt section, rather than in the overlying Vendian and Cambrian successions alone, as it was commonly noticed earlier.

Acknowledgments

This work was conducted under Government Contracts (0331-2019-0022 and 0266-2019-0006) and supported by the Russian Science Foundation (grant 17-17-01241).

References

Bazhenova T.K., Beletskaya S.N., Belyaeva L.S., Bikkenina D.A., Gurko N.N., Ivanovskaya A.V., Ipatov Yu.I., Kichueva U.O., Makarov K.K., Neruchev S.G., Parparova G.M., Rogozina E.A., Rudavskaya V.A., Solov'eva I.L., Faizullina E.M., Shapiro A.I., Shimanskii V.K., Shumenkova Yu.M., Aref'ev O.A., Gulyaeva N.D., Kulibakina I.B., Rabotnov V.T., Prokhorov V.S., Shadskii I.P. (1981). Organic geochemistry of the Paleozoic and Pre-Paleozoic Siberian platform and oil and gas potential. Leningrad: Nedra, 211 p. (In Russ.)

Bowring S.A., Grotzinger J.P., Isachsen C.E., Knoll A.H., Pelechaty S.M., Kolosov P. (1993) Calibrating rates of Early Cambrian evolution. *Science*, 261, pp. 1293-1298. https://dx.doi.org/10.1126/science.11539488

Cui H., Grazhdankin D.V., Xiao S., Peek S., Rogov V.I., Bykova N.V., Sievers N.E., Liu X.-M., Kaufman A.J. (2016). Redox-dependent distribution of early macro-organisms: Evidence from the terminal Ediacaran Khatyspyt Formation in Arctic Siberia. *Palaeogeography, Palaeoclimatology, Palaeoecology*, 461, pp. 122-139. https://doi.org/10.1016/j.palaeo.2016.08.015

Duda J.-P., Thiel V., Reitner J., Grazhdankin D. (2016). Opening up a window into ecosystems with Ediacara-type organisms: preservation of molecular fossils in the Khatyspyt Lagerstatte (Arctic Siberia). *Palaontologische Zeitschrift*, 90(4), pp. 659-671. https://doi.org/10.1007/s12542-016-0317-5

Grazhdankin D. (2004) Patterns of distribution in the Ediacaran biotas: facies versus biogeography and evolution. *Paleobiology*, 30, pp. 203-221. http://dx.doi.org/10.1666/0094-8373(2004)030<0203:PODITE>2.0.CO;2

Gusev A.I. (1950). Geology, coal content and oil content of the lower reaches of the Olenek River. *Proceedings of the Institute of Arctic Geology of the Ministry of Geology of the USSR*, 1, 101 p. (In Russ.)

Karlova G.A. (1987). The first finds of skeletal fauna in the Turkut suite of the Olenek uplift. *Doklady Akademii nauk*, 292(1), pp. 204-205. (In Russ.)

Kashirtsev V.A. (1988). Natural bitumen of the northeast of the Siberian platform. Yakutsk, 103 p. (In Russ.)

Kashirtsev V.A. (2004). Genetic families of Late Precambrian and Cambrian oils (naphthides) in the east of the Siberian platform. *Russian Geology and Geophysics*, 7, pp. 846-851.

Kashirtsev V.A., Parfenova T.M., Golovko A.K., Nikitenko B.L., Zueva I.N., Chalaya O.N. (2018). Phenanthrene biomarkers in the organic matter of Precambrian and Phanerozoic deposits and in the oils of the Siberian platform. *Russian Geology and Geophysics*, 59(10), pp. 1720-1729. (In Russ.) https://doi.org/10.15372/GiG20181013

Kashirtsev V.A., Parfenova T.M., Moiseev S.A., Chernykh A.V., Novikov D.A., Burshtein L.M., Dolzhenko K.V., Rogov V.I., Melnik D.S., Zueva I.N., Chalaya O.N. (2019). Direct signs of oil and gas potential and source deposits of the Sukhan sedimentary basin of the Siberian platform. *Russian Geology and Geophysics*, 60(10), pp. 1472-1487. (In Russ.)

Kaufman A.J. (2019) The Ediacaran-Cambrian transition: A resource-based hypothesis for the rise and fall of the ediacara biota. *Chemostratigraphy across major chronological boundaries, Geophysical Monograph 240, First Edition*, pp. 115-142. https://doi.org/10.1002/9781119382508.ch7

Kontorovich A. E., Kashirtsev V. A., Filp R. P. (1995). Biogopans in Precambrian sediments of the northeast of the Siberian platform. *Doklady RAN*, 345(1), p. 106-110. (In Russ.)

Kontorovich A.E., Melenevskii V.N., Timoshina I.D., Makhneva E.A. (2000). Group of Upper Precambrian oils of the Siberian platform. *Doklady RAN*, 370(1), pp. 92-95. (In Russ.)

Melnik D., Parfenova T., Grazhdankin D., Rogov V. (2019). Deposition of the Khatyspyt facies, Northeastern Siberia. *29th International Meeting on Organic Geochemistry (IMOG-2019)*. Abstracts. Gothenburg, Sweden. https://doi.org/10.3997/2214-4609.201902903

Melnik D.S., Parfenova T.M., Rogov V.I. (2019). Geochemistry of saturated hydrocarbon biomarkers of dispersed organic matter of the Khatyspyt Formation of the Neoproterozoic (northeast of the Siberian Platform). *Proc. 2nd All-Russ. sci. conf .: Actual problems of the geology of oil and gas of Siberia*. Novosibirsk, pp. 96-99. (In Russ.)

Nagovitsin K.E., Rogov V.I., Marusin V.V., Karlova G.A., Kolesnikov A.V., Bykova N.V., Grazhdankin D.V. (2015). Revised Neoproterozoic and Terreneuvian stratigraphy of the Lena-Anabar Basin and north-western slope of the Olenek Uplift, Siberian Platform. *Precambrian Research*, 270, pp. 226-245. https://doi.org/10.1016/j.precamres.2015.09.012

Natapov L. M. (1962). Deposits of the Domanik formation type in the northeast of the Siberian platform. *Sovetskaya geologiya*, 11, p. 110-112. (In Russ.)

Parfenova T. M., Kochnev B. B, Nagovitsin K. E., Ivanova E. N., Kashirtsev V. A., Kontorovich A. E. (2010). Geochemistry of organic matter of the Khatyspyt Formation (Vendian, northeast of the Siberian Platform). *Proc. Sci.Conf.: Advances Organic Geochemistry*. Novosibirsk: INGG SO RAN, pp. 265-268. (In Russ.)

Peters K.E., Walters C.C., Moldowan J.M. (2005). The biomarker guide. 2nd ed. New York: Cambridge University Press, 1155 p. https://doi.org/10.1017/CBO9780511524868

Petrov Al.A. (1984). Hydrocarbons of oil. Moscow: Nauka, 263 p. (In Russ.)

Rogov V.I., Karlova G.A., Marusin V.V., Kochnev B.B., Nagovitsin K.E., Grazhdankin D.V. (2015). The formation time of the first biostratigraphic zone of the Vendian of the Siberian hypostratotype. *Russian Geology and Geophysics,* 56(4), pp. 735-747. (In Russ.). https://doi.org/10.15372/GiG20150408

Rogov V.I., Marusin V., Bykova N.V., Goy Y., Nagovitsin K.E., Kochnev B.B., Karlova G., Grazhdankin D.V. (2012). The oldest evidence of bioturbation on Earth. *Geology*, 40, pp. 395-398. https://doi.org/10.1130/G32807.1

Rogov V.I., Marusin V., Bykova N.V., Goy Y., Nagovitsin K.E., Kochnev B.B., Karlova G., Grazhdankin D.V. (2012). The oldest evidence of bioturbation on Earth: Reply. *Geology*, 41(5), p. 290. https://doi.org/10.1130/G32807.1

Soldatenko Y., AlbaniA.El, Ruzina M., Fontane C., Nesterovsky V., Paquette J.-L., Meunier A., Ovtcharova M. (2019). Precise U-Pb age constraints on the Ediacaran biota in Podolia, East European Platform, Ukraine. *Scientific Reports*, 9, Article number 1675. https://doi.org/10.1038/s41598-018-38448-9

Stoupakova A.V., Suslova A.A., Bolshakova M.A., Sautkin R.S., Sannikova I.A. (2017). Basin analysis for the search of large and unique fields in the Arctic region. *Georesursy = Georesources*, Special issue, pp. 19-35. http://doi.org/10.18599/grs.19.4

Vaz Dos Santos E.N., Hayes J.M., Takaki T. (1998). Isotopic biogeochemistry of the Neocomian lacustrine and Upper Aptian marine-evaporitic sediments of the Potiguar Basin, Northeastern Brazil. *Organic Geochemistry*, 28(6), pp. 361-381. https://doi.org/10.1016/S0146-6380(98)00007-2

Zhuravlev V.S., Sorokov D.S. (1954) The litho-stratigraphic unit of the Cambrian sediments of the Olenek uplift. *Proc. of the Institute of Arctic geology*, 43, pp. 27-48. (In Russ.)

Zumberge J.A., Love G.D., Cardenas P., Sperling E.A., Gunasekera S., Rohrssen M., Grosjean E., Grotzinger J.P., Summons R.E. (2018). Demosponge steroid biomarker 26-methylstigmastane provides evidence for Neoproterozoic animals. *Nature Ecology & Evolution*, 2(11), pp. 1709-1714. https://doi.org/10.1038/s41559-018-0676-2

About the Authors

Dmitrii S. Melnik – Junior Researcher, Laboratory of the problems of geology, exploration and development of hard-to-recover oil, Trofimuk Institute of Petroleum Geology and Geophysics of the Siberian Branch of the Russian Academy of Sciences; Postgraduate Student, Novosibirsk State University

3, Ak.Koptyug ave., Novosibirsk, 630090, Russian Federation

E-mail: MelnikDS@ipgg.sbras.ru

Tatyana M. Parfenova – Cand. Sci. (Geology and Mineralogy), Deputy Director for Research, Trofimuk Institute of Petroleum Geology and Geophysics of the Siberian Branch of the Russian Academy of Sciences; Senior Lecturer, Novosibirsk State University

3, Ak.Koptyug ave., Novosibirsk, 630090, Russian Federation

Vladimir I. Rogov – Researcher of the Precambrian paleontology and stratigraphy laboratory, Trofimuk Institute of Petroleum Geology and Geophysics of the Siberian Branch of the Russian Academy of Sciences

3, Ak.Koptyug ave., Novosibirsk, 630090, Russian Federation

Manuscript received 18 October 2019;
Accepted 5 March 2020;
Published 30 June 2020

ORIGINAL ARTICLE
DOI: https://doi.org/10.18599/grs.2020.2.45-55

The microelement composition of caustobioliths and oil generation processes – from the D.I. Mendeleev's hypothesis to the present day

S.A. Punanova
Institute of Oil and Gas Problems of the Russian Academy of Sciences, Moscow, Russian Federation
E-mail: punanova@mail.ru

Abstract. The past 2019 is the year of the 150th anniversary of the Periodic Law discovery by D.I. Mendeleev. The international community has recognized it as the International Year of the Periodic Table of Chemical Elements. This initiative was made by the Russian Academy of Sciences, which was supported by UNESCO and the UN General Assembly. The law of D.I. Mendeleev is an interdisciplinary phenomenon, the universal language of communication between scientists – not only chemists, but also doctors, biologists, physicists, geochemists, geologists, and probably many other specialties.

The article presents the features of microelements (ME) distribution in various classes of caustobiolites in connection with the Mendeleev's Periodic Table. Their comparative assessment was carried out. MEs were identified that are concentrated in oils and shales in increased ore concentrations. Theories of oil generation developed by D.I. Mendeleev and other scientists, possible sources of ME in oils, features of the correlation dependencies of ME of the composition of oils and the Earth's crust at different levels. The polygenic source of ME in oils is substantiated, which is associated both with sedimentary rocks and organic matter (OM) buried in them, and the occurrence of ME in oils introduced from deep zones of the Earth's crust. A comparative assessment of ME composition of oil and gas basins and the composition of various geological substances indicate that the bulk of MEs are inherited by oils from OM. High enrichment by moving elements is associated with the migration activity during the formation of oil fields, while the correlation of ME oils with the chemical composition of the lower crust indicates the involvement of lower crustal fluids in this process.

Keywords: Mendeleev's Periodic Table of Chemical Elements, hydrocarbon, caustobiolith, organic matter, clay rocks, sources of microelements, oil generation, Earth's crust, clarks composition

Recommended citation: Punanova S.A. (2020). The microelement composition of caustobioliths and oil generation processes – from the D.I. Mendeleev's hypothesis to the present day. *Georesursy = Georesources*, 22(2), pp. 45-55. DOI: https://doi.org/10.18599/grs.2020.2.45-55

Introduction

There are several generally recognized geochemical classifications of elements, which are based on the Periodic Law of D.I. Mendeleev. Classifications of V.M. Goldschmidt (1923), V.I. Vernadsky (1927), A.E. Fersman (1933), N.A. Solodov (1932), A.N. Zavaritskii (1944) and others subdivide chemical elements according to their geochemical similarity, i.e., on the basis of their joint concentration in certain natural systems (Saukov, 1975).

According to the classification proposed by V.M. Goldschmidt and constructed taking into account the position of elements in the periodic system (such as electronic structure of atoms and ions, the specificity of affinity for certain anions, the position of this element on the atomic volume curve), all chemical elements are divided into 4 groups: lithophilic, chalcophilic, siderophilic and atmophilic.

V.I. Vernadsky laid down the geochemical facts as the basis of his classification: the history of chemical elements in the Earth's crust, the phenomena of radioactivity, the reversibility or irreversibility of migration (cyclicity) of elements. According to the classification of V.I. Vernadsky (Table 1), the largest number of chemical elements falls into the group of "cyclic" or organogenes (Vernadsky, 1954). Their geochemical history is expressed in circular processes (cycles), of which living matter is important for the course.

The group of cyclic elements according to V.I. Vernadsky is accepted by us as biogenic in studies on the ME assessment of caustobiolites composition.

No. group	Group	Elements	Number of elements	Content, %
I	Noble gases	He, Ne, Ar, Rr, Xe	5	5.44
II	Noble metals	Ru, Rh, Pd, Os, Ir, Pt, Au	7	7.66
III	Cyclic elements	H, Be, B, C, N, O, F, Na, Mg, Al, Si, P, S, Cl, K, Ca, Ti, V, Cr, Mn, Fe, Co, Ni, Cu, Zn, Ge, As, Se, Sr, Zr, Mo, Ag, Cd, Sn, Te, Ba, Hf, W, Re, Hg, Tl, Pb, Bi	44	47.82
IV	Dispersed elements	Li, Sc, Ga, Br, Rb, Y, Nb, In, I, Cs, Ta	11	11.95
V	Radioactive elements	Po, Rn, Ra, Ac, Th, Pa, U	7	7.61
VI	Rare earth elements	La, Ce, Pr, Nd, Pm, Sm, Eu, Gd, Tb, Dy, Ho, Er, Tm, Yb, Lu	15	16.30

Table 1. Geochemical groups of elements according to V.I. Vernadsky

When studying many ore deposits, N.A. Solodov identified 8 classes of chemical compounds: oxyphilic metals, siderophilic metals, non-metals, noble gases, lanthanides, radioactive elements, noble metals, sulfurophilic metals and metalloid elements.

In the given classifications, the inclusion of the same elements in different groups is not excluded. The classification of A.N. Zavaritskii, who divided the Table of D.I. Mendeleev into 10 blocks: 1) noble gases; 2) rock elements; 3) magmatic emanations; 4) elements of the iron group; 5) rare elements, rare earth elements; 6) radioactive elements; 7) metal ore elements; 8) metalloid and metallogenic elements; 9) platinum elements; 10) heavy halogens (Zavaritskii, 1944). A comparative analysis of caustobioliths using Mendeleev's Table shows in color the separation of elements into classes precisely according to A.N. Zavaritskii.

Comparative assessment of microelements in caustobiolites

More than 60 elements are identified in oil and its derivatives. It seems that only technical limitations prevent the detection in oils of almost all elements of the Periodic Table of Mendeleev. Their concentrations are low, but they carry important information.

As applied to them in petroleum geochemistry, the term microelements (ME) (less commonly "Trace elements" or "Spurenelementen"), introduced by A.P. Vinogradov for Zn, Br, Mn, Cu, I, As, B, F, Pb, Ti, V, Cr, Ni, Sr, found in living matter from 1 to 100 g/t; elements in concentrations from 100 to 1000 g/t were designated by him as macroelements (Vinogradov, 1931, 1956).

To assess the nature of MEs accumulation in caustobiolites, a comparison was made of 42 MEs in coals, oils (the ash content of which is assumed to be 20% and 0.1%, respectively) and shale (oil and black shale with an ash content of 50 and 80% and an OM content of 20-80% and 8-20%) of the majority of the world's basins (Table 2) (Punanova, 1974; Yudovich, Ketris, 1994, 2005, 2006; Shpirt, Punanova, 2010, 2012; Babaev, Punanova, 2014).

For comparison, the average contents – clarks of elements were used in clay rocks with an ash content of more than 90% and OM less than 8% (Vinogradov, 1962, 1970) and living matter (Kovalskii, 1970; Bowen, 1966).

The degree of ME concentration by caustobiolites (Qi) and their ashes (Qi^A) compared with their average contents in clay rocks (K) was taken as the estimated parameters. For the clarke value, a correction factor of 1.13 was used, which was not previously taken into account for calculating Qi^A, which is associated with calcining of clay rocks at a temperature of 550-900 °C, their dehydration, and weight reduction by 12-14%, which leads to a corresponding increase in the ME content in an average of 13% (Shpirt, Punanova, 2007). Oils contain insignificant amounts of mineral impurities (ash content is usually ≤0.1%), and MEs are concentrated only in organometallic compounds in a relatively small fraction with a high molecular weight, as a result of which the ME content in them is usually low. For these reasons, the concentration of ME in oil is much lower than its average content in clayey rocks. Therefore, ME contents comparison in terms of oil ash, i.e. Qi^A parameter is more informative.

The large range of changes takes place in the element concentrations in natural objects, significantly increased concentrations of many elements in the caustobiolite ash, the difference in oil ash from the content of ME from coal ash, shale and clay rocks: enrichment of the ash of oils Hg, Mo, Se, Co, Ni, V and depletion of Be, Sc, La, Pb, Zr, Ti (Fig. 1). Such significant differences in a large number of MEs can be explained by different initial organic material (higher and lower ground vegetation for coal and planktonogenic for oils and shales), as well as conditions for further OM conversion (by the redox environment, burial rate, depth and stage of compensation for deflection).

To determine the dependence of ME concentration on their general geochemical characteristics in various types of caustobiolites, the geochemical classification of A.I. Perelman was applied (Perelman, 1989).

MEs	K_1 – clarks of clay rocks	Q_i			Q_i^A				Group of MEs*
		Coal	Shale		Coal	Shale		Oil	
			oil	black		oil	black		
Li	60	0.25	1.0	0.52	1.1	1.77	0.57	–	1
Rb	130	0.12	1.07	0.57	0.53	1.95	0.63	**2.3**	1
Cs	2.0	0.32	**2.5**	**2.35**	1.42	**4.42**	**2.57**	**27.2**	1
Sr	450	0.23	0.6	0.42	1.02	0.97	0.46	0.88	1
Ba	800	0.16	0.7	0.625	0.7	1.24	0.69	0.33	1
Be	3.0	0.7	1.0	0.67	**3.1**	1.77	0.74	0.15	2
Sc	10	0.27	**1.5**	1.2	1.19	**2.65**	1.33	0.25	2
Y	26	0.29	1.0	1.0	1.28	1.85	1.11	–	2
Yb	2.2	0.43	–	1.27	1.9	–	1.41	–	2
La	90	0.13	0.4	0.31	0.58	0.7	0.34	0.09	2
Ce	50	0.42	**1.6**	1.16	1.86	**2.8**	1.28	–	2
Eu	0.95	0.42	–	1.26	1.86	–	1.4	1.43	2
Nd	26	0.36	–	1.27	1.59	–	1.41	–	2
Sm	4.5	0.38	–	1.2	1.68	–	1.33	–	2
Pr	7.1	0.34	–	0.59	1.5	–	0.65	–	2
Gd	3.8	0.47	–	1.24	**2.1**	–	1.37	–	2
Ga	20	0.32	1.0	0.8	1.4	1.77	0.88	**3.4**	2
Ge	1.6	**1.5**	1.2	**1.5**	**6.6**	**2.1**	1.67	1.32	2
B	100	0.63	1.3	0.56	**2.79**	**2.3**	0.62	–	2
Ti	4500	0.36	0.3	0.67	1.59	0.6	0.74	0.00004	3
Zr	200	0.18	0.8	0.6	0.8	1.42	0.66	0.035	3
Hf	3.0	0.4	1.3	1.4	1.77	**2.39**	1.55	–	3
Th	12	0.32	0.4	0.58	1.4	0.67	0.64	0.08	3
Sn	10	0.11	0.5	0.39	0.49	0.88	0.43	0.012	3
V	130	0.19	1.0	**1.58**	0.82	1.77	1.75	**268**	3
Nb	11	0.2	**1.6**	1.0	0.88	**2.74**	1.11	–	3
Mo	2	1.2	1.0	**10**	**5.3**	1.77	**11.1**	**538**	3
W	1.8	1.3	1.2	**1.6**	**5.75**	**2.1**	1.77	–	3
U	3.7	0.59	0.9	**2.3**	**2.6**	1.59	**2.55**	**4.8**	3
Re	0.0002	**<5**	**2.5**	**4500**	**<22.5**	**4.4**	**4978**	–	3
Cu	57	0.2	0.8	1.22	0.93	1.42	1.34	**5.7**	5
Ag	0.1	0.5	0.8	**10**	**2.2**	1.42	**11.1**	**37.2**	5
Au	0.003	**10**	0.7	**2.3**	**44**	1.15	**2.55**	**147.5**	5
Zn	80	0.35	1.25	**1.6**	1.55	**2.2**	1.77	**26**	5
Hg	0.05	**3.0**	**3.6**	**5.4**	**15.9**	**6.4**	**5.97**	**45000**	5
Pb	20	0.64	1.1	1.05	**2.8**	1.95	1.15	0.028	5
As	13	**1.45**	1.0	**2.3**	**6.4**	1.77	**2.54**	**16.9**	6
Se	0.6	**5**	**25**	**14.5**	**25**	**44**	**15.9**	**427.4**	6
Cr	100	0.14	1.0	0.96	0.62	1.77	1.06	**4.3**	7
Mn	850	0.18	0.6	0.47	0.78	1.06	0.52	0.3	7
Co	19	0.24	1.0	0.95	1.04	1.86	1.04	**14.9**	7
Ni	95	0.11	0.7	0.74	0.47	1.33	0.81	**132**	7

*Table 2. The degree of caustobioliths enrichment with microelements (Shpirt, Punanova, 2007). * groups by (Perelman, 1989); A dash in the table means that the average content of the element has not been established; MEs are shown in bold are, the enrichment of which is higher than caustobioliths clarke (Q> K), the so-called "typomorphic"[1], characteristic (Yudovich, 1978).*

[1] *Ya.E. Yudovich and M.P. Ketris, the authors of this term, no longer use it, believing it is incorrect, and instead proposed the term coaleophilic elements for coal (Yudovich, Ketris, 2002) and oileophilic for oil. According to the author, it's a very successful term that will be used in future works.*

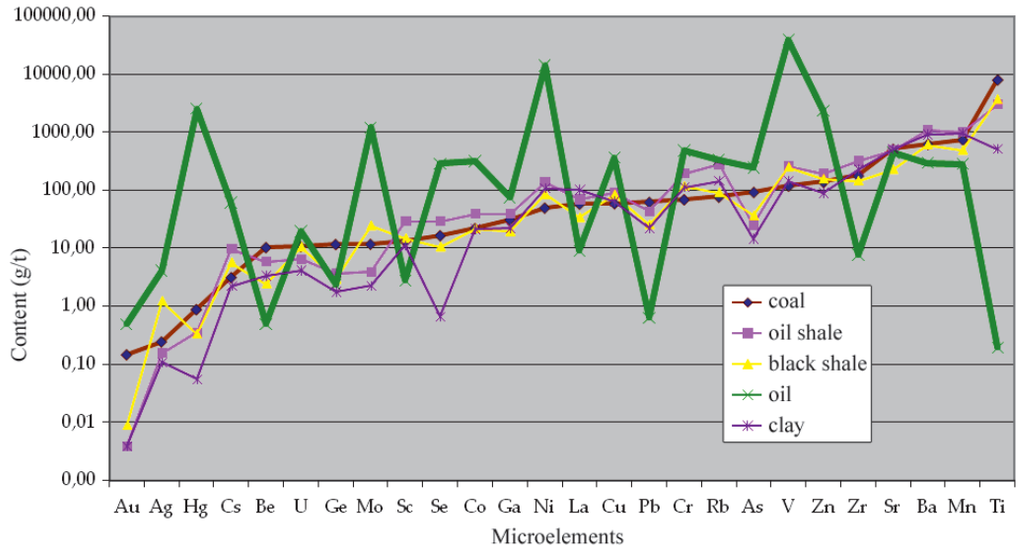

Fig. 1. The average content of microelements in the ash of caustobioliths and clay rocks (ranked by coal)

It was repeatedly used in studies of coal and black shales (Yudovich, Ketris, 1994; 2002; 2005; 2006), with the following ME groups highlighted: 1) typical cationogenic lithophiles; 2) cationic and anionic lithophiles with constant valency; 3) cationic anionic lithophiles with variable valency; 4) typical anionic lithophiles; 5) metals – thiophils; 6) non-metals – thiophils; 7) siderophiles of the iron group.

Table 2 shows a similar grouping of MEs, but group 4 is excluded, since there is no reliable information on the halogen content in oils and coal, and boron is transferred to group 2. Elements are grouped, as a rule, not in accordance with this classification. Traditional geochemical characteristics do not always allow us to explain or predict the degree of concentration of trace elements in caustobiolites, probably due to the fact that during their development the authors do not take into account the specific features of ME interaction with organic components of caustobiolites and, possibly, do not take into account their content in the initial humic or sapropelic material.

By high values of caustobioliths enrichment with microelements, especially oil and black shale ash, ME of groups 5, 6 and 7 (thiophils and siderophiles) – Hg, Se, Au, Ni, Ag, Zn, As, Co, Cr, with the exception of Cu are quite homogeneous. From ME of the 1st group, only Cs is concentrated in caustobiolites. Lanthanides having very similar chemical properties (group 2) differ significantly in their degree of concentration in caustobiolites. This peculiar distribution of individual lanthanides, for example, Eu is also detected for the oils of individual deposits (Gottikh et al., 2009). All caustobiolites are significantly enriched only in Mo and Re (group 3). It should be noted the differentiation in coals of alkali metals and REEs in terms of the Qi^A coefficients: for Li, Rb, Sc, La, Qi^A <Ki, and for Cs, Y and other lanthanides higher than 1.13Ki.

Works (Yudovich, Ketris, 2005, 2006), as previous publications of these authors (Yudovich, Ketris, 2002) present calculations of clarke concentrations of elements in coals. When replenishing analytical data, these figures are recalculated by the authors. The authors write: "The basis for the calculations was created by M.P. Ketris is a unique Coal Geochemistry Database with tens of thousands of analyzes across all coal basins in the world. This database, continuously updated with new analytical data, made it possible to quickly form fairly homogeneous samples and calculate sample averages, and then *evaluate coal clarke as the median content in the aggregate of sample averages*" (Yudovich, Ketris, 2006, p. 488, authors emphasized).

In our studies of comparing the ME of caustobioliths composition, we rely on the calculations performed by us and published in a number of articles and monographs (Shpirt, Punanova, 2012).

Figure 2 shows the degree of ME concentration (Qi^A) calculated on the ash of caustobiolites. The curves in the graph are ranked by the Qi^A of oils. The most dramatic differences are observed when comparing the ME contents in oil and clay rocks. A large group of elements is distinguished by which oil ash is significantly enriched in comparison with clay – Co, As, Zn, Cs, Ag, Ni, Au, V, Se, Mo, Hg, Cu. The contents of Ti, Pb, Zr, Th, La, Be are significantly lower than their contents in clays, and the concentrations of Sc, Mn, Ba, Sr, Ge, Rb, Ga, Cr are very close. Concentrations of the majority of MEs in coals are either lower or not statistically different from their average contents in clay rocks (1.13Ki values) and only statistically higher for Au, Se, Mo, Hg, Ge, As. Significantly less difference in the degree of enrichment of the ME of oil and black shales compared with clay clarks: black shales are enriched in Ag, Se, Mo, Hg, and combustibles are enriched in Cs, Se.

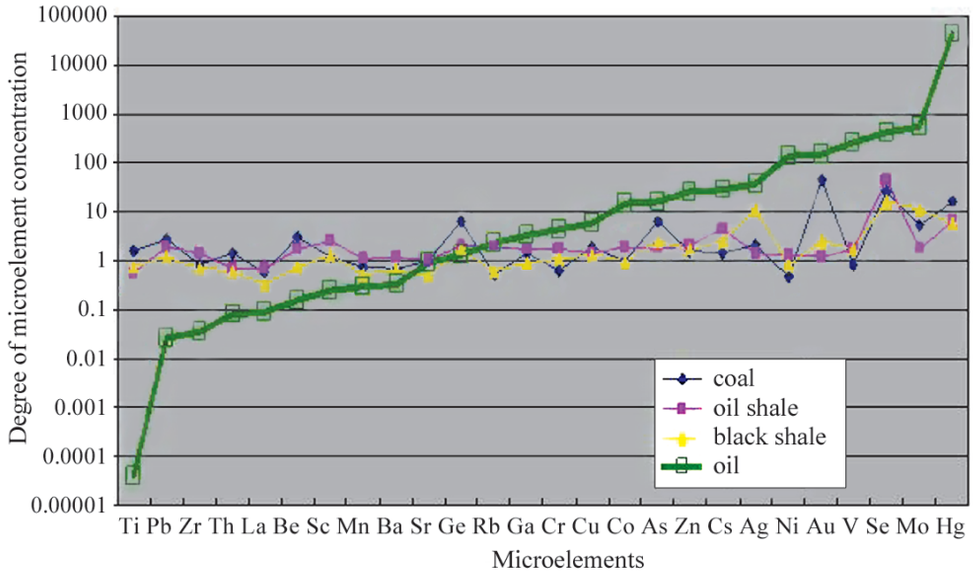

Fig. 2. The degree of microelement concentration in the ash of caustobioliths and shales in relation to clay clarks (ranked by oil)

It can be stated that the same MEs (biophilic elements) are characterized by the highest degree of concentration in all types of caustobiolites, which confirms their genetic unity.

Unfortunately, a number of elements with undefined average data were excluded when plotting. The conclusions obtained are obviously valid only for the average ME contents in caustobiolites, while the comparative indicators for oils, shales, and coals of individual deposits may be different due to the significant difference in the ME contents from the average.

Table 3 shows the "typomorphic" elements, classified by the values of the coefficients Qi>1.4 and Qi^A>2.0, in coal, oil shale (combustible and black) and oils, arranged in rows in decreasing Qi or Qi^A. MEs with approximately the same values of Qi or Qi^A are given in parentheses.

The common "typomorphic" MEs (by dry weight content) for coals and shales (black or combustible) are Au, Se, Hg, Re; coals differ from schists only in "typomorphic" Ge. A significantly larger number of MEs can be considered as "typomorphic" in the value of the Qi^A parameter, i.e. according to the contents calculated on the ash of caustobiolites. By the number of "typomorphic" MEs according to this parameter, caustobiolites are located in the sequence: oil (16) > coal (14) > oil shale (12) > black (9). The number of "typomorphic" elements is given in parentheses. Caustobiolites have many common "typomorphic" MEs. In terms of Qi^A, Ag, Au, As, Hg, Mo, Re, Se, U, W are common "typomorphic" MEs for coals, black shales and oils. According to the Qi^A parameter, MEs that are "typomorphic" for only one type of caustobiolite can be distinguished , namely: for coal – Ge and Be, possibly Pb, probably Gd; oil shale – Ce, Nb, Sc, Hf; there are no black shales; oils – V, Ni, Co, Cu, Cr, probably Ga, Rb. Therefore, in comparison with other types of caustobioliths, oil ash is the richest ME. It differs both in the number of all "typomorphic" MEs and in the number of "typomorphic" MEs that are characteristic of only one type of caustobioliths considered, which may indicate the complexity and multifactorial nature of oil formation processes.

Figures 3 and 4 using the Periodic Table of D.I. Mendeleev present a comparative average characteristic of ME concentration in oil ashes and in black shales relative to clay clarks and taking into

Caustobiolites	"Typomorphic" MEs	
	By dry weight Q_i > 1.4	By ashe Q_i^A > 2.0
Coal	Au, Se, Hg, Re, Ge, As	Au, Se, Hg, Re, **Ge**, As, W, Mo, **Be**, (B, **Pb**), U, Ag, **Gd**
Oil shale	Se, Hg, (Re, Cs), (Ce, Sc, Nb)	Se, Hg, (Re, Cs), **Ce, Sc, Nb, Hf,** B, Zn, (W, Ge)
Black shale	(Zn, W, Ge, V), Re, Se, (Ag, Mo), Hg, (Cs, As, Au, U)	Re, Se, (Ag, Mo), Hg, (Cs, As, Au, U)
Oil	-	Hg, Mo, Se, **V**, Au, **Ni,** Ag, Cs, Zn, As, **Co,** U, **Cu, Cr, Ga, Rb**

Table 3. "Typomorphic" MEs in various caustobiolites. MEs that are "typomorphic" for only one type of caustobiolite are shown in bold

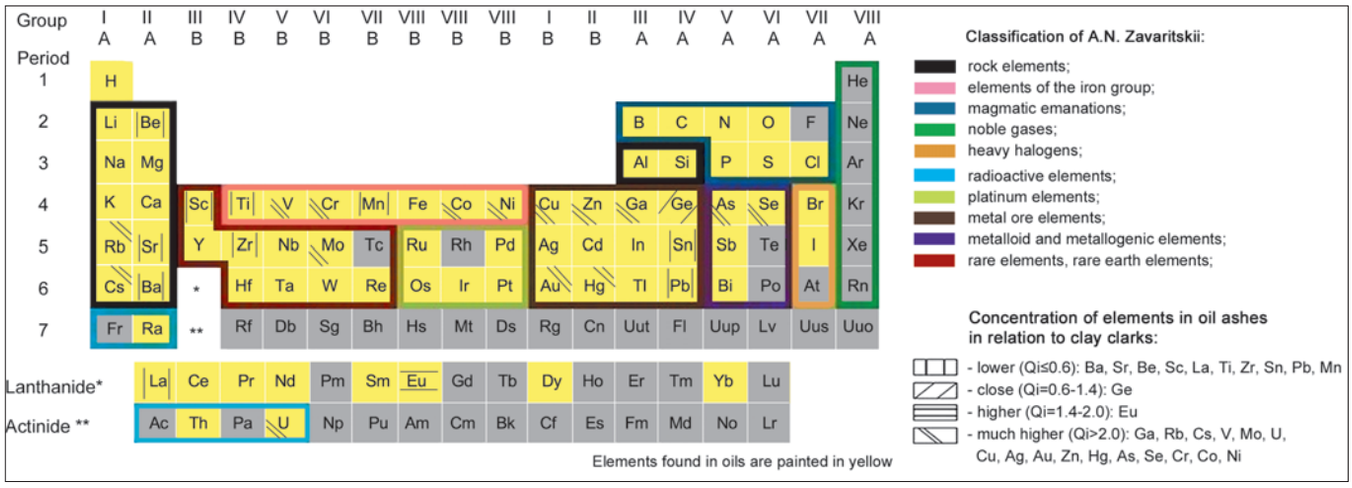

Fig. 3. Element concentrations in oil ashes relative to clay clarks

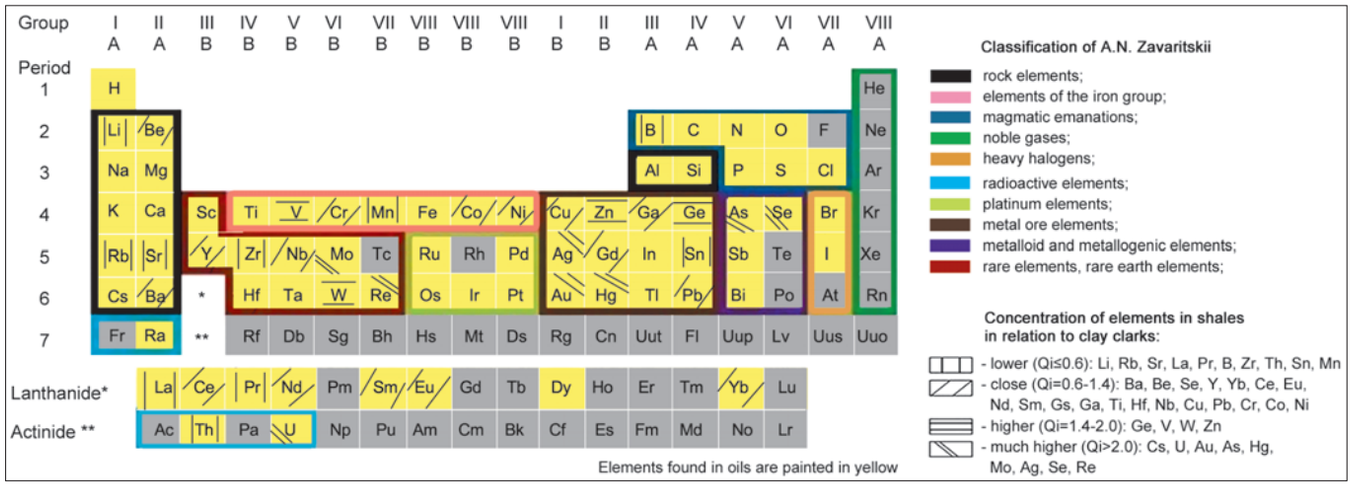

Fig. 4. Element concentrations in oil shales relative to clay clarks

account the classification of elements according to A.N. Zavaritskii. We have identified four gradations of statistical evaluation. An analysis of these data underlines the wide variety of ME composition in caustobiolites. The group of elements enriching caustobiolites includes rock elements, iron groups, metal, rare, metalloid, and radioactive. In terms of enrichment, two groups of elements are distinguished. The maximum values are characteristic of the so-called elements highly mobile under the Earth's crust (Hg, Se, Mo, Sb, As, Cd, Pb, Bi, etc.), which probably indicates the activity of migration processes during the formation of hydrocarbon (HC) deposits.

In some cases, the enrichment values are similar to the concentrations of elements in ore deposits, which makes it possible to use caustobiolite deposits in a complex manner, i.e. and as a potential source of a number of ore elements.

This provision indicates the relevance of the instructions of D.I. Mendeleev on the extreme value of oil as a complex chemical feedstock.

Sources of MEs in oils and problems of naftidogenesis

D.I. Mendeleev was a versatile scientist and, along with the development of the Periodic Law and the creation of the Periodic Table of Chemical Elements, was widely known and a significant contributor to other fields of science. October 15, 1876 at a meeting of the Russian Chemical Society D.I. Mendeleev presented a report in which he offered his views on the problem of oil formation. According to his hypothesis, during formation of mountains, water flows deep into the Earth through faults and/or cracks. In the interaction of water with iron carbides under the influence of high temperatures and pressure, iron and hydrocarbon oxides are formed, which rise upward along the same faults and, filling up porous rocks, accumulate and form oil deposits (Mendeleev, 1877). Probably the work of D.I. Mendeleev at the Baku oil fields and in Pennsylvania (USA), as well as his chemical experiments, which testified to the possibility of such processes, reinforced his ideas. Model of D.I. Mendeleev still serves as one of the starting points

of the abiogenic origin of oil hypothesis in its various modifications, and according to (Pikovskii, 2012), the majority of those issues put forward by D.I. Mendeleev are relevant today, and are the subject of study and discussion today.

M.V. Lomonosov is another great Russian scientist and the founder of an alternative biogenic model of oil generation. M.V. Lomonosov was one of the first who drew attention to the problem of the "emergence" of oil. In 1763, in the famous work "On the Layers of the Earth," he wrote about oil as follows: "Meanwhile, it is expelled by underground heat from prepared coals of brown and black oil matter and appears in different crevices and cavities, dry and moist, filled with water...". Since it was believed (and is believed) that coals came from plant debris, oil was also attributed to plant origin, "... oil was formed as a result of decomposition of organic matter under the influence of underground heat" (Lomonosov, 1763). Currently, after almost 150 years since the proclamation of D.I. Mendeleev of his views and more than 250 years since the publication of the work of M.V. Lomonosov's problems of naphthytogenesis are still competing with biogenic and abiogenic models of oil formation. There are also concepts of oil polygenesis (Dmitrievskii, 2008, etc.).

A significant contribution to the development of oil generation models is made by V.I. Vernadsky, I.M. Gubkin, N.B. Vassoevich, A.E. Kontorovich, N.A. Kudryavtsev, P.N. Kropotkin, B. Tisso and D. Velte, K. Peters and J. Moldovan and many, many other researchers.

At the 29th World Congress on Organic Geochemistry held in September in Sweden (All Abstracts EAGE-IMOG, 2019), most of the reports were devoted to the results of studying, at a modern instrumental level, of structural features and the conversion of initial organic material into oil hydrocarbon during diagenesis and metamorphism considering different oil and gas basins of the world. In the framework of the "sedimentary-migration theory", the source of oil generation is "living matter" (the term of V.I. Vernadsky), which, when immersed and heated in the sedimentary strata, is gradually transformed into "micro-oil" (Vassoevich et al., 1967).

Scattered hydrocarbons, then migrating along the sedimentary stratum under the influence of a stress field and saturating various types of reservoir traps, form deposits. According to V.I. Vernadsky (1954), confirmed by further geochemical studies, the total amount of dispersed oil in the sedimentary shell of the Earth is much higher than the total amount of oil in the fields (Galimov, Kamaleeva, 2015; Tisso, Velte, 1981; Kontorovich, 2004; Neruchev, Smirnov, 2007; Neruchev, 2013; Skorobogatov, Solov'ev, 2013; Mukhametshin, 2019) and others. Within the framework of such a model, increased OM concentrations in sedimentary rocks are the main factors controlling the oil and gas potential of the basin, heating them to the required temperature (stagewise catagenetic transformation), and the presence of insulating screens fluid supports and trap reservoirs. In this regard, it is worth highlighting a rather vivid statement by V.I. Vernadsky on the unity of shale and oil hydrocarbons: "Two types of deposits for oil accumulations can be noted: 1) accumulation in sedimentary rocks; 2) penetration (saturation) of bituminous shale hydrocarbons. Both types can be considered as parts of the same phenomenon. Being in shale contains the largest masses of oil". Summing up all his evidence base of the biogenic hypothesis, V.I. Vernadsky came to the conclusion that "the formation of oils is of great importance in transferring the energy of the Sun through living matter to the deeper layers of the planet" (Vernadsky, 1994 a, b)

Existing abiogenic models can describe the synthesis of only some components of oils, but not of all their diversity, not to mention hydrocarbons - chemofossilia-biomarkers. Chemofossilia are fossil biomolecules, their recognizable fragments and genetic analogues, which are undoubted and often found in oils fragments of living matter (Peters, Moldovan, 1993; Vassoevich et al., 1967) and others.

The development of the oil genesis theory led to the development of more complex models of oil generation. Back in 1993, the founders of modern petroleum organic geochemistry B.A. Sokolov and A.N. Guseva (1993) wrote: "Oil and gas are renewable natural resources and their development should be built on a scientifically based balance of hydrocarbon generation volumes and extraction during field exploitation." These authors draw attention to the high rates of chemical reactions during the destruction of organic matter and its transformation into mobile gas-liquid hydrocarbons (which occurs under certain natural conditions), which are completely incompatible with the rates of sedimentary strata subsidence and their catagenetic transformation due to slow heating. Hydrocarbon fluid motion also occurs at much greater speeds than previously assumed. Oil manifestations in the rift depressions of the Gulf of California (Guyamas field), in the caldera of the Uzon volcano in Kamchatka serve as examples. Under the influence of high temperatures of hydrotherms, from the sedimentary rocks OM, immature oils were formed here, whose age is estimated at several hundred years (Simoneit, 1986; Sokolov, Guseva, 1993; Punanova, Vinogradova, 2017).

In the modern version of the oil origin theory, the nonlinear (i.e., strongly thermodynamically nonequilibrium) nature of naftidogenesis is indicated and the contribution of abiogenic sources to the formation of hydrocarbon deposits is allowed (Kontorovich,

2004). In the framework of the fluid dynamic model, the importance of an active fluid regime is emphasized when intense upward and downward fluid flows provide the supply and removal of matter and energy from the focus of oil generation (Sokolov, 1996).

As can be seen from the above, the process of oil formation is complex in nature, due to a combination of exogenous and endogenous factors. In assessing the influence of deep and sedimentary processes on the oil formation, interpretation of the data on the ME composition of naphthides can significantly help.

To date, there is no single, well-defined point of view on the source of ME in oils. The analysis and generalization of a large amount of factual material gives us the opportunity to argue for the existence of three sources of ME in oils – inherited from living matter, borrowed by oil from surrounding rocks and formation water and introduced into permeable zones from deep sections of the Earth's crust, i.e. their polygenic origin (Punanova, 2004; Rodkin, Punanova, 2019).

It has been established that when studying the processes of oil formation, the "biogenic" elements (defined by V.I. Vernadsky, 1954) that are present in oils: V, Ni, Zn, Cu, Fe, Co, As, Mo, Ag, I, Br, B et al. Comparison of the "concentration fields" of a large group of elements in oil, oil ash and living matter showed that it is precisely these "biogenic" elements that show the closest similarity between oil and living matter, but a significant difference from the distribution of elements in clay rocks (Punanova, 2004, 2016). Based on this, it has been suggested that the source of a large group of elements in oils is living matter. The inheritance of the ME composition of oils from the initial OM is confirmed by detailed studies conducted by us in the Volga-Ural, Timan-Pechora, North Caucasus-Mangyshlak, West Siberian and other oil and gas basins. With the "oil – dispersed OM" correlation, the composition of precisely "biogenic" elements shows clear genetic relationships, the oil source strata are diagnosed, the types of OM are differentiated, and parallelism in the stages of their catagenetic transformation is established (Punanova, 2017). Features of the "biogenic" elements distribution in oils are clearly linked to the genetic code of oils, expressed in a specific composition of their biotags.

There are MEs that could accumulate in oil during its interaction with formation water and sedimentary rocks. The metal content of oils is to some extent determined by the enrichment by metals of the surrounding rocks both within the sedimentation basin and in the areas of demolition of terrigenous material, and the presence of ore deposits. These can be rock-forming elements, or elements with variable valency – Si, Al, Ti, K, Na, Ca, Mg, Ba, Sr, U, etc. The exchange of elements between oil and the environment, i.e. borrowing is recorded in the oils of the Timan-Pechora oil and gas deposits, the South Tajik Depression and other regions and is reflected in model experiments (Punanova, 2017).

The fact that so-called "abiogenic" elements – As, Hg, Sb, Li, Al, B, radioactive, lanthanides, REEs – are found to be very important in oils (Vinokurov et al., 2010). Despite the poor knowledge of these elements and their very low concentration, he points to the possibility of introducing elements into the oil through the fracture zones in the body of the basement formations, to the effect on the composition of oils of the upper and lower continental crusts on the ME, to the probability of hydrocarbon accumulations directly in the deep deposits of the earth bark – in loose basement rocks, in unconventional reservoirs. All this is an additional argument in favor of a wide and comprehensive study of the basement, as an unconventional hydrocarbon storage device and a possible ME supplier.

However, the assignment of elements identified in oils to a particular group of sources – to inherited, borrowed or introduced, is very conditional. Some "biogenic" elements (V, As, Cu, Fe) in certain geological and geochemical conditions enter the oil from the environment, while a number of borrowed elements (K, Na, Mg, Ca) can be partially inherited from the initial OM. The same may apply to abiogenic elements. Some of them can also be associated with living matter and with the original organic matter. However, despite the polygenicity of the source of all MEs in oils, the biogenic complex of elements is different from the composition of the host rocks and magmatic emanations and is dominant. It is paragenetically bound in oils and organisms and initially forms the ME type of oil – vanadium or nickel.

The materials presented above on the polygenic character of ME composition of oils are partly of a qualitative nature, making it impossible to quantitatively compare the contribution of the lower and upper crust components and living matter to the formation of the ME in oils. To obtain quantitative estimates of the close relationship between the ME of the oil composition with various reservoirs and biota, the correlation coefficients between the concentrations of chemical elements were calculated (Rodkin et al., 2016). These studies are described in detail in previous works (Punanova, Rodkin, 2019; Rodkin, Punanova, 2019), in which it was shown that for some oil and gas basins there is a systematically higher correlation between the ME composition of oils and the chemical composition of the middle and lower continental crust than with the upper one (according to analytical data (Fedorov et al., 2007; Taylor, McLennan, 1988)). A more detailed study of oils in fields of the Romashkino group of the Volga-Ural oil and gas basin showed that downstream from the Tula sediments of the Lower Carboniferous to the Pashian sediments of the Upper Devonian, the relationship between the ME

composition of oils and the composition of the crust of various levels is steadily increasing. Moreover, the magnitude of the correlation of the ME composition of oils with various geo reservoirs and the chemical composition of biota is noticeably smaller than for coal and shale, which apparently indicates a more complex multifactorial nature of naphthydogenesis. In this case, a high correlation between the ME composition of the studied oils and the composition of both marine and terrestrial biota (r = 0.81) is revealed. Moreover, the relation between the ME composition of oils and the ME composition of terrestrial biota is somewhat higher, which corresponds to the data on the mixed type of the initial organics in these deposits – sapropelic-humic. The number of elements by which the correlation coefficients of concentration logarithms were calculated was different in different cases, but always quite large, varying from 30 to 50. When comparing biogenic (V, Cr, Co, Ni, Cu, Zn) and conditionally deep (Li, Be, La, Sm, Al, Eu) elements in the satellite oils of the Romashkino group of fields (according to analytical data (Maslov et al., 2015)), as well as in the oils of the Abdrakhmanovsky and Berezovsky areas (according to analytical data (Ivanov et al., 2013)), uncorrelated changes in various samples of the concentrations of these two groups of elements were established. On the contrary, when comparing the nature of the distribution of element contents in one putative genetic group, biogenic, namely V and Ni, there is a close relationship between the concentrations of these elements in the oil and gas complexes of different age in the Romashkino group of fields. The uncorrelated changes in the concentrations of biogenic and deep elements with a fairly high correlation of changes in the concentrations of elements within these groups indicates the independent supply of biogenic and deep elements from various sources, and the total concentration of biogenic elements is about 3 orders of magnitude higher, which reflects the crucial role of OM in the oil formation (Punanova, Rodkin, 2019).

Other regularities of the correlation between the ME of the oil composition and the composition of the Earth's crust were obtained using the oils of the West Kamchatka oil field and oil manifestations of the Uzon volcano caldera (according to analytical data (Dobretsov et al., 2015)). Higher correlation coefficients of the oil composition with the composition of the upper crust, not lower one, are noted here. It seems that the traced characteristics of the correlation can be explained by oil ontogenesis in the studied mineral water bodies, which are caused by the peculiarities of geodynamics and the tectonic structure (Kravchenko, 2004). Research of N.B. Vassoevich, V.I. Sokolov, K. Peters, J.M. Moldovan, A.A. Petrov, V.A. Chakhmakhchev, V.F. Kamyanov, A.K. Golovko et al. showed that in the sedimentary section of the Earth's crust, according to the vertical evolutionary zonation of hydrocarbon formation and transformation due to changes in depth, temperature gradient, pressure and type of initial organics, the composition of hydrocarbon systems generated in the bowels is transformed – from heavy oils to light and condensates. Thus, oils of increased catagenic transformation are more susceptible to deep processing and are characterized by a set of ME associated with lighter oil components, some of which are probably associated with deep processes in the bowels of the Earth, with the products of mantle emanation in areas of its activation and high geodynamic stress. Often, the abnormal enrichment of oil in the hyperegenesis zone of V, Ni, Mo, Re, Cd, Hg and other elements can be explained by their endogenous input under the influence of intrusions and hydrothermal accumulations of asphalt bitumen mainly within the folded areas (Ural, Koryak-Kamchatka, Andean, Apennine and etc.) and the introduction of Hg, Cd, Sb into oil with gas emanations in the zones of deep faults (the Pre-Carpathian Trough, California basins, etc.). Oil deposits of this type, as a rule, of vanadium metallogeny are associated with active geodynamic zones of the reformation and relocation of tectonic structures (Goldberg et al., 1990; Yakutseni, 2005; Punanova, 2017). The oils of these oil and gas regions are characterized by relatively higher correlation coefficients of the ME composition of the lower crust compared to the upper. On the other hand, the oils of the main oil formation zone and early generation oil bear the influence of the upper sedimentary crust to a greater extent, contain more elements associated with the starting organic material: V, Ni, Mo, Co, etc., and exhibit higher correlation dependencies of its ME composition in the upper crust compared to the lower crust (Punanova, Rodkin, 2019; Punanova, 2019).

Conclusion

Thus, the distribution of MEs in various classes of caustobioliths in connection with the Periodic Table of D.I. Mendeleev was characterized, their comparative assessment was carried out and MEs were identified that are concentrated in oils and shales in elevated, sometimes ore concentrations. The interpretation of hydrocarbon deposits as a production resource as well as of a number of ore elements additionally justifies the relevance of D.I. Mendeleev indication on the extreme value of oil as a complex chemical feedstock.

Theories of naftidogenesis and the contributions of D.I. Mendeleev are briefly described. Analysis of the ME of oil compositions of various oil and gas basins, the Earth's crust of different levels and biota suggests that the bulk of the ME is inherited by oil from OM rocks, which confirms the organic source of hydrocarbon oil. High enrichment with moving elements also indicate the activity of migration processes during the formation of

hydrocarbon accumulations, while the high correlation of ME oils with the chemical composition of the lower crust indicates the involvement of lower crustal fluids in the migration process. These new data on the influence of the Earth's crust composition of at various levels on the ME characterization of oils emphasize the complex nature of oil formation and the influence of deep processes.

A deeper introduction of a large amount of factual material on the composition of microelements of naphthides into the system of the Periodic Law of Chemical Elements is to be made, which will open up perhaps still unknown pages of this connection and will help to correctly solve the most important issues of petroleum geology and geochemistry.

It is important to continue developing naftidogenesis theory, is not constrained by the restrictive framework, and it goes clearly along the lines that were predetermined many years ago: M.V. Lomonosov pointed to the source – the substance – the living, and D.I. Mendeleev – on thermodynamics, the influence of deep-seated processes that supply heat to transform organics. A microelement tag of caustobioliths confirms the validity of these views.

Acknowledgements

This work was carried out as part of a state assignment on the topic: "Development of the scientific and methodological foundations of the search for large hydrocarbon accumulations in non-structural traps of a combined type within platform oil and gas basins", AAAA-A19-119022890063-9

The author thanks the reviewer Doctor of Geological and Mineralogical Sciences Ya.E Yudovich for the in-depth study of the manuscript and valuable and constructive comments.

References

Babaev F.R., Punanova S.A. (2014). Geochemical aspects of the trace element composition of oils. Moscow: Nedra, 181 p. (In Russ.)

Dmitrievskii A.N. (2008). Polygines of oil and gas. *Doklady Academii Nauk*, 419(3), pp. 373-377. (In Russ.)

Dobretsov N.L., Lazareva E.V., Zhmodik S.M. et al. (2015). Geological, hydrogeochemical and microbiological features of the oil platform of the Uzon caldera (Kamchatka). *Russian Geology and Geophysics*, 56(1-2), pp. 56-88. (In Russ.)

Fedorov Yu.N., Ivanov K.S., Erokhin Yu.V., Ronkin Yu.L. (2007). Inorganic geochemistry of oil in Western Siberia (the first results of a study using ICP-MS). *Doklady Academii Nauk*, 414(3), pp. 385-388. (In Russ.)

Galimov E.M., Kamaleeva A.I. (2015). Source of hydrocarbons from the supergiant oil field Romashkino (Tatarstan) – inflow from the crystalline basement or oil source sediments? *Geochemistry International*, 53(2), pp. 95-112. https://doi.org/10.1134/S0016702915020032

Goldberg I.S., Mitskevich A.A., Lebedeva G.V. (1990). Hydrocarbon-metal-bearing provinces of the world, their formation and allocation. *Coll. papers: Problems of resource assessment and integrated development of natural bitumen, high viscosity oils and associated metals*. Leningrad: VNIGRI, pp. 49-60. (In Russ.)

Gottikh R.P., Vinokurov S.F., Pisotskii B.I. (2009). Rare earth elements as geochemical criteria for endogenous sources of trace elements in oil. *Doklady Academii Nauk*, 425(2), pp. 223-227. (In Russ.)

Ivanov K.S., Biglov K.Sh., Erokhin Yu.V. (2013). The trace element composition of the oils of the Republic of Tatarstan (on the example of the Romashkinskoye field). *Vestnik of the Institute of Geology of the Komi Science Centre UB RAS*, 8, pp. 2-6. (In Russ.)

Kontorovich A.E. (2004). Essays on the theory of naftidogenesis: Selected articles. Ed. S.G. Neruchev. Novosibirsk: SO RAN, Geo, 545 p.(In Russ.).

Kovalskii V.V. (1970). Biogenic elements. Great Soviet Encyclopedia, 3rd ed., pp. 327-328. (In Russ.)

Kravchenko K.N. (2004). Basin basis of the general theory of naftidogenesis. Moscow: Priroda, 66 p. (In Russ.)

Lomonosov M.V. (1763). On the layers of the Earth. The second addition to the "First foundations of metallurgy or ore business. St. Petersburg: Imperial Academy of Sciences, pp. 237-416. (In Russ.)

Maslov A.V., Ronkin Yu.L., Lepikhina O.P., Izotov V.G., Sitdikova L.M. (2015). Trace elements in the oils of some satellite fields of the Romashkinsky oil field (Republic of Tatarstan). *Litosfera = Lithosphere*, 1, pp. 53-64. (In Russ.)

Mendeleev D.I. (1877). The origin of oil. *Zhurnal Russkogo khimicheskogo obshchestva i fizicheskogo obshchestva* [Journal of the Russian Chemical Society and Physical Society]. Is. 2, part chem., pp. 36-37. (In Russ.)

Mukhametshin R.Z. (2019). About the "facts of renewability" of hydrocarbon reserves in the developed oil and gas fields. *Proc. Int. Sci.-Pract. Conf.: Hydrocarbon and mineral resources potential of the crystalline basement*. Kazan: Ikhlas, pp. 242-245. (In Russ.)

Neruchev S.G. (2013). Transformation of planet Earth by living matter of the biosphere. *Neftegazovaya Geologiya. Teoriya I Praktika = Petroleum Geology - Theoretical and Applied Studies*, 18(1). (In Russ.) http://www.ngtp.ru/rub/10/4_2013.pdf

Neruchev S.G., Smirnov S.V. (2007). Assessment of potential hydrocarbon resources based on modeling the processes of their generation and formation of deposits. *Neftegazovaya Geologiya. Teoriya I Praktika = Petroleum Geology - Theoretical and Applied Studies*, 2. (In Russ.) http://www.ngtp.ru/rub/1/013.pdf

Perel'man A.I. (1989). Geokhemistry. 2nd edition. Moscow: Vysshaya shkola, 420 p. (In Russ.)

Pikovskii Yu.I. (2012). Memoirs of D.I. Mendeleev on the mineral origin of oil (modern reading). *Proc.: Earth degassing and the genesis of oil and gas fields*. Moscow: GEOS, pp. 198-239. (In Russ.)

Punanova S.A. (1974). Trace elements of oils, their use in geochemical studies and the study of migration processes. Moscow: Nedra, 244 p. (In Russ.)

Punanova S.A. (2004). About the polygenic nature of the source of trace elements of oils. *Geokhimiya = Geochemistry*, 8, pp. 893-907. (In Russ.)

Punanova S.A. (2017). Trace elements of naphthides in the process of ontogenesis of hydrocarbons due to petroleum potential. *Dr. geol.-min. sci. diss*. Moscow, 288 p. (In Russ.)

Punanova S.A. (2019). Trace elements of naphthides in oil and gas basins. *Doklady Academii Nauk*, 488(5), p. 103-107. (In Russ.)

Punanova S.A., Rodkin M.V. (2019). Comparison of the contribution of differently depth geological processes in the formation of a trace elements characteristic of caustobiolites. *Georesursy = Georesources*, 21(3), pp. 14-24. https://doi.org/10.18599/grs.2019.3.14-24

Punanova S.A., Vinogradova T.L. (2017). Geochemical features of oils of hydrothermal origin. *Geologiya, geofizika i razrabotka neftyanyh i gazovyh mestorozhdeniy = Geology, geophysics and development of oil and gas fields*, 6, pp. 32-36. (In Russ.)

Rodkin M.V., Punanova S.A. (2019). Ideas of D.I. Mendeleev and processes of naftidogenesis. *Priroda*, 10, pp. 14-21. (In Russ.)

Rodkin M.V., Rundkvist D.V., Punanova S.A. (2016). On the question of the relative role of the bottom and upper crust processes in the formation of the trace element composition of oils. *Geokhimiya = Geochemistry International,* 11, pp. 1025-1031. (In Russ.)

Saukov A.A. (1975). Geochemistry. 4th ed. Moscow: Nauka, 477 p. (In Russ.)

Shpirt M.Ya., Punanova S.A. (2007). Comparative evaluation of the trace element composition of coal, oil and shale. *Khimiya tverdogo topliva*, 5, pp. 15-29. (In Russ.)

Shpirt M.Ya., Punanova S.A. (2010). Features of the microelement composition of coals, shales and oils of various sedimentary basins. *Khimiya tverdogo topliva*, 4, pp. 57-65. (In Russ.)

Shpirt M.Ya., Punanova S.A. (2012). Microelements of caustobioliths. Problems of genesis and industrial use. Saarbrucken. Germany: Lambert Academic Publishing, 367 p. (In Russ.)

Simoneit B.R.T. (1986). Organic Maturation and Oil Formation: The Hydrothermal Aspect. *Geokhimiya = Geochemistry International*, 2, pp. 236-254. (In Russ.)

Skorobogatov V.A., Solov'ev N.N. (2013). Comparative analysis of the conditions of oil and gas accumulation in the West Siberian and Arab-Persian megabasins. *Vesti gazovoi nauki*, 5(16), pp. 43-52. (In Russ.)

Sokolov B.A. (1996). Fluidodynamic model of oil and gas formation. *Moscow University Geology Bulletin*, 4, pp. 28-36. (In Russ.)

Sokolov B.A., Guseva A.N. (1993). About the possibility of fast modern generation of oil and gas. *Moscow University Geology Bulletin*, 3, pp. 39-46. (In Russ.)

Teilor S.R., Mak-Lennan S.M. (1988). Continental crust: its composition and evolution. Moscow: Mir, 384 p. (In Russ.)

Tisso B., Velte D. (1981). Formation and distribution of oil. Moscow: Mir, 501 p. (In Russ.)

Vassoevich N.B., Guseva A.N., Leifman I.E. (1967). Biogeochemistry of oil. *Geokhimiya = Geochemistry International*, 7, pp. 1057-1084. (In Russ.)

Vernadsky V.I. (1954). Chemical elements and the mechanism of the Earth's crust. Selec. papers, v. 1. Moscow: USSR Academy of Sciences, pp. 513-519. (In Russ.)

Vernadsky V.I. (1994a). Essays on geochemistry. 8th ed. In the book: *Library of Works of Ac. V.I. Vernadsky. Proceedings in geochemistry*. Moscow: Nauka, pp. 159-468. (In Russ.)

Vernadsky V.I. (1994b). Biosphere. 5th ed. In the book: *Library of Works of Ac. V.I. Vernadsky. Living matter and the biosphere*. Moscow: Nauka, pp. 315-401. (In Russ.)

Vinogradov A.P. (1931). The chemical elemental composition of marine organisms in connection with the issues of their systematics and morphology. *Priroda*, 3, pp. 230-254. (In Russ.)

Vinogradov A.P. (1956). Regularities of distribution of chemical elements in the Earth's crust. *Geokhimiya = Geochemistry International*, 1, pp. 6-52. (In Russ.)

Vinogradov A.P. (1962). SThe average content of chemical elements in the main types of igneous rocks of the earth's crust. *Geokhimiya = Geochemistry International*, 7, pp. 551-571. (In Russ.)

Vinogradov A.P. (1970). Biogeochemistry. BSE. 3rd ed., v. 3, pp. 329-330. (In Russ.)

Vinokurov S.F., Gottikh R.P., Pisotskii B.I. (2010). Features of the distribution of lanthanides in resinous-asphaltene fractions is one of the geochemical criteria for the sources of trace elements in oil. *Geokhimiya = Geochemistry International*, 4, pp. 377-389. (In Russ.)

Yakutseni S.P. (2005). Prevalence of hydrocarbon raw materials enriched with heavy impurity elements. Environmental risk assessment. St.Petersburg: Nedra, 372 p. (In Russ.)

Yudovich Ya.E., Ketris M.P. (2006). Valuable impurities in coals. Yekaterinburg: Nauka, 538 p. (In Russ.)

Yudovich Ya.E. (1978). Geochemistry of fossil coals. Leningrad: Nauka, 264 p. (In Russ.)

Yudovich Ya.E., Ketris M.P. (1994). Impurity elements in black shales. Yekaterinburg: Nauka, 304 p. (In Russ.)

Yudovich Ya.E., Ketris M.P. (2002). Inorganic substance of coals. Yekaterinburg: UrO RAN, 422 p. (In Russ.)

Yudovich Ya.E., Ketris M.P. (2005). Toxic impurity elements in fossil coals. Yekaterinburg: UrO RAN, 655 p. (In Russ.)

Yudovich Ya.E., Ketris M.P. (2006). Valuable impurities in coals. Yekaterinburg: Nauka, 538 p. (In Russ.)

Zavaritskii A.N. (1944). Introduction to petrochemistry of igneous rocks. AN SSSR. (In Russ.)

About the Author

Svetlana A. Punanova – Dr. Sci. (Geology and Mineralogy), Leading Researcher, Institute of Oil and Gas Problems of the Russian Academy of Sciences

3, Gubkin st., Moscow, 119333, Russian Federation

Manuscript received 10 October 2019;
Accepted 8 May 2020; Published 30 June 2020

ORIGINAL ARTICLE
DOI: https://doi.org/10.18599/grs.2020.2.56-66

Mineralogical and geochemical aspects of rare-earth elements behavior during metamorphism (on the example of the Upper Precambrian structural-material complexes of the Bashkir megaanticlinorium, South Urals)

S.G. Kovalev[1], A.V. Maslov[1,2], S.S. Kovalev[1]*
[1]*Institute of Geology – Subdivision of the Ufa Federal Research Centre of the Russian Academy of Sciences, Ufa, Russian Federation*
[2]*Zavaritsky Institute of Geology and Geochemistry of the Ural Branch of the Russian Academy of Sciences, Yekaterinburg, Russian Federation*

Abstract. The article provides new data on geochemistry and mineralogy of rare-earth elements (REE) in rocks of structural-material complexes of the Bashkir megaanticlinorium, which underwent metamorphic transformations of various nature: contact metamorphism (Suran section); syn- and postgenetic contact-dislocation metamorphism (Shatak complex) and hydrothermal metamorphism (Uluelga-Kudashmanovo zone). It has been established that when a magmatic melt is exposed to sediments, the latter are enriched with REEs with the formation of rare earth minerals (monazite, allanite, xenotime et al.). The study of the chemical composition of monazites and allanites showed that all variations of oxides in the composition of the former are due to isomorphous Ce-Ca-Th substitutions in the structure of minerals, but redistribution of these elements was an independent process characteristic of each structural-material complex. The study of allanites made it possible to establish the presence of isomorphism according to the Ca↔Ce, La, Nd principle, as well as the sharp difference between the characterized minerals in the amount of MgO, Fe* and MnO from analogues from other regions, which indicates the presence of a regional component in the chemical compositions of minerals altogether, geotectonic settings of mineralization formation. The temperature regimes of mineral-forming processes with metamorphic transformations of rocks calculated from chlorite and muscovite compositions (344-450°C – Suran section, 402-470°C – Shatak complex, 390-490°C – Uluelga-Kudashmanovo zone) indicate the possibility of stable coexistence of the association monazite-allanite. It was established that when a magmatic melt on the sedimentary substrate of the frame, the lanthanides enrich the exocontact rocks with the formation of newly formed REE-mineral associations. At the same time, the processes of formation of rare-earth mineralization are largely determined by the physicochemical parameters and thermobaric conditions of the accompanying and subsequent metamorphism.

Keywords: South Ural, Bashkir megaanticlinorium, structural-material complexes, Upper Precambrian, rare-earth elements, contact metamorphism, monazite, allanite

Recommended citation: Kovalev S.G., Maslov A.V., Kovalev S.S. (2020). Mineralogical and geochemical aspects of rare-earth elements behavior during metamorphism (on the example of the Upper Precambrian structural-material complexes of the Bashkir megaanticlinorium, South Urals). *Georesursy = Georesources*, 22(2), pp. 56-66. DOI: https://doi.org/10.18599/grs.2020.2.56-66

Introduction

The genetic nature of the rare-earth mineralization of metamorphogenic type is the subject of lively discussion (Savko et al., 2010). There are at least two points of view on the rare-earth minerals (REE) behavior in the processes of metamorphism.

According to the first, the formation and decomposition of rare-earth phases during metamorphism occurs without the participation of rock-forming aluminosilicates, which practically do not contain REE. Such phenomena are described in metapelites, where in detail the following is documented: the appearance of allanite during decomposition of detrital monazite under conditions of the green shale facies (Smith, Barero, 1990; Wing et al., 2003); a change in the paragenesis of florensite with monazite by the association of allanite with synchitis with high-pressure metamorphism (Janots et al., 2006); the replacement of allanite with monazite under the conditions of the epidote-amphibolite facies (Wing et al., 2003; Janots et al., 2009; Tomkins, Pattison, 2007, etc.). The formation of monazite during partial decomposition of REE-containing apatite in the rocks of the Bohemian

*Corresponding author: Sergey G. Kovalev
E-mail: kovalev@ufaras.ru

array has also been established (Finger, Krenn, 2006). In addition, apatite and sphene monazite has been described in the Rogaland orthogneisses in southwestern Norway (Bingen et al., 1996).

The second point of view suggests that silicates, upon decomposition of which monazite is formed, can contain significant amounts of light REE and phosphorus (Lanzirotti, Hanson, 1996; Kohn, Malloy, 2004; Gibson et al., 2004). These ideas are based on a significant increase in the number of monazite with the advent of staurolite and data on high contents of light lanthanides and phosphorus in pomegranate, plagioclase, biotite, muscovite, and chlorite, while they were not found in staurolite (Kohn, Malloy, 2004). In addition, the growth of monazite and xenotime due to partial decomposition of pomegranate in metapelites has been described in the Canadian Cordilleras (Gibson et al., 2004) and in contact metamorphism in North Labrador (McFarlane et al., 2005).

Recently, we have obtained extensive new material on the geochemistry and mineralogy of REE in the Riphean deposits of the Bashkir meganticlinorium (South Urals), which allows us to characterize rare-earth mineral formation in structural-material complexes that underwent metamorphic transformations of various nature using the example of a number of model objects: 1) "Suran section" where contact metamorphism is manifested in a "pure" form; 2) "Shatak complex" with syn- and post-genetic contact-dislocation metamorphism; 3) "Uluelga-Kudashmanovo zone", within which hydrothermal metamorphism is developed.

Geological and geochemical characteristics of objects

The Suran section is represented by carbonaceous shales, siltstones and carbonate rocks of the Lower Riphean Suranian Formation (Fig. 1), penetrated by igneous bodies of various thicknesses (from 1-2 m to 60 m).

Shales and silt shales consist of small (0.000n ... 0.00n cm) quartz grains, numerous elongated sericite flakes, feldspar tablets of close dimension and nest-like streaky chlorite secretions. The rocks are schistose with the formation of directive micro-textures, underlined by sericite flakes. Thin filamentous veins composed of sericite are observed. Carbon matter is relatively rare

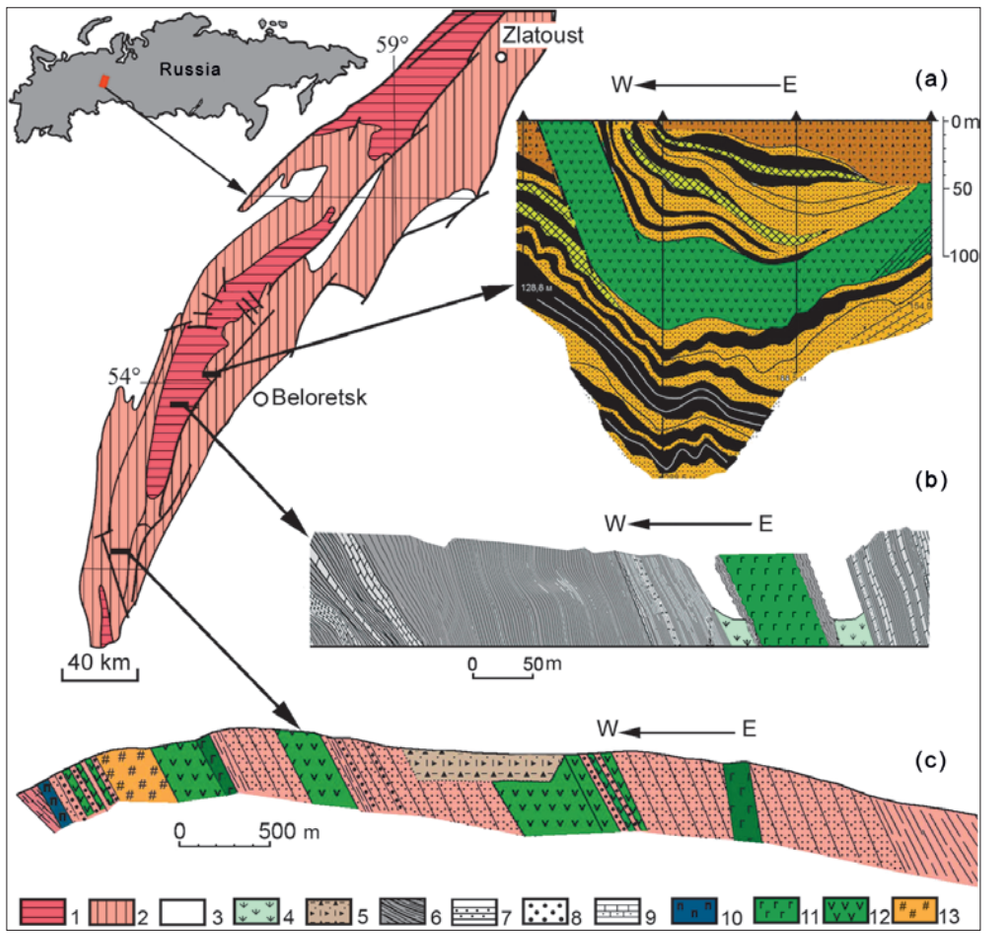

Fig. 1. Geological scheme of the western slope of the Southern Urals and the structure of the Uluelga-Kudashmanovo (a), Suran (b) and Shatak (c) sections. 1 – Lower Riphean deposits; 2 – Middle Riphean deposits; 3 – Upper Riphean-Paleozoic deposits; 4 – sodded areas; 5 – screes, weathering crust; 6 – clay shales; 7 – siltstones, shaly silts, sandstones; 8 – conglomerates; 9 – carbonate rocks with a variable amount of terrigenous component; 10 – picrites; 11 – gabbro, gabbro-dolerite; 12 – basalts; 13 – rhyolites.

in the form of thin veins or clots of irregular shape, unevenly scattered throughout the rock. Streakiness is expressed in the presence of dark and light-colored bands of variable thickness (from fractions of mm to 1-1.5 cm).

Carbonate rocks are represented by dark gray limestones, clayey limestones and fine crystalline dolomites.

The igneous rocks of the Suran section – coarse-grained metamorphosed gabbro of normal alkalinity, the primary minerals of which are plagioclase and clinopyroxene – have been preserved only in the form of relics. Clinopyroxene is amphibolized and chloritized, and plagioclase is albitized. The b odies of gabbroids have sub-consonant contacts with the host rocks, which suggests their occurrence in the form of multi-tier reservoir intrusions (sills) (Kovalev et al., 2017).

Exocontact rock is a fine-grained epidote-feldspar-sericite-quartz aggregate with nest-shaped chlorite secretions and irregular-shaped accumulations of tabular-prismatic amphibole crystals. Locally, along the veins, carbonatization develops – coarse-grained calcite or its heterogeneous aggregates and intergrowths.

The Shatak complex is a stratified volcanic-sedimentary association, which lies at the base of the Middle Riphean section of the Bashkir meganticlinorium (Fig. 1). Sedimentary rocks make up about 75% of its volume and are mainly represented by conglomerates and sandstones. Siltstones, shaly silts and shales are relatively rare. Conglomerates are developed at several stratigraphic levels. They are 70-80% composed of well-rounded fragments of quartzite sandstones and quartzites, less often of ferruginous quartzite-sandstones and microquartzites. Cement is a quartz sandy material and finely scaled sericite-chlorite mass. Sandstones are 80-90% composed of fragments of quartz with chlorite-sericite cement (Kovalev, Vysotsky, 2006).

The igneous rocks of the Shatak complex are represented by picrites, basalts and rhyolites. Picrites form a reservoir intrusion with a visible thickness of about 25-30 m, located on the border with the underlying sediments of the Yushinsky formation of the Lower Riphean. Metabasalt is green, greenish-gray, medium-fine-grained rock, which is characterized by microdoleritic, microphytic, apointersertic and porphyritic structure. They are composed of clinopyroxene, plagioclase, hornblende, titanomagnetite and magnetite. Secondary minerals are represented by amphibole of the actinolite-tremolite series, chlorite (pennin-clinochlor), epidote, sericite, titanite, leukoxen and hematite. Riolites are light gray rocks with a porphyry fluid and schlieren-taxite structure. The bulk is composed of a fine-grained quartz-feldspar aggregate. Acid plagioclase (andesine-oligoclase) is present in porphyry manifestations. Dark-colored minerals are represented by greenish-brown biotite and chlorite. Apatite, allanite, monazite, titanite, epidote are found as accessory.

The Uluelga-Kudashmanovo zone is structurally confined to the Ishlinsky graben. It is located directly within the Yuryuzan-Zyuratkul regional fault, representing a narrow (100-250 m) strip of submeridional strike, traced at a distance of about 15 km (Fig. 1).

Metaterrigenous rocks of the zone are represented by sericite-quartz siltstones and carbonaceous shales of the Mashak Formation of the Middle Riphean (Parnachev et al., 1986). The rocks are characterized by a significant dislocation – crushing, corrugation, microbudding, rolling of quartz fragments with mosaic, cloud extinction, and the formation of plastic flow textures. Metasomatic recrystallization is expressed in the growth of quartz fragments and the enlargement of sericite with the formation of coarse-grained (up to 5 mm elongation) muscovite. Silica and carbonation are widely developed in rocks. The main difference between carbon-containing schists and siltstones is the lower dimension of quartz grains and the presence of carbonaceous matter, which forms layered-strip-like, cord-like and lumpy precipitates. In siltstones and shales, sulfide mineralization of the metamorphogenic type, represented by pyrite, pyrrhotite, sphalerite, chalcopyrite and galena, is widespread. The amount of sulfides on average is 0.1-0.5 wt. %, increasing in black shale horizons to 10-15 wt. %, where they form vein-disseminated mineralization (Kovalev et al., 2013).

The igneous rocks of this zone are intrusive bodies of gabbro-dolerite and effusives of the main composition. Albitite veins with a thickness of 15-20 cm, consisting of xenomorphic albite grains, coarse-grained (0.5-0.8 mm) muscovite, and a small amount of quartz and chlorite, were established in the upper part of the section. Intrusive rocks are largely metamorphosed. In the schist zones, they are transformed into carbonate-epidote (clinitoisite) -albit-quartz-chlorite schists and epidote-albite-quartz-amphibole rocks of massive texture. The metabasalts are composed of misoriented leaves of segregated plagioclase, clinopyroxene substituted by epidote and chlorite, and also products of volcanic glass devitrification. Together with the thin intercalations of lithocrystalline plastic tuff sandstones, they are schistose and are represented by epidote-quartz-chlorite formations.

Each of the structural-material complexes described is an independent unit, the mineralogical and geochemical analysis of which allows us to characterize the behavior of rare-earth elements in the process of its formation and transformation. As reference values for terrigenous rocks of the Suran section, REE contents in unchanged/"background"[1] rocks of the Suranian Formation of the lower Riphean of the Bashkir meganticlinorium are considered, for the sediments of the

Uluelga-Kudashmanovo zone, the content of lanthanides in clastic rocks of the Zigazino-Komarovskian Formation middle Riphean of the same structure are considered (Maslov et al., 2008).

The REE contents normalized to the upper continental crust (Taylor, McLennan, 1985) in the exocontact rocks of the Suran section and unchanged/"background"[1] deposits of the Suranian formation, with the general trend similarity, differ quantitatively, which is clearly recorded in graphs (Fig. 2a) and in their average amounts – 165.9 ppm for the former and 118.4 ppm for the latter. The same trend is clearly visible in the

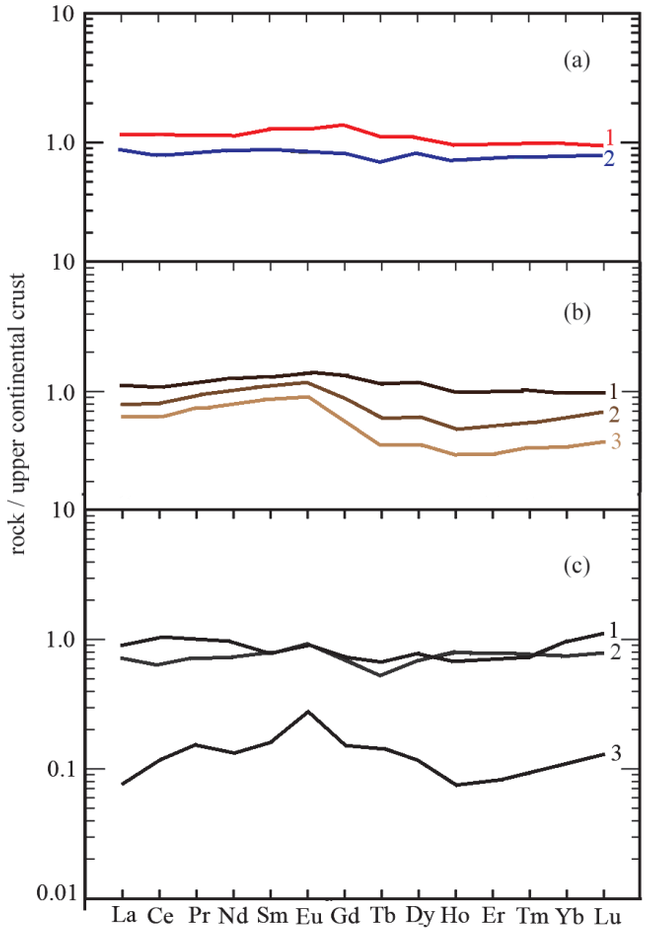

Fig. 2. Average REE contents normalized to the upper continental crust (Taylor, McLennan, 1985) in the rocks of the Suran section (a), the Shatak complex (b) and the Uluelga-Kudashmanovo zone (c). a: 1 – exocontact rocks (n = 16); 2 – unchanged deposits of the Suranian formation (n = 11); b: 1 – shales (n = 21); 2 – siltstones (n = 5); 3 – sandstones (n = 8); in: 1 – sulfidized carbonaceous shales (n = 3); 2 – unchanged deposits of the Zigazino-Komarovskian formation (n = 11); 3 – carbon-containing shales (n = 8). n is the number of analyzes.

[1]*Unchanged/"background" rocks here refer to as relatively slightly altered post-sedimentation (mainly isochemical) processes of sandstones, siltstones and clay shales of the lower and middle Riphean of the Bashkir meganticlinorium, which do not bear obvious signs of material remobilization, the impact of metamorphic-metasomatic processes or the introduction of ore components (Maslov, Kovalev, 2014).*

Y – Ce diagram (Fig. 3a), where the amounts of Y and Ce in the exocontact rocks ($Ce_{av.}$ = 72.02 ppm; $Y_{av.}$ = 22.26 ppm) significantly exceed the contents of these elements in unaltered sediments of the Suran suite ($Ce_{av.}$ = 50.45 ppm; $Y_{av.}$ = 9.8 ppm).

A different picture in the distribution of REE is characteristic of terrigenous rocks of the Shatak complex. From the analysis of normalized contents (Fig. 2b) it follows that the amounts of REE directly depend on the lithological composition of the rocks (sandstones – $\sum REE_{av.}$ – 95.62 ppm; siltstones – $\sum REE_{av.}$ – 123.22 ppm; shales – $\sum REE_{av.}$ – 162.76 ppm), which is most likely the result of the sorption abilities of the substance. Moreover, as can be seen from the Y – Ce diagram (Fig. 3b), the scatter in the contents of these elements in the shales is significant (Ce – 16.2-157.0 ppm; Y – 3.81-61.4 ppm), which may serve as an indirect sign REE redistribution in the process of metamorphic transformation of complex rocks.

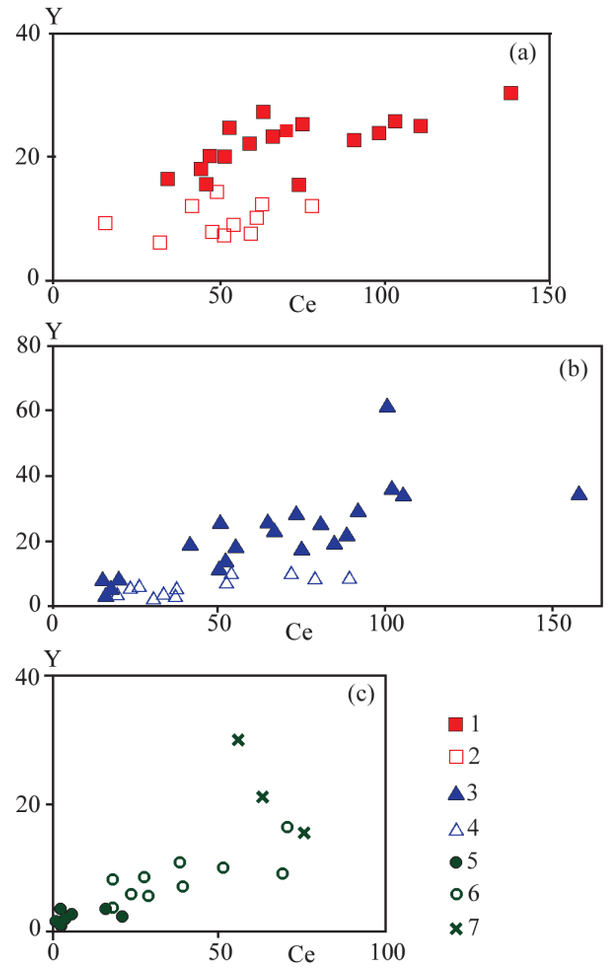

Fig. 3. Y – Ce diagrams for rocks of the Suran section (a), the Shatak complex (b) and the Uluelga-Kudashmanovo zone (c). 1 – exocontact rocks; 2 – unchanged / "background" deposits of the Suranian formation; 3 – shales; 4 – siltstones and sandstones not divided; 5 – carbon-containing shales; 6 – unchanged / "background" deposits of the Zigazino-Komarovskian formation; 7 – sulfidized carbonaceous shales.

The variations in REE contents caused by hydrothermal metamorphism processes are especially evident when analyzing the rocks of the Uluelga-Kudashmanovo zone. For example, sharply reduced REE amounts were found in carbon-containing shales, not only in comparison with uniform "background" rocks of the Zigazino-Komarovskian Formation, but also with average contents of these elements in the earth's crust (Fig. 2c), and the trend itself has a complex configuration. At the same time, in sulfidized shales with a sulfide content of at least 50% of the sample volume, the amount of REE increases by almost 10 times (∑REE in the carbon-containing shales – 16.67 ppm; ∑REE in the sulfidized shales – 137.43 ppm) , which indicates the redistribution of rare earth elements in the process of metamorphogenic sulfide formation.

Research methods

The contents of rare-earth elements in 48 samples were obtained by inductively coupled plasma mass spectrometry (ICP-MS) at the Russian Geological Research Institute (VSEGEI) (St. Petersburg). The accuracy of REE measurements was (in ppm): La – 0.01; Ce – 0.01; Pr – 0.01; Nd – 0.01; Sm – 0.005; Eu – 0.005; Gd – 0.01; Tb – 0.005; Dy – 0.01; Ho – 0.005; Er – 0.01; Tm – 0.005; Yb – 0.01; Lu – 0.005.

The study of REE minerals was carried out on a REMM-202M scanning electron microscope with a Z-5 X-ray energy dispersive spectrometer (SiLi detector, resolution 140 ev), secondary (SE) and reflected (COOMPO) detectors of electrons at the Institute of Mineralogy of the Ural Branch of the RAS (Miass). For quantitative analysis, pure metal standards and/or synthetic and natural mineral standards were used.

Rare earth mineralization

REE minerals are found in the rocks of all studied structural-material complexes. They are represented by monazite, xenotime, calcium cyanoanilite, allanite, yttrium-containing epidote, cerianite, REE-containing thorite and a significant amount of unidentified REE and Th-REE compounds of complex composition (Kovalev et al., 2017).

Monazite is the most abundant mineral. Almost complete absence of faceted crystals is a characteristic feature of all studied monazites (Fig. 4). The mineral is found in the form of xenomorphic grains forming clusters of irregular shape, sometimes in the form of elongated columnar discharge (Fig. 4a, b). It was found both in metaterrigenous and apomagmatic rocks in the Uluelga-Kudashmanovo zone. In terms of chemical composition, all monazites are cerium species ($Ce_{av.} \geq La_2O_3+Pr_2O_3+Nd_2O_3+Sm_2O_{3av.}$). Separate crystals contain Sm_2O_3, Gd_2O_3, ThO_2, UO_2, FeO and SiO_2, and the content of silicon oxide in unidentified phases rises to 49.89-54.67 wt. %. In the monazite of the Shatak complex, the REE contents are subject to significant fluctuations. In particular, monazite with 20.42 wt. % Nd_2O_3 and 12.32 wt. % Sm_2O_3. In addition, all the studied minerals belong to Th-containing varieties of monazite

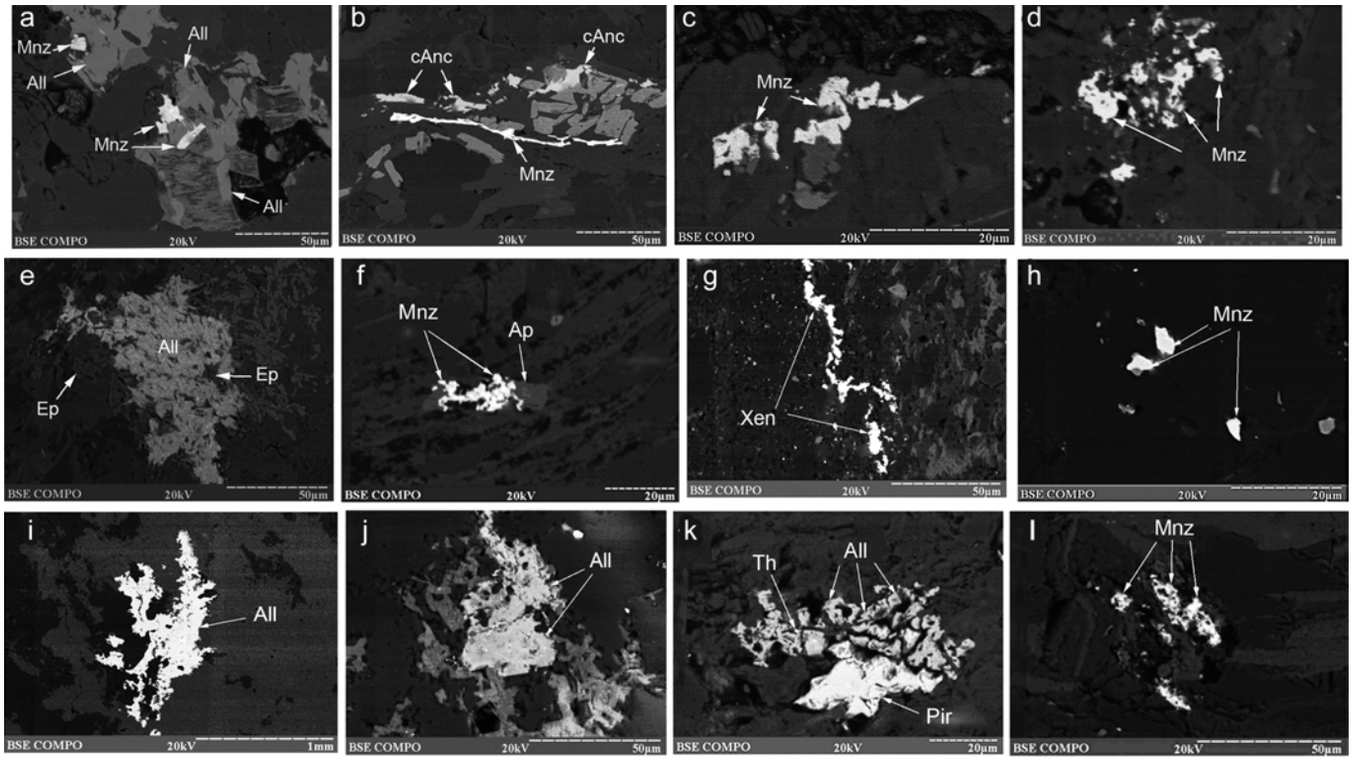

Fig. 4. Microphotographs of rare-earth minerals from the rocks of the Suran section (a – f), the Shatak complex (g – j) and the Uluelga-Kudashmanovo zone (k – l). Mnz – monazite; cAnc – calcioankilite; Xen – xenotime; All -allanite; Ep – epidote; Th – torit; Pir – pyrrhotite; Ap – apatite.

with Ce_2O_3 contents varying over a wide range (from 13.35 to 35.71 wt.%).

Xenotim in the rocks of the Suran section and the Uluelga-Kudashmanovo zone is found in the form of independent xenomorphic secretions or in paragenetic intergrowths with monazite and associations with rutile and muscovite. It contains SiO_2, FeO, ThO_2, and UO_2. In the rocks of the Shatak complex, xenotime was found in the form of chain-streaky segregations composed of intergrowths of faceted crystals or xenomorphic precipitates, as well as rims on zircon crystals. Xenotime "microbranches" are located in conglomerate cement and have a complex branching and discontinuous shape (Fig. 4g). In the chemical composition of xenotime, in addition to the characteristic impurity Gd, Dy, Tb, Ho, Yb, Nd and Sm are established. In addition, U-Th-containing differences are also found.

Calcioankilite, first discovered in 2016 in terrigenous rocks of Russia (Kovalev, Kovalev, 2017), was established in exocontact rocks of the intrusive body of gabbro of the Suran section in association with monazite, muscovite, chlorite, albite, and titanite (Fig. 4b) . It is represented by intergrowths of elongated prisms or xenomorphic secretions. By chemical composition, it belongs to the cerium variety of calcioankylite (0.98-0.99 f.k. Ca, (La + Pr)/(Ce + Nd) = 0.36).

Allanite occurs in the form of intergrowths of tabular crystals (Fig. 4a), and also forms granular aggregates up to 200 μm in size (Fig. 4 e,i,j) often in association with epidote, thorite, and iron sulfides (Fig. 4k). By chemical composition, all the discovered minerals belong to the cerium ($Ce_2O_3 \geq La_2O_3 + Pr_2O_3 + Nd_2O_3$). Ferruginous allanites (FeO – 10.49-10.64 wt.%) with a low content of MgO (0-0.21 wt.%) and MnO (0-0.08 wt.%) are found in the Uluelga-Kudashmanovo zone; in the Shatak complex zonal ones are found (in wt.%: La – edge 3.03, center – 1.33; Ce – 6.67 and 4.62; Nd – 2.55 and 2.03; Al_2O_3 – 20.18 and 22.98; SiO_2 – 37.34 and 39.37; CaO – 15.07 and 17.45, respectively). In addition, relatively large (up to 1 mm in elongation) xenomorphic allanite precipitates of nonstoichiometric composition ($(Ca_{0.71}Ce_{0.22}La_{0.07}Pr_{0.05}Nd_{0.11})_{1.16}(Al_{0.31}Fe_{0.50}Mg_{0.03})_{0.84}(Si_{1.98}Al_{1.02})_3O_8$; $(Ca_{0.67}Ce_{0.26}La_{0.07}Pr_{0.04}Nd_{0.11})_{1.15}(Al_{0.33}Fe_{0.50}Mg_{0.02})_{0.85}(Si_{1.98}Al_{1.02})_3O_8$; $(Ca_{1.76}Ce_{0.17}La_{0.07}Nd_{0.07}Pr_{0.04})_{2.11}(Al_{2.07}Fe_{0.78}Mg_{0.04})_{2.89}(Si_{3.54}Al_{0.46})_4O_{14}$), in which the total amount of REE (at Ce> Nd> La> Pr) varies from 20.48 wt. % to 33.37 wt. % were found in the upper part of the Shatak complex in the horizon of interbedded sandstones and shales. Compounds close in $((Ca_{1.31}La_{0.18}Ce_{0.42}Nd_{0.08}Pr_{0.06})_{2.05}(Al_{2.03}Fe_{0.81}Mg_{0.10}Mn_{0.01})_{2.95}(Si_{3.70}Al_{0.30})_4O_{14}$ and $(Ca_{0.55}Ce_{0.21}La_{0.10}Pr_{0.03}Nd_{0.06})_{0.95}(Al_{0.63}Fe_{0.33}Mg_{0.03}Mn_{0.01}Ti_{0.05})_{1.05}(Si_{2.65}Al_{0.35})_3O_8$) with a total REE content – 20.01 wt. % and 18.51 wt. %, respectively, were found in conglomerates from the base of the complex.

There is a Y-containing epidote in association with allanite (Fig. 4f) in the rocks of the Suran section, in the form of prismatic crystals, their intergrowths, and xenomorphic precipitates of 300-400 μm in size. The presence of yttrium in its chemical composition suggests that the mineral is part of the isomorphic series epidote – allanite.

A comparative analysis of the chemical composition of minerals described above makes it possible to characterize the features of mineral formation in various structural-material complexes. In Fig. 5, the CaO – ThO_2 diagram for monazites is presented, from which it can be seen that all minerals are quite clearly grouped into three fields. The first one characterizes monazites from rocks of the Uluelga-Kudashmanovo zone, which are characterized by the presence of ruthenium-free varieties and the maximum amounts of calcium in the composition of minerals. Monazites from exocontact rocks of the Suran section (field II) differ in significant variations in CaO contents with relatively small changes

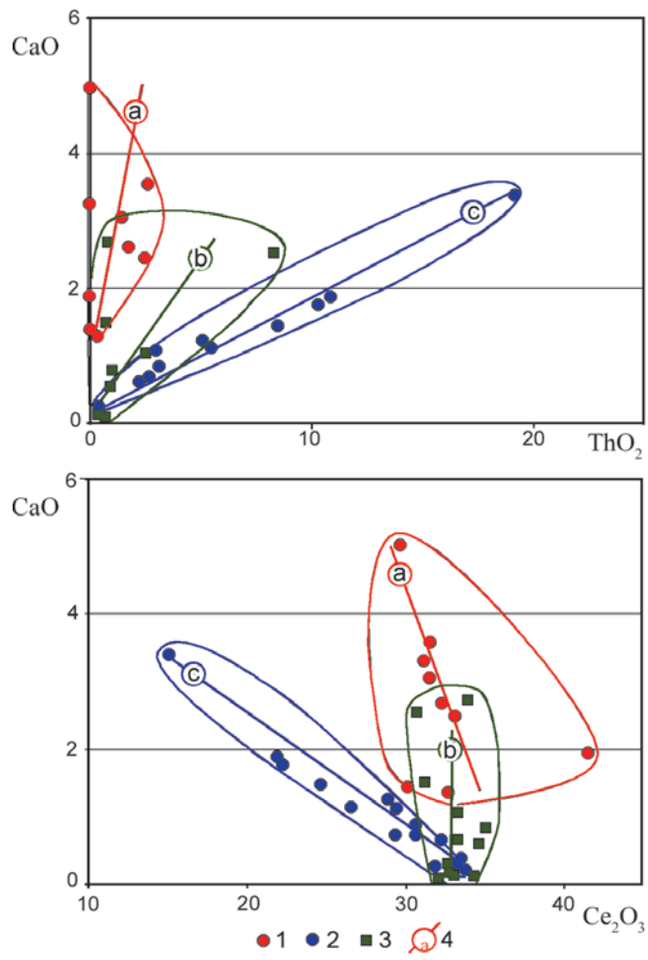

Fig. 5. Diagrams of CaO – ThO_2 and CaO – Ce_2O_3 for monazites from the Upper Precambrian structural-material complexes of the Bashkir megaanticlinorium. 1 – Suran section; 2 – Shatak complex; 3 – Uluelga-Kudashmanovo zone; 4 – trends in the content of components (a – Suran section; b – Uluelga-Kudashmanovo zone; c – Shatak complex).

in the amounts of thorium. The minerals of the third group (Shatak complex) have a well-defined direct relationship between the contents of CaO and ThO_2 with an approximation coefficient of 0.96 and the presence of varieties with a maximum amount of ThO_2. Between the minerals of the first and second groups, common features of changes in the contents of oxides are visible. They are characterized by the presence of two "local trends" (the first is a sharp increase in the amount of calcium and the second is a direct relationship between the contents of CaO and ThO_2). This is most likely due to a certain similarity of contact and hydrothermal metamorphism and, possibly, to the presence of two generations of monazites, one of which was formed from REE of the fluid phase, and the second during metamorphic recrystallization of a phosphate-containing sedimentary substrate.

A similar picture of the distribution of monazites by genetic groups is also clearly visible on the CaO-Ce_2O_3 diagram (Fig. 5), from the analysis of which it follows that the relationships between the indicated oxides in each group are characterized by aspecificity: for monazites from the Suran section, there is a significant spread in cerium content and a weakly manifested inverse relationship between CaO and Ce_2O_3; minerals from the rocks of the Uluelga-Kudashmanovo zone differ in significant variations in CaO amounts with small changes in Ce_2O_3; monazites from rocks of the Shatak complex are characterized by a clearly manifested inverse relationship between calcium and cerium with an approximation coefficient of 0.94.

In general, all the oxide variations in Fig. 5 are due to isomorphic substitutions of Ce-Ca -Th in the structure of monazite. The fundamental conclusion follows from the above description of minerals and analysis of diagrams, that the redistribution of these elements was realized in an independent process characteristic of each structural-material complex.

In addition to monazite, allanite is a mineral characteristic of the rocks of all the described complexes. For a comparative analysis of the chemical composition of allanites, we used data on minerals from the Paleoproterozoic carbon schists of the Tim-Yastrebovsky paleorift (Voronezh crystalline array) (Savko et al., 2010) and to allanites from the metamorphic schists of the Puyva Formation of the Subpolar Urals (Kovalchuk, 2015). The results are plotted on the MgO-Fe*, MnO-Fe*, Al_2O_3-CaO, Ce_2O_3-CaO, Nd_2O_3-CaO, La_2O_3-CaO diagrams (Fig. 6).

From the consideration of these diagrams it follows that, firstly, allanites from structural-material complexes of the Urals and carbonaceous schists of the Tim-Yastrebovsky paleorift sharply differ in the amount of MgO, Fe* and MnO, forming local disjoint fields, which indicates the presence of a "regional component" in the chemical compositions of minerals, most likely due to geotectonic conditions of mineralization formation. Secondly, between the contents of Al_2O_3 and CaO in allanites from all structural-material complexes, a direct relationship is established; in this case, the maximum

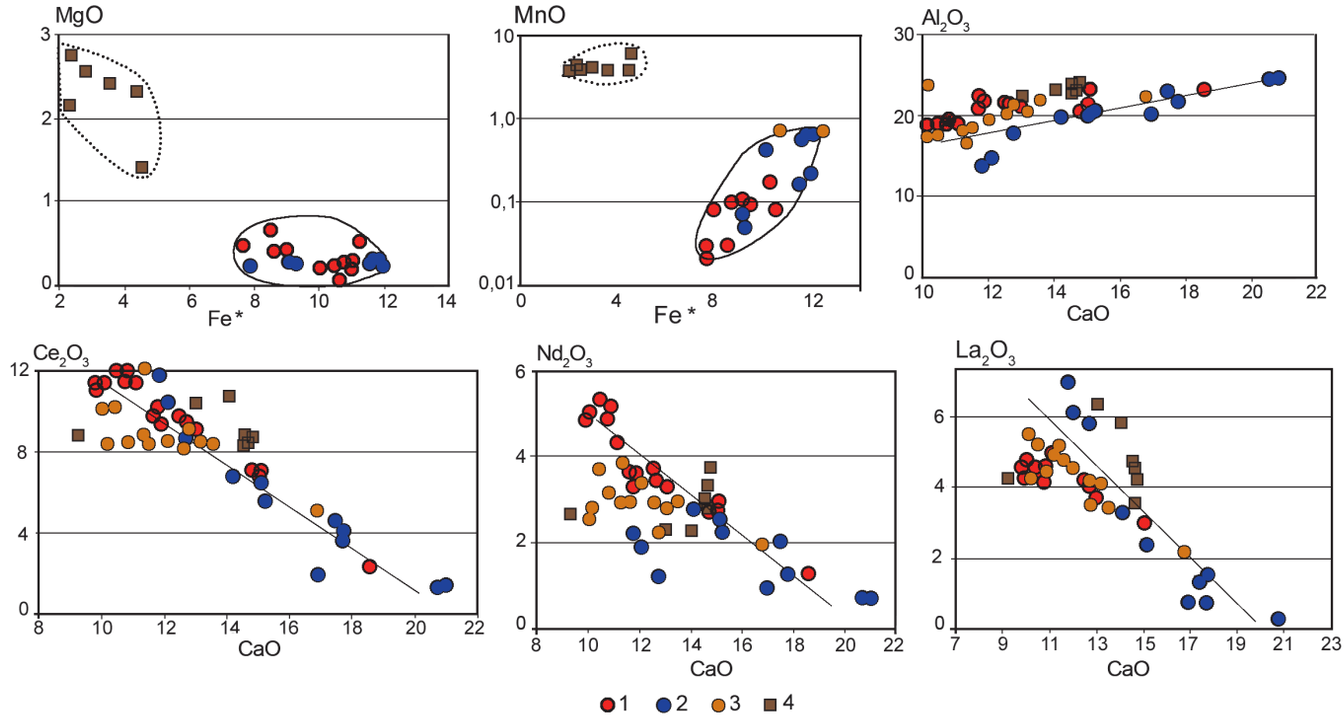

*Fig. 6. Diagrams of element contents (wt.%) in the allanites of the Suran section and the Uluelga-Kudashmanovo zone (1), the Shatak complex (2), the metamorphic schists of the Puyva Formation of the Subpolar Urals (3, according to Kovalchuk, 2015) and the Tim-Yastrebov structure of the Voronezh crystalline array (4, according to Savko et al., 2010). Fe * – total iron in the form of FeO.*

dispersion of the quantities of both components is characteristic of minerals from the complexes described in this work. Thirdly, all allanites of the Ural region are characterized by an inverse relationship between the calcium content on the one hand and REE on the other, indicating a wide isomorphism according to the Ca ↔ Ce, La, Nd principle, which, as shown above, is also characteristic of monazites; at the same time, this dependence is absent in allanites from carbon schists of the Tim-Yastrebovsky paleorift (a change in the amount of calcium occurs at almost constant contents of Ce, Nd, and La).

Thermobaric metamorphism parameters

The chemical compositions of chlorites were used to evaluate the thermal parameters of metamorphism of the characterized complexes. The temperatures of their formation were calculated by the formula $T = –61{,}9229+321{,}9772\times Al^{IV}$ (Kranidiotis, MacLean, 1987).

In accordance with the classification (Drits, Kossovskaya, 1991), chlorites from exocontact rocks of the Suran section fall into the fields of Fe-Mg chlorites of clastogenic formations and Fe-Mg and Mg-Fe chlorites of the main igneous rocks, and the temperature range of their formation is 212-344 °C (Fig. 7) with a relatively small fluctuation in the iron content (0.4-0.5). The confluence of the figurative points of the studied chlorites to the indicated fields and small variations in the iron content indicate their formation from the fluid phase under the influence of magmatic melt on the rocks of the frame. The formation temperatures of chlorites from apomagmatic rocks of the Uluelga-Kudashmanovo zone are in the range of 171-377 °C, and from metaterrigenous ones – 148-410 °C. At the same time, it is clearly seen that chlorites from para- and orthoporods significantly differ in iron content (Fig. 7). This is due to the fact that Mg-chlorites of the ortho-rocks are the result of the replacement of clinopyroxenes, and Fe-chlorites were formed during the hydrothermal process, covering both igneous and terrigenous rocks, which is confirmed by the confinement of all points of the composition of the studied minerals to the field of Fe-Mg-chlorites of clastogenic formations on the geocrystallochemical classification diagram of V.A. Drits and A.G. Kossovskaya (1991).

The subdivision of minerals into two groups – "high-magnesian" and "low-magnesian", is also characteristic of chlorites of the Shatak complex (Fig. 7). The temperature range for the formation of the first ones is ~ 308-350 ° C; of the latter ~ 318-402 °C. According to the classification of V.A. Dritsa and A.G. Kossovskaya (1991) chlorites of the Shatak complex correspond to Fe-Mg-chlorites of clastogenic formations and Fe-Mg- and Mg-Fe-chlorites of the main igneous rocks, which

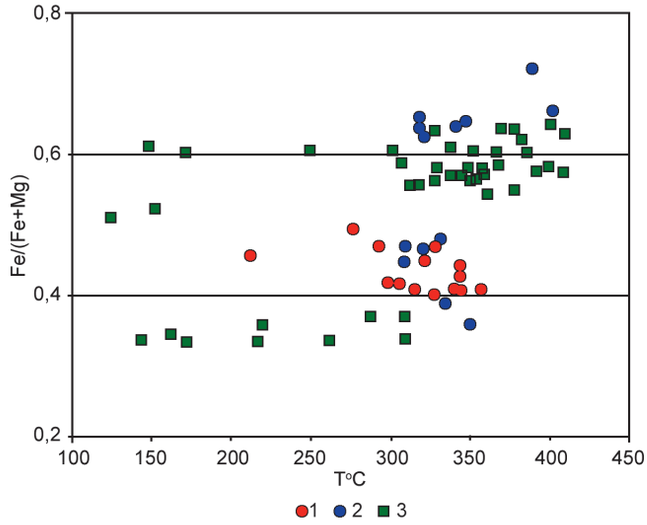

Fig. 7. Fe/(Fe+Mg)–T °C diagram for chlorites from rocks of various Upper Precambrian structural-material complexes of the Bashkir meganticlinorium. 1 – Suran section: 2 – Shatak complex; 3 – Uluelga-Kudashmanovo zone.

indicates the formation of minerals in a single process of transformation of the complex rocks.

In addition to chlorites, in order to determine the thermobaric conditions for the metamorphism of the described complexes, we analyzed the compositions of light mica. The thermobaric parameters of their formation are shown in Fig. 8a, the analysis of which shows that the maximum temperature corresponded to ~ 450 °C, and the pressure was ~ 6-7 kbar. In this case, a rather well-pronounced tendency to a decrease in temperature with increasing pressure is observed. Thus, variations in the P-T parameters indicate the existence of two stages of metamorphism in the Suran section. The first stage (max T, min P) is an exocontact metamorphism; the second stage (min T, max P) is stress pressure with regional metamorphism.

In the rocks of the Uluelga-Kudashmanovo zone, muscovite is present both in the form of small-scaled varieties (sericite), which are part of the cement of shales and silt shales, and in the form of relatively large-sheeted crystals and their aggregates, which are found in terrigenous and apomagmatic rocks. Interpretation of the position of points in the Si – Na/Na + K diagram (Fig. 8c) indicates that light mica in the apomagmatic rocks of the indicated zone formed in the intervals: pressure ~2.0-9.8 kbar; temperature – 390-450 °C. In this case, the minimum temperatures do not coincide with the minimum pressure, which indicates the predominance of stress load during metamorphism. For terrigenous rocks, the scatter of temperature and pressure values is close to those characteristic of apomagmatic formations (T = ~390-490 °C, P = ~2.5-9.9 kbar). As well as for apomagmatic rocks, the maximum and minimum temperatures and pressures established for terrigenous formations do not correlate between themselves.

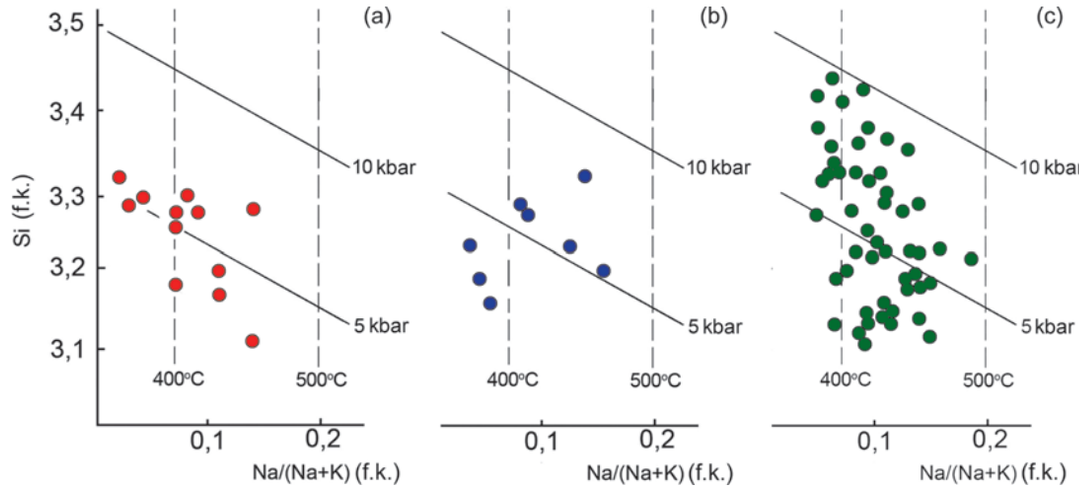

Fig. 8. Si (f.k.)–Na/(Na+K) (f.k.) diagrams for light mica from terrigenous complexes of the Bashkir meganticlinorium (a – Suran section; b – Shatak complex; c – Uluelga-Kudashmanovo zone). Pressure isogradic line (Chopin, 1981; Massonne, Schreyer, 1989); temperature isogradic line (Dobretsov et al., 1974; Krogh, Raheim, 1978).

In terrigenous rocks of the Shatak complex, newly formed muscovite is found in coarse clastic sediments of the Kuzelginsky sub-formation in association with a chloritoid and epidote. An assessment of the thermobaric parameters of its formation (Fig. 8b) showed that the maximum temperature and pressure corresponded to: T = ~470 °C, P = ~8 kbar, and the minimum were: T = ~380 °C, P = ~3 kbar.

Discussion of results and conclusions

The question of the matter sources during the formation of rare-earth mineralization, as noted above, remains the subject of heated debate. The general sequence of the change of REE index minerals with progressive metamorphism of metapelites is described as follows: detrital monazite → metamorphic allanite → metamorphic monazite → apatite (Smith, Barero, 1990; Wing et al., 2003; Finger, Krenn, 2007; Janots et al.,. 2009; Savko et al., 2010, etc.). At the same time, estimates of the thermobaric parameters of these substitutions, as well as the mechanisms of mineral reactions in the above studies vary significantly.

On the example of materials from the Suran section, it was shown that rare-earth mineralization is formed during exocontact metamorphism, where igneous rocks are the source of REE. Moreover, mineral associations include both monazite and allanite, although cases where monazite and allanite are found in the same paragenesis are quite rare (Savko et al., 2010, and others). Based on the established fact of the formation of rare-earth mineralization as a result of exocontact metamorphism, we can consider the genetic conditions for the formation of REE mineralization in other structural-material complexes described in this work.

Due to the fact that igneous rocks are one of the sources of REE, and metamorphism is the main process of rare-earth mineralization formation, it is logical to link these processes with the geodynamic regimes of the territory's development at certain time stages. The igneous rocks of the Surans section belong to the Middle Riphean (Larionov et al., 2006), the first third of which was characterized by the manifestation of plume processes (Puchkov, Kovalev, 2013, Puchkov, 2013, Ernst, 2014), accompanied by active riftogenesis and wide spread of magmatism within the Bashkir megaanticlinorium in all its manifestations (dikes and sills, dike swarms and belts, volcanic-plutonic associations and intrusive stratified arrays).

The introduction of magmatic melts in the upper horizons of the crust with fluid development of sedimentary substrate in such geodynamic settings led to the formation of exocontact and fluid-magmatic types of rare-earth mineralization, differing in the scale of local manifestation of magmatism (in the case of single bodies, an exocontact type is formed (Suran section); in the case of plutonic association the fluid-magmatic type is formed (Shatak complex) .The fact that rare-earth mineralization in the rocks of the named complexes was formed in a single process is evidenced by a well-defined inverse relationship between the CaO content and the sum of REE in the monazites and allanites of each complex with approximation coefficients of 0.975 and 0.967 respectively (Fig. 9a, b).

The thermal conditions for the reaction of allanite ↔ monazite have not been precisely established to date. Most authors believe that allanite replaces monazite in the range of 400-450 °C and remains stable up to the amphibolite facies. Monazite reappears in the temperature range 450-530 °C (Smith, Barero, 1990; Wing et al., 2003; Janots et al., 2006 and others). In addition, it was found that the decomposition temperature of allanite with the formation of monazite can vary depending on the contents of CaO and Al_2O_3 in the rocks (Wing et al., 2003). It is important for our

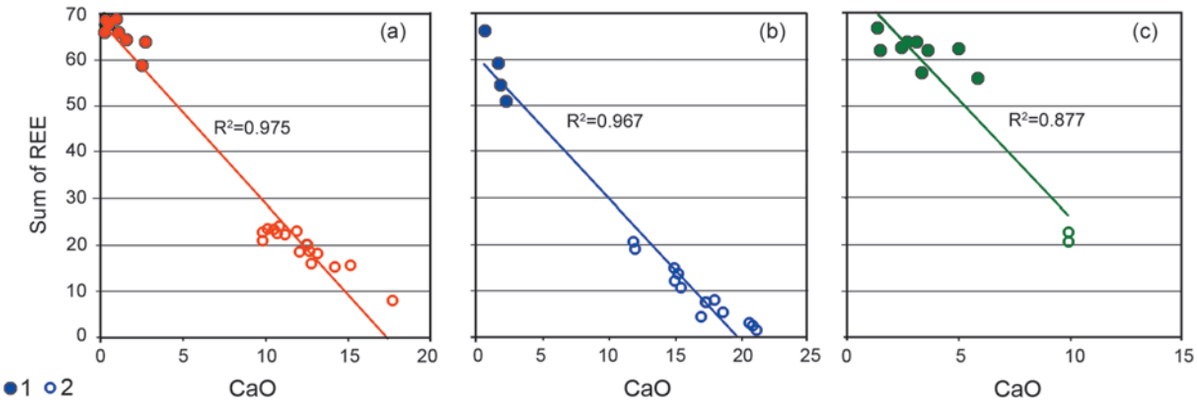

Fig. 9. The diagrams sum of REE – CaO for monazites (1) and allanites (2) from rocks of the Suran section (a), the Shatak complex (b) and the Uluelga-Kudashmanovo zone (c).

studies that the calculated temperature regime of mineral formation (344-450 °C – Suran section, 402-470 °C – Shatak complex) is close to the coexistence temperatures of both phases.

The main mechanism for the formation of rare-earth minerals in the rocks of the Uluelga-Kudashmanovo zone was a hydrothermal type metamorphism, which manifested itself in this zone ~ 600 Ma ago (Kovalev et al., 2013). According to modern geodynamic constructions, in the Vendian, the territory of the region developed in a compression mode (Puchkov, 2000), and the physicochemical conditions of mineral formation were determined by the functioning of local multidimensional fluid-hydrothermal systems, which were formed when rifting magmatism was replaced by processes of water crustal palingenesis and regional metamorphism. A specific feature of the mineral-forming processes of this stage was the redistribution of REE during metamorphic sulfide formation (Fig. 2), as well as significant variations in the CaO content in the monazite composition (Fig. 5) with the previously established isomorphic substitution of thorium for calcium in the mineral structure and the appearance of thorium-free high-calcium monazite and native thorium minerals (Kovalev et al., 2017). Moreover, the maximum temperature of metamorphism of 390-490 °C, as well as in the structural-material complexes described above, suggests the coexistence of both monazite and allanite. In this situation, the possibility of the monazite formation due to the decomposition of allanite cannot be ruled out, although this has not been found in a direct study of mineralization.

Thus, the behavior of REEs in the Late Precambrian structural-material complexes of various compositions and genetic nature of the Bashkir megaanticlinorium is determined by the effect of magmatic melt of the main composition on the sedimentary substrate of the frame, in which lanthanides enrich exocontact rocks. It leads to the appearance of newly formed REE-mineral associations. The formation of rare-earth mineralization are largely controlled by physicochemical parameters and thermobaric conditions of concomitant and subsequent metamorphism.

Acknowledgments

The work was performed as part of the State assignment, topic No. 0252-2017-0012.

References

Bingen B., Demaiffe D., Hertogen J. (1996). Redistribution of rare earth elements, thorium, and uranium over accessory minerals in the course of amphibolite to granulite facies metamorphism: the role of apatite and monazite in orthogneisses from southwestern Norway. *Geochim. Cosmochim. Acta*, 60(8), pp. 1341-1354. https://doi.org/10.1016/0016-7037(96)00006-3

Chopin C. (1981). Talc-phengite: a widespread assemblage in high-grade pelitic blueschists of the Western Alps. *J. Petrol.,* 22(4). pp. 628-650. https://doi.org/10.1093/petrology/22.4.628

Dobretsov N.L., Lavrentiev Yu.G., Ponomareva L.G., Pospelova L.N. (1974). Statistical studies of white micas of the glaucophans schist strata. *Coll. papers: Statistical methods in geology,* 236, pp. 113-133. (In Russ.)

Drits V.A., Kossovskaya A.G. (1991). Clay minerals: mica, chlorite. Moscow: Nauka, 176 p. (In Russ.)

Ernst R.E. (2014). Large igneous provinces. London: Elsevier, 653 p. https://doi.org/10.1017/CBO9781139025300

Finger F., Krenn E. (2006). Three metamorphic monazite generations in a high_pressure rocks from Bohemian Massif and the potentially important role of apatite in stimulating polyphase monazite growth along a PT loop. *Lithos,* 95, pp. 103-115. https://doi.org/10.1016/j.lithos.2006.06.003

Gibson D.H., Carr S.D., Brown R.L., Hamilton M.A. (2004). Correlations between chemical and age domains in monazite, and metamorphic reactions involving major pelitic phases: an integration of ID-TIMS and SHRIMP geochronology with Y-Th-U X-ray mapping. *Chem. Geol.,* 211, pp. 237-260. https://doi.org/10.1016/j.chemgeo.2004.06.028

Janots E., Engi M., Rubatto D., Berger A., Gregory C., Rahn M. (2009). Metamorphic rates in collisional orogeny from in situ allanite and monazite dating. *Geology,* 37(1), pp. 11-14. https://doi.org/10.1130/G25192A.1

Janots E., Negro F., Brunet F., Coffee B., Engi M., Bouybaoene M.L. (2006). Evolution of REE mineralogy in HP-LT metapelites of the Septide complex, Rif, Morocco: monazite stability and geochronology. *Lithos,* 87, pp. 214-234. https://doi.org/10.1016/j.lithos.2005.06.008

Kohn M.J., Malloy M.A. (2004). Formation of monazite via prograde metamorphic reactions among common silicates: Implications for age determinations. *Geochim. Cosmochim. Acta,* 68(1), pp. 101-113. https://doi.org/10.1016/S0016-7037(03)00258-8

Kovalev S.G., Vysotsky I.V. (2006). A new type of noble metal mineralization in terrigenous rocks of the Shatak graben, western slope of the southern Urals. *Lithology and Mineral Resources,* 41(4), pp. 371-377. (In Russ.) https://doi.org/10.1134/S0024490206040079

Kovalev S.G., Michurin S.V., Vysotsky I.V., Kovalev S.S. (2013). Geology, mineralogy and metallogenic specialization of carbon-containing strata of the Uluelginsko-Kudashman zone (western slope of the South Urals). *Lithosphere (Russia)*, 3, pp. 67-88. (In Russ.)

Kovalev S.G., Kovalev S.S., Vysotsky S.I. (2017). Th – REE mineralization in Precambrian rocks of the Bashkir meganticlinorium: species diversity and genesis. *Zapiski RMO = Proceedings of the Russian Mineralogical Society*, 5, pp. 59-79. (In Russ.)

Kovalev S.S., Kovalev S.G. (2017). The first find of calcioankilite in terrigenous rocks of the Bashkir meganticlinorium. *Geologiya. Izvestiia Otdeleniya nauk o Zemle i prirodnykh resursov Akademii nauk Respubliki Bashkortostan,* 23, pp. 45-50. (In Russ.)

Kovalev S.S., Kovalev S.G., Timofeeva E.A. (2017). New data on the geology, geochemistry and mineralogy of the Suran and Inturatov sections (Bashkir meganticlinorium). *Geologicheskiy sbornik*, 13, pp. 101-118. (In Russ.)

Kovalchuk N.S. (2015). Rare-earth mineralization in metamorphic schists of the Puyvinskaya suite (RF2), Subpolar Ural. *Vestnik of the Institute of Geology of the Komi Science Centre UB RAS*, 10, pp. 38-44. (In Russ.) https://doi.org/10.19110/2221-1381-2015-10-38-44

Kranidiotis P., MacLean W.H. (1987). Systematic of Chlorite Alteration at the Phelps Dodge Massive Sulfide Deposit, Matagami, Quebec. *Economic Geology*, 82, pp. 1808-1911. https://doi.org/10.2113/gsecongeo.82.7.1898

Krogh E.J., Raheim A. (1978). Temperature and pressure dependence of Fe-Mg partitioning between garnet and phengite, with particular reference eclogits. *Contrib. Mineral Petrol.,* 66(1), pp. 75-80.https://doi.org/10.1007/BF00376087

Lanzirotti A., Hanson G.N. (1996). Geochronology and geochemistry of multiple generations of monazite from the Wepawaug Schist, Connecticut, USA: implications for monazite stability in metamorphic rocks. *Contrib. Mineral. Petrol.,* 125, pp. 332-340. https://doi.org/10.1007/s004100050226

Larionov N.N., Bergazov I.R. (2006). State geological map of the Russian Federation. Scale 1: 200 000. Sheet N-40-XXII (explanatory note). Ufa, 185 p. (In Russ.)

Maslov A.V., Kovalev S.G. (2014). Noble metal specialization of terrigenous rocks of the lower and middle Riphean of the Bashkir anticlinorium (Southern Urals). *Geology and mineral resources of Siberia*, 3(2), pp. 11-14. (In Russ.)

Maslov A.V., Nozhkin A.D., Podkovyrov V.N., Letnikova E.F., Turkina O.M., Grazhdankin D.V., Dmitrieva N.V., Isherskaya M.V., Krupenin M.T., Ronkin Yu.L., Gareev E.Z., Vescheva S.V., Lepikhina O.P. (2008). Geochemistry of fine-grained terrigenous rocks of the Upper Precambrian of Northern Eurasia. Yekaterinburg: UB of RAS, 274 p. (In Russ.)

Massonne H.J., Schreyer By.W. (1989). Stability field of the high-pressure assemblage talc+phengite and two new phengite barometers. *Europ J. Mineral.,* 1, pp. 391-410. https://doi.org/10.1127/ejm/1/3/0391

McFarlane C.R.M., Connelly J.N., Carlson W.D. (2005). Monazite and xenotime petrogenesis in the contact aureole of the Makhavinekh Lake Pluton, northern Labrador. *Contrib. Mineral. Petrol.,* 148, pp. 524-541. https://doi.org/10.1007/s00410-004-0618-7

Parnachev V.P., Rotar A.F., Rotar Z.M. (1986). Middle Riphean volcanic-sedimentary association of the Bashkir meganticlinorium (Southern Urals). Sverdlovsk: UC AN USSR, 105 p. (In Russ.)

Puchkov V.N. (2000). Paleogeodynamics of the Southern and Middle Urals. Ufa: Dauria, 146 c. (In Russ.)

Puchkov V.N. (2013). Plumes in the geological history of the Urals. *Bull. MOIP, Otd. geol.,* 88(4), pp. 64-73. (In Russ.)

Puchkov V.N., Kovalev S.G. (2013). Plume events in the Urals and their relationship with subglobal epochs of riftogenesis. *Coll. papers: Continental rifting, associated processes.* Irkutsk: IZK SB RANS, pp. 34-38. (In Russ.)

Savko K.A., Korish E.Kh., Pilyugin S.M., Polyakova T.N. (2010). Phase equilibria of rare-earth minerals during metamorphism of carbonaceous schists of the Tim-Yastrebovskaya structure, Voronezh crystalline massif. *Petrology,* 18 (4), pp. 402-433. (In Russ.) https://doi.org/10.1134/S0869591110040053

Smith H.A., Barero B. (1990). Monazite U-Pb dating of staurolite grade metamorphism in pelitic schists. *Contrib. Mineral. Petrol.,* 105, pp. 602-615. https://doi.org/10.1007/BF00302498

Taylor S.R., McLennan S.M., (1985). The continental crust; its composition and evolution. Cambrige: Blackwell, 312 p.

Tomkins H.S., Pattison D.R.M. (2007). Accessory phase petrogenesis in relation to major phase assemblages in pelites from the Nelson contact aureole, southern British Columbia. *J. Metam. Geol.,* 25, pp. 401-421.https://doi.org/10.1111/j.1525-1314.2007.00702.x

Wing B.A., Ferry J.M, Harrison T.M. (2003). Prograde destruction and formation of monazite and allanite during contact and regional metamorphism of pelites: petrology and geochronology. *Contrib. Mineral. Petrol.,* 145, pp. 228-250. https://doi.org/10.1007/s00410-003-0446-1

About the Authors

Sergey G. Kovalev – Director, Dr. Sci. (Geology and Mineralogy), Institute of Geology – Subdivision of the Ufa Federal Research Centre of the Russian Academy of Sciences

16/2, Karl Marx st., Ufa, 450077, Russian Federation

E-mail: kovalev@ufaras.ru

Andrey V. Maslov – Chief Researcher, Corresponding Member of the Russian Academy of Sciences, Dr. Sci. (Geology and Mineralogy), Zavaritsky Institute of Geology and Geochemistry of the Ural Branch of the Russian Academy of Sciences

15, Vonsovsky st., Yekaterinburg, 620016, Russian Federation

Sergey S. Kovalev – Junior Researcher, Institute of Geology – Subdivision of the Ufa Federal Research Centre of the Russian Academy of Sciences

16/2, Karl Marx st., Ufa, 450077, Russian Federation

Manuscript received 14 January 2020;
Accepted 24 April 2020; Published 30 June 2020

ORIGINAL ARTICLE
DOI: https://doi.org/10.18599/grs.2020.2.67-76

The development of numerical forecasting systems of primary sources of gold on the results of placer sampling in the example Vagran placer cluster (North Urals)

A.V. Lalomov[*], *A.A. Bochneva, R.M. Chefranov*
Institute of Geology of Ore Deposits, Petrography, Mineralogy and Geochemistry of the Russian Academy of Sciences, Moscow, Russian Federation

Abstract. Based on the results of field research, as well as data from stock reports, two types of placer gold were identified within the Vagran placer cluster, which are indicators of primary mineralization. They are used as benchmarks for developing a digital system for predicting parameters and localizing primary sources of placer gold.

Formalized typomorphic characteristics of placer gold (size, roundness, fineness, sorting and content of trace elements), combined in multiplicative indicators, make it possible to forecast the composition and localization of the primary mineralization with greater confidence than ordinary parameters separately. The data required for such an assessment do not require additional field and highly qualified laboratory studies, they are contained in standard reports on the heavy minerals testing, and, in contrast to the characteristics of individual indicator types of placer gold, they give more stable results.

The study of the correlation system allowed to identify characteristic indicators for the primary mineralization of gold-sulfide-quartz and hypogenic-hypergenic types, and to give recommendations for conducting prospecting and exploration in order to identify the primary gold content of the cluster. The proposed method of creating forecast estimates allows to computerize the process of determining the prospects for primary mineralization of territories.

Keywords: placer deposits, strategic metals, modeling, forecast, multiplicative indicators

Recommended citation: Lalomov A.V., Bochneva A.A., Chefranov R.M. (2020). The development of numerical forecasting systems of primary sources of gold on the results of placer sampling in the example Vagran placer cluster (North Urals). *Georesursy = Georesources*, 22(2), pp. 67-76. DOI: https://doi.org/10.18599/grs.2020.2.67-76

During 200 years of exploitation of gold deposits of Urals main part of mining gold was produced from placer deposits, but at present, the main prospects for maintaining of the gold production in this region are associated with primary ore bodies. Available placers and its halos can be used as a search criterion for primary gold deposits. To assess the potential of long-term developing ore-placer clusters for endogenous mineralization, including new non-traditional types (Barannikov, 2009), it is necessary to carry out of material and spatial-genetic relationships in the series "primary gold source– intermediate host – placer".

Despite almost a century of mining of gold placers on the territory of the Vagran cluster, some questions related to the primary sources of gold remain unresolved. It is believed that at the stage of Mesozoic peneplanation of the Ural folded belt, placer gold was released from the zones of ore mineralization of the gold-sulfide-quartz type, and then re-deposited in the formation of the Quaternary alluvial complex through the weathering crust systems and erosion-structural depressions (ESD) (Barannikov, 2009; Sazonov et al., 2001).

To find out the primary sources of placer gold, it is necessary to carry out specialized field work and laboratory research. The algorithm proposed by the authors based on formalizing standard typomorphic characteristics of placer gold and further combining them into multiplicative indicators makes it possible to automate, significantly simplify and optimize the process of forecasting of the ore mineralization.

Geology and primary metallogeny of Vagran cluster

The Vagran cluster, which we took as a model, is located within Sur'ya-Promyslovsky and Ashkinsky metallogeny zones of Northen Urals, the border between

[*]*Corresponding author: Alexander V. Lalomov*
E-mail: lalomov@mail.ru

them runs along a regional meridionally oriented fault. In both ore zones, rocks of the black shale formation are developed: in the Ashkinsky – Upper Riphean and in the Sur'ya-Promyslovsky – mainly Ordovician ages. The size of the studied part of this cluster is 12.5 by 15 km.

The Riphean complex consists of metamorphosed terrigenous sediments, the lower part of which is dominated by coarser-grained varieties (chlorite-sericite shales, quartzite-sandstones, rarely quartzite conglomerates), the upper part – clay chlorite-quartz shales and phyllites) (Sazonov, Velikanov, 2010). The Ordovician complex is represented by gray and black carboniferous-quartzite and carboniferous-phyllite shales with subordinate layers of carbonate-containing varieties; in the upper part there are basic volcanics with corresponding layers of quartz porphyrites. The complex is intruded by a series of dolerite and gabbro-dolerite dikes. There are single dikes of metamorphosed granitoids, more common bodies of metadolerites (Fig. 1). According to geophysical data, a large buried granitoid massif is located within the cluster (Petrov et al., 2015).

Currently, single quartz veins with a sulfide content up to 0.5-2.0%, represented by pyrite, rarely chalcopyrite and tennantite, which show weak but widespread gold mineralization with a gold content of 0.2 ppm, rarely of 2-5 ppm, which have been identified within the Vagran cluster. In addition, weak gold content (of 0.5-1.0 ppm) accompanies linear zones of shale and pyritization, locations of crushing in metamorphic shales and

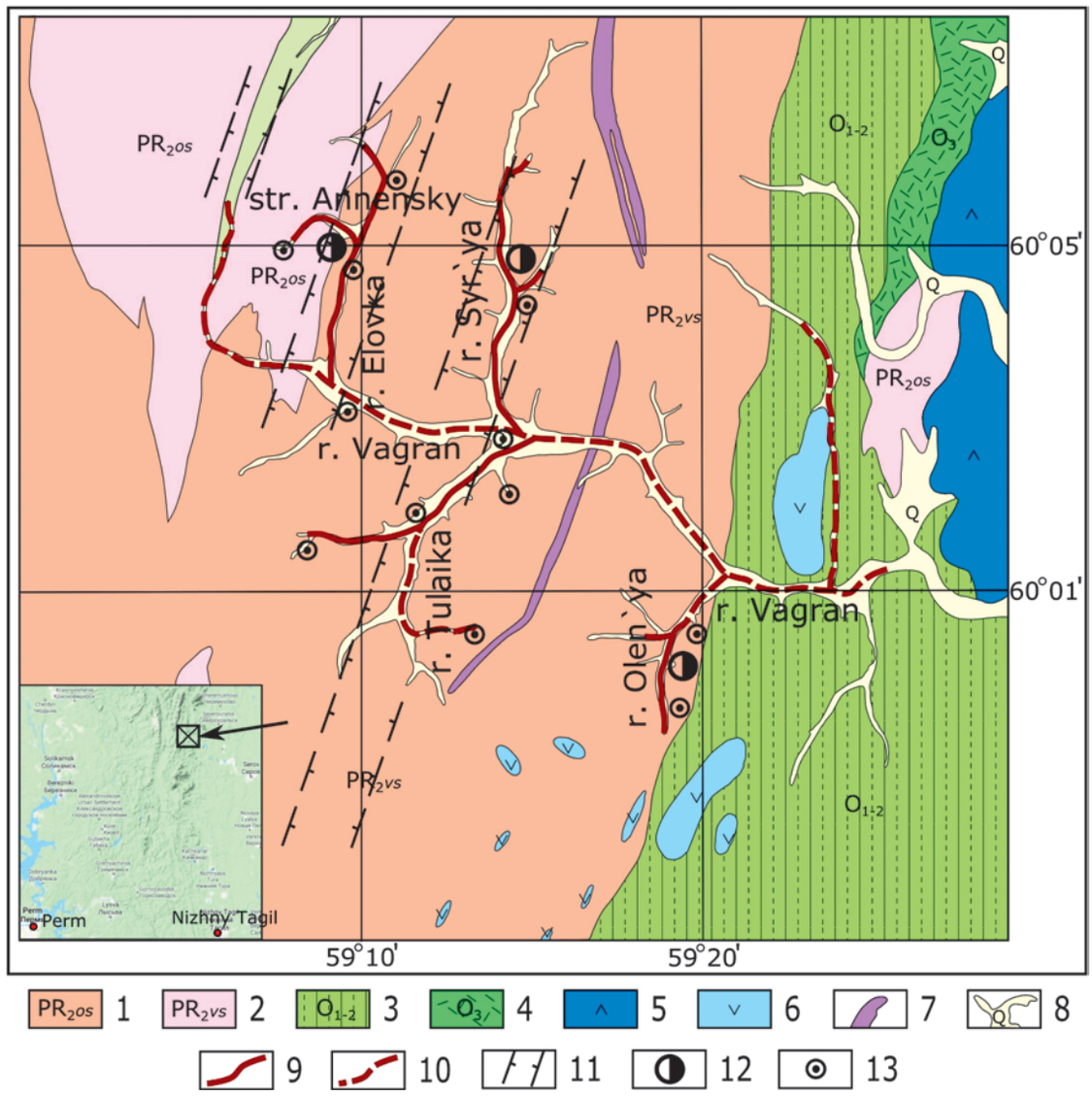

Fig. 1. Geological map of Vagran gold-bearing placer cluster base on a Report (Novitskiy et al., 1967). 1, 2 – metamorphosed clastic sediments of Upper Proterozoic (Riphean): 1 – quartzite, and sandstone of Oslyan Formation, 2 – carbonate-black shale strata with the basic volcanics of the Visim Formation; 3 – Lower-Middle Ordovician (black carbon-quartzite and carbonaceous-phyllite shales with subordinate layers of carbonate-containing varieties); 4 – Upper Ordovician (basic volcanics with under lying layers of quartz porphyry); 5 – gabbro-hornblende, biotite-hornblende amphibolites; 6 – altered gabbro; 7 – albite gneiss, gneissogranite and interstratified porphyry; 8 – Quaternary alluvial sediments; 9, 10 – gold placers: 9 – industrial importance, 10 – non-industrial; 11 – erosion-structural depressions; 12 – primary gold deposits; 13 – sample positions.

listvenite-like zones of hydrothermally altered rocks (Novitskiy et al., 1967).

The ore occurrence of gold-sulfide-quartz type has been identified in the headwater of Sur'ya Creek. It is represented by a zone of veined-disseminated mineralization of pyrite, chalcopyrite, sphalerite, gray copper ores and other sulfides, sulfoarsenides, tellurides with a gold content of 8 ppm and platinum of 3.7 ppm (Petrov et al., 2015). It is assumed that quartz-vein bodies with gold-sulfide-quartz mineralization, which served as sources of placers of Jurassic, Early Miocene and Quaternary age, were mostly eroded at similar ore occurrences at the level of the modern erosive section (Barannikov, Azovskova, 2017), and Sur'ya ore occurrence is the bottom parts of this gold mineralization.

In addition to gold-polysulfide-quartz orogenic mineralization, new non-traditional geological and industrial types for the Urals were established in the adjacent territory: gold-shale "Sukhoy log type", gold-argillisite and ore-bearing chemical weathering crusts (Lezhepekov, 2006; Petrov, 2014).

The mineralization of the hypogenic-hypergenic type, which singled out last time, is associated with the prospects of identifying new gold deposits in the Urals. The mineralization is associated with the stitch zones, disjunctive dislocations and strain zones. The hypogenic component is caused by the development of low-temperature hydrothermal metasomatites, while the hypergenic component is caused by the presence of chemical weathering crusts. Activation of low-depth low-temperature processes of gold ore genesis took place in several stages: Early Mesozoic ($T\text{-}J_1$), Late Mesozoic (J_2-K) and Cenozoic (Pg_3-Q), which generally coincided with the phases of post-collisional tectonic-magmatic activation of the region (Shub et al., 1993). A distinctive feature of this type of mineralization is the dominance of fine-grained and fine gold, as well as a wide range of probity and the absence of hypergenic changes (Gryaznov et al., 2007; Barannikov, Azovskova, 2017).

Placer metal content is localized in the headwaters of Vagran River and its tributaries within Quaternary watercourses of I-III orders. The productive layer of mainly alluvial genesis lies on fractured bedrocks, which is represented by metamorphosed shales, siltstones and sandstones, or on weathered eluvial deposits; in some cases, the layer lies on a false bottom at the base of the second (mid-Quaternary) cycle of alluvial system development. The gold distribution both in thickness and width, as well as strike of placers is uneven.

Sample collection and data of previous investigations

The material for the study based on data from sampling of alluvial, slope and eluvial sediments within the modern and mined quarriers and river-bedded material of natural streams, which were held on the territory of placer cluster over an area of approximately 400 km^2, and were taken from "Report on geological exploration at the Vagranskoe deposit of alluvial gold" (Novitskiy et al., 1967). At the field stage of research bulk samples of the river valley sediments each with an approximate weight of 20 kg were hand-panned to heavy mineral concentrate, from which the gold was extracted by separation in a heavy liquid in the laboratory of Institute of Geology of Ore Deposits, Petrography, Mineralogy and Geochemistry of the Russian Academy of Sciences (IGEM RAS). Within the Vagran cluster, a total of 20 points were tested (which were then combined and the total number of points was 10) and 372 grains of placer native gold were obtained (Lalomov et al., 2020).

Obtained gold grains were studied for morphology on binocular. Back-scattered-electron (BSE) images of the gold were taken for 94 original grains using a Scanning Electron Microscope (SEM) GSM 5610LV. 112 grains were later analyzed by electron microprobe at the Analytical Laboratory of IGEM RAS using JEOL JXA-8200 electron microbrobe (Japan) by analyst E. Kovalchuk. 7 grains with inclusions and pronounced rim-core zoning were studied in detail with SEM and energy dispersive spectrometer INCA-Energy 450 by analyst L.O. Magazina (IGEM RAS).

Data on the geological structure of the cluster, grain-size composition and fineness of gold was taken from the report (Novitskiy et al., 1967).

In previous works (Lalomov et al., 2020; Lalomov et al., 2017) the authors identified five types of gold, which differ in morphology, chemical composition and structure of gold particles (Fig. 2). The first type

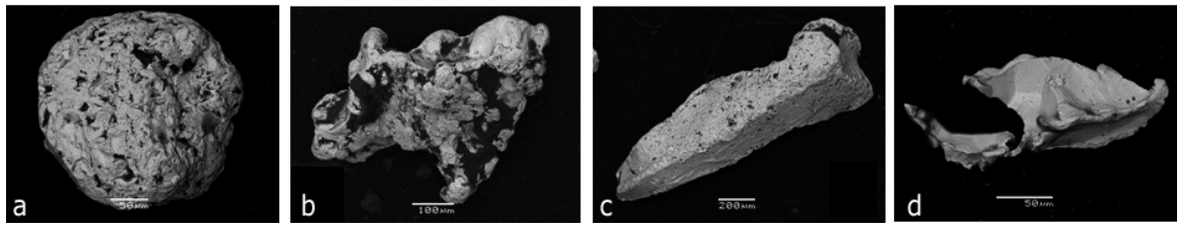

Fig. 2. Morphological types of concentrate gold of the Vagran cluster. a – medium to well-rounded with high fineness (type I); b – medium to subrounded with high fineness (type II); c – idiomorphic and interstitial with high fineness (type IV); d – irregular angular to sub-angular with medium and low fineness with high content of silver and mercury (type V).

(I) is classified as rounded and well-rounded particles of high fineness and absence of gold-rich rim zone, whereas second type (II) are characterized by rounded to sub-rounded gold grains of high gold fineness and absence of gold-rich rim zone. Morphologically third type (III) is identify to grains of types I and II, but it has high gold fineness rim zone of hypergenic origin. Gold of fourth type (IV) is idiomorphic and interstitial with high gold fineness without gold-rich rim zone, which is characterized mezothermal level of mineralization zone at first. Gold grains of fifth type (V) are sub-angular, medium to low gold fineness with an increased content of silver and mercury (Table 1).

The distribution of the selected types of gold within Vagran cluster is uneven: types I and II are found throughout the territory, while the periphery is dominated by more rounded gold of the type I. Gold of types III and IV tends to the ESD zones. V-type gold is poorly connected to the modern relief and driangle system and is controlled by the North-Western strike zone, which is diagonal to the structures of the Urals.

The similarity of composition of the first four types of gold indicates the similarity of their primary source, which is attributed to gold-sulfide-quartz formation, at the same time the differences can be explained by zoning of primary mineralization and history of transformation of native gold in hypergenesis. The least distant from the source (least rounded) is gold of type II.

The characteristics of V-type gold indicate a second primary source of gold, discovered at later stages of

	Types of gold				
	I	II	III	IV	V
Shape and surface	Gold grains are of a spherical shape with rough, rarely slightly smooth and pitted surface.	Grains are with rough slightly smooth. The shape of the gold is mainly dendritic, wire-like, leaf-like, and the internal structure is uniform.	Similar to grains of type I and II	Gold of idiomorphic and interstitial morphology with a rough surface.	Gold particles are presented angular monocrystalline secretions of idiomorphic and xenomorphic particles with smooth and conchoidal surface.
Roundness	Well-rounded and rounded	Rounded and sub-angular	Well, rounded and sub-angular	Moderate traces of roundness	sub-angular and angular
Fineness	933 (882- 970) *	931 (901- 957)	In core 932 (882- 970), in rim-zone - 986 (967- 997)	948 (923- 966)	828 (571- 901)
Trace elements (wt.%)	Ag 6.18 (2.03- 11.62); Cu 0.15 (0.06- 1.08); Hg (0.154- 0.268) - in single grains	Similar to type I	Ag 6.38; Cu 0.15.	Ag 4.76.; Cu 0.17.	Ag 15.8.; Hg of 1.15
% in placers	36.7	28.8	13.8	9.2	11.5 (0 - 76.5)
Internal structure	Mostly homogeneous, there is a lumpy, spongy and layered structure, formed when rolled into spherical aggregates of irregularly shaped gold particles during transportation.	Mostly homogeneous in individual grains inclusions of cobaltite.	High fineness rim-zone (10-40 microns)	Without rim zone. The internal structure is uniform, similar in composition to grains of type I and II.	The structure is uniform, with veinlets enriched with mercury. Thin (3-5 microns), highly enriched (fineness 923-967) rim zone in the individual grains.
Localities	They are distributed throughout the cluster, have signs of transfer and long-term stay in the zone of hypergenesis.		It tends to ESD zones.	It tends to Sos'vinskaya ESD zone.	There are signs of short-distance drift and a relatively short time spent in the hypergenesis zone.
	Well-rounded gold predominates on the flanks of the cluster.	Dendritic rounded gold predominates in the central part of the cluster and decreases on the flanks.			

*Table 1. Distinguished types of placer gold (Lalomov et al., 2020). * Average content (variations of values).*

formation of the cluster placers, at the same time weak roudness indicating its minimal displacement. The distribution of gold of this type over the area is poorly controlled by driangle system: the increased content is confined to a linear zone diagonally oriented in relation to the folded structures of the Urals. Presumably, the source of this gold is hypogenic-hypergenic mineralization (Lalomov et al., 2020).

Thus, gold halos of the types II and V have the greatest connection with primary mineralization and can serve as indicators of primary ore mineralization, which were used as a model for creating complex search indicators.

The development of forecasting multiplicative indicators

When prospecting of gold deposits applies a complex of methods, among which the most important is the heavy mineral concentrate sampling. At the same time, not only the total gold content in alluvium sediments is informative, but also its morphology, first of all, its roundness, which indicates the degree of its distance

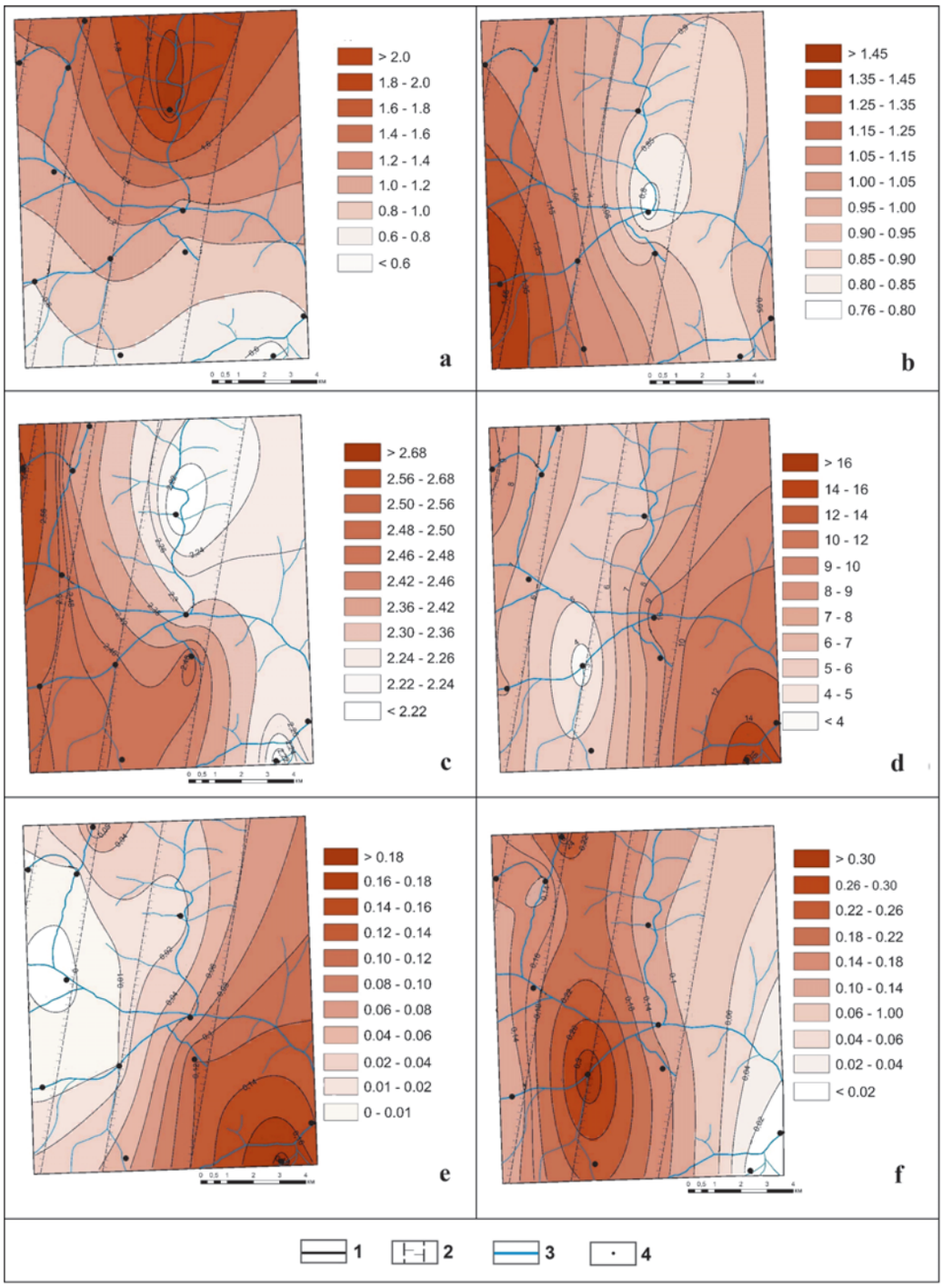

Fig. 3. The distribution of formalized indicator characteristics over the cluster area: a – size, b – sorting, c – roundness, d – content of Ag, e – content of Hg, f – content of Cu. 1 – cluster boundaries, 2 – erosion-structural depressions, 3 – watercourses, 4 – sampling points.

from the primary source. At the present stage, different types of concentrate gold are additionally distinguished, its composition, structure and nature of inclusions are studied, which allows us to establish the types of primary sources and the history of gold conversion in the hypergenesis zone.

Sometimes such data is sufficient to solve the problem of identifying the primary source of placers, but most often the level of features individually is not sufficiently informative, and methods are needed to obtain complex indicators that are more contrasting than individual factors. The various study of the Vagran cluster's gold concentrate allowed us to formulate and test methods for creating and applying such complex indicators on its example.

In order to create a computerized system for predicting primary mineralization, the following steps have been taken sequentially:

- the main indicator characteristics (IC) of placer native gold haloes are highlighted, the direction and degree of their connection with indices of basic mineralization are determined;
- formalized (quantitative assessment) of these IC has been done;
- within the framework of the GIS project of the Vagran cluster, the quantitatively evaluated IC received spatial reference;
- based on the correlation analysis, the primary IC are combined into multiplicative indicators constructed taking into account the directivity of the influence of the parameters on the overall predicted result.

The created computerized system allows to collect, store, process and visualize data at all stages of the process of creating forecast estimates.

To solve the problem, we used the following typomorphic IC of placer gold – weighted average size, sorting (formalized by the coefficient of variation of the size), roundness according to a 5-point scale from 0 (non-rounded) to 4 (very well rounded grains) for different types and for the sample as a whole, the fineness and content of trace elements: silver, copper and mercury (Fig. 3). All the obtained characteristics are spatially linked within the framework of the GIS project in the ArcGis package.

The formalization of sorting through the coefficient of variation is caused by a number of reasons: the distribution entropy according to S.I. Romanovsky requires a more detailed analysis of particle size distribution (Romanovsky, 1988); the classical sorting coefficient using trask quantiles (Trask, 1932) is not universal, it is suitable for the most rough estimation of granulometric composition (Logvinenko, Sergeeva, 1986). The magnitude of the standard deviation depends on the size of the particles being analyzed, therefore, the coefficient of variation (the dimensionless value of the standard deviation of the size divided by the weighted average particle size) is, in this case, the most representative indicator of the sorting of gold particles by size.

Ordinary indicators far from always can unambiguously characterize the forecast potential of the studied area for various types of mineralization, therefore, multiplicative indicators (MI) were used, similar to those used in geochemistry to increase the contrast of indicator features. MI is calculated according to the formula in which the numerator contains the products of the results of the analysis of elements (in our case, IC) of positive correlation with the desired type of mineralization, and the denominator contains the product of neutral or negative indicators of the desired parameter (Grigoryan et al., 1983).

Due to the directed amplification of correlated useful signals, the influence of fluctuations (background) is minimized, and therefore the multiplicative halos show a closer connection with the geological and structural features of ore bodies and deposits, which significantly increases the reliability of their interpretation. When m elements are multiplied, the anomaly amplitude increases m times, and the variance only $\sqrt{m}$ times. Accordingly, the contrast of the anomaly increases by a factor of $\sqrt{m}$. MI also gives a more stable result, reducing the influence of random deviations and errors (Voroshilov, 2011).

To create generalized predictive characteristics, a matrix of pair correlation coefficients between them and the gold content of types II and V, which are the reference indicators of primary mineralization, was constructed (Table 2). Based on these data, MI were formulated that characterize the zones most promising for searches for bedrock sources of gold.

The second type of gold ("C_{II}") has a positive correlation with the particle size and copper content, and negative correlation with the sorting, roundness and silver and mercury content. MI-1 characterizes (through the prevalence of type II gold) the bedrock sources of the gold-sulfide-quartz formation, discovered at the stage of peneplanation and passed through the intermediate hosts. It can be calculated by the formula:

$$MI\text{-}1 = (K \times Cu) / (S \times O \times Ag \times Hg) \quad (1)$$

The fifth type of gold ("C_V") has positive correlation with content of silver and mercury, and the negative correlation with particle size, sorting, particle roundness and copper content. MI-2 characterizes (through the prevalence of type V gold) the bedrock sources of the hypogenous-hypergenic type, discovered at the Quaternary stage. It can be calculated by the formula:

$$MI\text{-}2 = (Ag \times Hg) / (K \times S \times O \times Cu) \quad (2)$$

The data from Table 2 demonstrates that MI-2 has a real stable correlation with the type V gold content ($R = 0.86$), more significant than the correlation

	C_{II}	C_V	K	S	O	Ag	Hg	Cu	MI-1	MI-2
C_{II}		**-0.59**	0.44	-0.12	-0.31	-0.61	-0.34	0.31	**0.46**	-0.48
C_V			-0.54	-0.52	-0.45	0.80	0.80	-0.56	-0.53	**0.86**
K				-0.10	-0.05	-0.60	-0.60	0.36		
S					0.61	-0.37	-0.50	0.18		
O						-0.33	-0.46	0.43		
Ag							0.81	-0.79		
Hg								-0.54		
Cu										

Table 2. Matrix of pair correlation coefficients (R) between typomorphic indicator characteristics, the content of indicator gold types and obtained multiplicative indicators (MI). Notes: "C_{II}", "C_V" – gold content of indicator types II and V in the total placer gold; "K" – the average size of the placer gold (fineness); "S" – sorting, expressed in terms of the coefficient of variation of dimension; "O" – roundness on a 5-point scale; "Ag", "Hg", "Cu" – the content of silver, mercury and copper in gold; "MI-1", "MI-2" values of multiplicative indicators. The critical value is R = 0.55 with a sample size of N = 10 and a confidence probability of α = 0.90.

relationships of individual characteristics, which allows MI-2 to be used as a criterion for allocating areas for the search for hypogenous-hypergenic mineralization.

The multiplicative indicator MI-1 has a less obvious connection with the zone of the primary source characterized by type II gold. Although MI-1 has a more stable correlation with the main indicator of gold-sulfide-quartz mineralization than individual IC (with the exception of silver content), the overall correlation stability (R = 0.46) is less than the critical value R = 0.55 at a confidence level of α = 0.90. Obviously, this is due to the fact that gold entered the placers not directly from the zones of primary mineralization, but through a system of intermediate

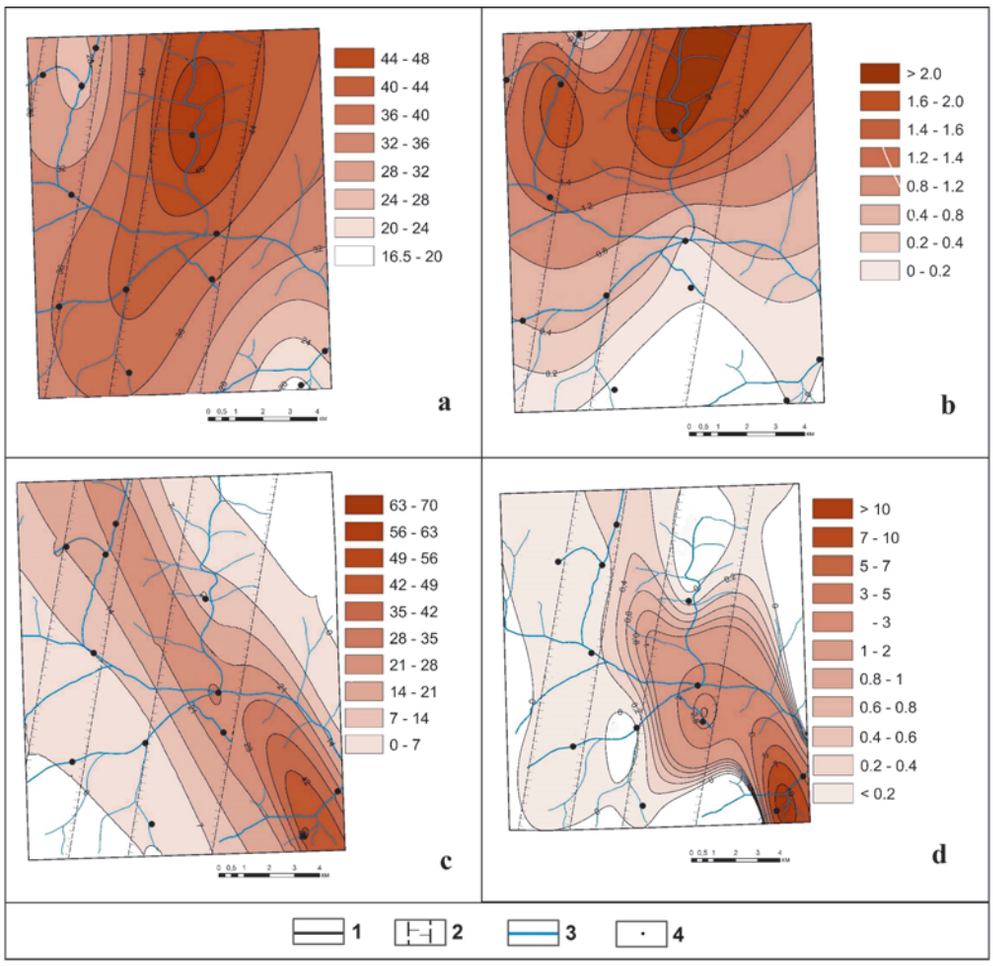

Fig. 4. Distribution of indicator types of bedrock gold and multiplicative indicators: a – gold of type II (%), b – MI-1, c – gold of type V (%), d – MI-2. 1 – boundaries of the site, 2 – erosion-structural depressions, 3 – watercourses, 4 – sampling points.

hosts, which introduced a distortion into the picture of the spatial-genetic relationships between the primary source and placer gold of Quaternary streams.

Although the silver content (which is equivalent to the fineness due to the low contents of other trace elements) is more contrasted in comparison with MI-1 (R = -0.61), separately use ID silver content may have an increased error and characterize the zonality of the variation in the fineness of a single source, rather than the presence of different formation sources. Therefore, the use of MI-1 gives a more stable and reasonable result.

A stable negative correlation between the contents of gold of types II and V (R = -0.59) confirms the assumption that these types of alluvial gold came from different sources.

The final results of data processing are presented in Fig. 4. Distributions of indicator types of gold II and V were adopted as reference indices of primary mineralization, and MI-1 and MI-2 were used as forecast criteria.

MI-1 has maximum value in the region of the middle and upper part of the valley of the Sur`ya River; the second, less pronounced maximum, is associated with the basin of the Elovka River (mouth of the Annensky creek). The values of MI-1 are reduced to the periphery of the cluster. This approximately coincides with the distribution of type II gold and confirms the assumption that the main primary source of alluvial gold of the cluster was localized in this zone.

The maximum values of MI-2 are concentrated in a linear zone extending from the middle course of the Olen`ya river through the site of confluence in the Vagran river Sur`ya, Tulaika rivers and Bazovy creek, to the upper part of the valley of river Elovka (above Annensky creek).

The available irregular sampling on the primary mineralization of the cluster is insufficient for the development of MI, therefore, in the proposed study, short transported placer gold was used as indicator sign of primary mineralization. Nevertheless, the identified prospective areas are confirmed by the available data on the bedrock gold mineralization. Revealed gold-sulfide-quartz mineralization in the upper river Sur'ya has gold contents up to 8 ppm (Petrov et al., 2015). It coincides with the maximum contents of type II gold and elevated values of MI-1. Unfortunately, available publications have not description of the typomorphic features of the bedrock gold, fineness is not indicated, therefore, the type of mineralization can be characterized only tentatively.

In the Olen`ya-Elovka zone, which corresponds to elevated gold contents of type V and MI-2, ore gold with a content of 2.0-6.9 ppm is presents in the selected bedrock samples. The silver content of 3.6-1.7 ppm and mercury 0.05-0.10 ppm indicates possible connection with type V placer gold. There is no doubt that the use of directly primary rock analyses as standards will increase the reliability of the method.

The prospective areas obtained from the multiplicative indicators can be used for setting up prospecting works for gold ore objects.

Thus, with respect to the forecast of the bedrock gold mineralization within the Vagran cluster, the most promising is the linear north-east – south-west strike zone, which controls the distribution in the placers of medium-grade mercury placer gold of low-temperature hypogenous-hypergenic type. It is assumed that it is determined by the linear zone of faults and/or deconsolidation of rocks established at the stage of postcolysis tectonic-magmatic activation. A weak manifestation of the relationship between the distribution of gold of the fifth type and elements of the hydrogrid indicates its late opening (Quaternary time), which suggests a small level of its erosion section and, accordingly, an increased ore potential.

The use of a computerized system for processing the data of heavy mineral concentrate sampling and the obtained multiplicative indicators can be used to predict the bedrock metal content. Although the distribution of indicator types of gold is more directly than the multiplicative indicators associated with bedrock mineralization, their direct application is complicated by a number of reasons:

- to highlight the indicator types of placer gold, indicating bedrock objects, it is necessary to test the entire investigated area and obtain placer gold samples for specialized studies;
- the bonds of placer gold with primary sources are manifested at the level of the internal structure of grains and their chemical composition, therefore, it is necessary to carry out specialized hardware analytical studies (electron microscopy, microprobe analysis in polished pieces);
- to distinguishing of the indicator types of the placer gold and for creation of forecast of primary mineralization, high qualification and extensive practical experience of the researcher in the study of primary mineralization and placer native gold are required. At present, the number of such specialists in Russia is not enough to conduct mass forecast estimates.

The proposed method allows to carry out a predictive assessment quickly, with less cost and in an automated mode:

- does not require special field and laboratory studies, uses standard data from geological reports on the study of placer gold deposits and aureoles;
- consists of standard operations within the framework of the developed algorithm and does not require high qualifications and extensive practical experience of the operator.

Currently, the method is under development and has a number of unresolved issues that will need to be investigated when continuing the work:

- IC were tested within a single gold-bearing cluster on two types of primary mineralization (gold-sulfide-quartz and hypogenous-hypergenic); the amount of used IC and the types of characterized primary mineralization types can be increased;

- at the current stage, placer gold with minimal signs of transfer, which has the maximum connection with primary mineralization, has been used as indicator types of primary sources; the application of this technique at sites with known ore mineralization will increase the reliability of the model;

- equations (1) and (2) solve the problem in a first approximation, based on the assumption of a linear nature of the relationship between IC and the ore potential of the territories. In the case of nonlinearity of these relationships, the calculation formulas of the MI can change, but the qualitative nature is likely to continue. The use of complex multiplicative indicators can reduce the influence of individual characteristics (even if they have a nonlinear correlation dependence) and strengthen the general regularities. This issue requires additional research in the subsequent stages of the development of the methodology.

Thus, in the current state, the proposed methodology is optimally applicable at the initial stages of forecasting and planning of the exploration, when the problem should be solved using available data and without additional research. In the case of confirmation of the forecast, it is recommended that more detailed work be undertaken on the prospective areas.

Conclusion

Based on the formalized (quantitatively estimated) indicator characteristics of placer gold, computer numerical modeling and GIS technologies using the example of the Vagran goldiferous cluster, a system for spatially calculating and positioning multiplicative indicators that evaluate the zone of the likely occurrence of primary metal bearing has been created.

The proposed methodology makes it possible at the initial stages of work to use the results of ordinary analyzes (including those contained in stock reports) for forecasting.

Obtained multiplicative indicators are oriented to forecasting of two types of mineralization (gold-sulfide-quartz and hypogenous-hypergenic); for other ore-bearing formations can be used other parameters, that will be the subject of further research.

Nevertheless, already in its present form, it can be used for planning geological exploration, and also serve as the basis for the further development of more detailed and accurate versions of the methodology, as well as expanding it to other geological and genetic types of mineralization.

Based on the conducted studies, a zone was identified within the Vagrans gold-bearing cluster that is promising for the identification of the primary bedrock mineralization of the hypogenous-hypergenic type.

Application of the developing method does not mean abandonment of existing methods for predicting of bedrock mineralization. It will not be able to completely replace the specialist, and therefore it will be used as a hybrid system operating in the "operator-computer" dialogue mode, which facilitates the decision-making process for the specialist. A similar approach is already used for the express assessment of gold ore occurrences in the Arctic zone of Russia (Chizhova et al., 2019).

Acknowledgments

The work was carried out as part of the state assignment under program No. 0136-2019-0006. Field work was carried out with financial support from the RFBR grant 18-05-00113. Analytical work was performed at the IGEM-Analytics Center in the framework of the IGEM Research Program.

References

Barannikov A. G., Azovskova O. B. (2017). Gold-bearing objects of hypogene-supergene type in the Urals. Convergence of signs of their difference from ore-bearing weathering crusts. *Izvestiya Uralskogo gosudarstvennogo gornogo universiteta = News of the Ural State Mining University*, 2, pp. 13-22. (In Russ.) https://doi 10.21440/2307-2091-2017-2-13-22

Barannikov A.G. (2009). Mesozoic gold-bearing placers of the Urals. *Otechestvennaya geologiya*, 2, pp. 22-33. (In Russ.)

Chizhova I.A., Lobanov K.V., Volkov A.V. (2019). Logical and information models for the forecast and rapid assessment of new gold deposits in the Arctic zone of Russia. *Arktika: ekologiya i ekonomika = Arctic: Ecology and Economy*, 4(36), pp. 107-117. (In Russ.) https://doi.org/10.25283/2223-4594-2019-4-107-117

Grigoryan S.P., Solovov A.P., Kuzin M.F. (1983). Instructions on geochemical methods of ore deposits prospecting. Moscow: Nedra, 191 p. (In Russ.)

Gryaznov O.N., Barannikov A.G., Savelieva K.P. (2007). Non-traditional types of gold-argillite mineralization in Mesozoi structures of the Urals. *Izvestiya Uralskogo gosudarstvennogo gornogo universiteta = News of the Ural State Mining University*, 22, pp. 41-53. (In Russ.)

Lalomov A.V., Chefranov R.M., Naumov V.A. et al. (2017). Typomorphic features of placer gold of Vagran cluster (the Northern Urals) and search indicators for primary bedrock gold deposits (2017). *Ore Geology Reviews*, 85, pp. 321-335. http://dx.doi.org/10.1016/j.oregeorev.2016.06.018

Lalomov A.V., Naumov V.A., Grigorieva A.V., Magazina L.O. (2020). Evolution of Vagren gold bering cluster (North Ural) and prospects for detecting of primary mineralization. *Geology of Ore Deposits* (in print). (In Russ.)

Lezhepekov M.A. (2006). Gold-bearing ore-placer nodes in the southern part of the Suryinsko-Promyslovsky mineralogenous zone. Abstract cand. sci. diss. Ekaterinburg: UGGU, 25 p. (In Russ.)

Logvinenko N.V., Sergeeva E.I. (1986). Methods for the determination of sedimentary rocks. Leningrad: Nedra, 240 p. (In Russ.)

Novitskiy V.Ya., Ushakov S.A., Sukhanov L.P. et al. (1967). Report on geological exploration at the Vagran deposit of alluvial gold with a reserve estimate on 01.07.1967. Severouralsk integrated expedition, Sosvinskaya GRP. Seveouralsk, Pokrovsk-Uralsky. No. TGF 30652. (In Russ.)

Petrov G.A. (2014). Prediction of noble metal mineralization in the pre-Paleozoic black shale strata of the central part of the Ural mobile belt. *Lithosphere (Russia),* 6, pp. 88-101. (In Russ.)

Petrov G.A., Aleksandrov V.V., Zubkov A.I., et al. (2015). To the

Problem of Ore Content of Black Shale of Vi-shera-Kutim Anticlinorium (Northern Urals). *Vestnik Permskogo universiteta. Geologiya = Bulletin* of *Perm University. Geology*, 4, pp. 32-42. (In Russ.)

Romanovsky S.I. (1988). Physical sedimentology. Leningrad: Nedra, 240 p. (In Russ.)

Sazonov V.N., Ogorodnikov V.N., Koroteev V.A. et al. (2001). Gold deposits of the Urals. Yekaterinburg: IGiG UrO RAN, 622 p. (In Russ.)

Sazonov V.N., Velikanov A.Ya. (2010). Ashka noble metal zone (Middle and North Urals): geological position, structural features, composition of ore bodies and associated metasomatites, practical significance. *Lithosphere (Russia)*, 4, pp. 116-127. (In Russ.)

Shub V.S., Barannikov A.G., Shub I.Z. et al. (1993). Gold of the Urals. Alluvial deposits (to the 250th anniversary of the gold industry of the Urals). Yekaterinburg: Nauka, 135 p. (In Russ.)

Trask P.D. (1932). Origin and environment of source sediment of petroleum. Houston, 281 p.

Voroshilov V.G. (2011). Geochemical methods of prospecting for mineral deposits. Tomsk: Tomsk Polytechnic University, 104 p. (In Russ.)

Manuscript received 17 March 2020;
Accepted 6 May 2020;
Published 30 June 2020

About the Authors

Alexander V. Lalomov – Dr. Sci. (Geology and Mineralogy), Leading Researcher, Institute of Geology of Ore Deposits, Mineralogy, Petrography and Geochemistry of the Russian Academy of Sciences

35, Staromonetny st., Moscow, 119017, Russian Federation
Tel: +7(499)2308427, e-mail: lalomov@mail.ru

Anna A. Bochneva – Cand. Sci. (Geology and Mineralogy), Leading Researcher, Institute of Geology of Ore Deposits, Mineralogy, Petrography and Geochemistry of the Russian Academy of Sciences

35, Staromonetny st., Moscow, 119017, Russian Federation

Roman M. Chefranov – Cand. Sci. (Geology and Mineralogy), Leading Researcher, Institute of Geology of Ore Deposits, Mineralogy, Petrography and Geochemistry of the Russian Academy of Sciences

35, Staromonetny st., Moscow, 119017, Russian Federation

ISSN 1608-5043 (Print)
ISSN 1608-5078 (Online)

Key title: «Georesursy»
Parallel title: «Georesources»

GEORESURSY

A peer-reviewed scientific and technical journal published since 1999

The journal is included/indexed in:

Clarivate Web of Science™	Web of Science Core Collection Emerging Sources Citation Index (ESCI)
Scopus	Scopus
CAS A DIVISION OF THE AMERICAN CHEMICAL SOCIETY	CAS (Chemical Abstracts Service) databases
GeoRef	GeoRef database
EBSCOhost	EBSCOhost™ databases
DOAJ DIRECTORY OF OPEN ACCESS JOURNALS	Directory of Open Access Journals (DOAJ)

The full-text electronic versions of the articles are freely available to the public on journal's website: **www.geors.ru**

Contacts:
Deputy Chief Editor - Daria Khristoforova
E-mail: mail@geors.ru
Tel: +7 (843) 239-05-30